This is to certify that the

dissertation entitled

Cellular Aspects of Aluminum Toxicity: Aluminum uptake by Neuroblastoma Cells and Inhibition of Inositol Phosphate Formation by Aluminum in Neuroblastoma Cells

presented by

Biao Shi

has been accepted towards fulfillment
of the requirements for

Ph.D degree in Microbiology

A. Haug
Major professor

Date 30 Oct. 1991

CELLULAR ASPECTS OF ALUMINUM TOXICITY:

ALUMINUM UPTAKE BY NEUROBLASTOMA CELLS AND INHIBITION OF

INOSITOL PHOSPHATE FORMATION BY ALUMINUM IN NEUROBLASTOMA CELL

By

Biao Shi

A DISSERTATION

Submitted to
Michigan State University
in partial fulfillment of the requirements
for the degree of

DOCTOR OF PHILOSOPHY

Department of Microbiology and Public Health

1991

ABSTRACT

CELLULAR ASPECTS OF ALUMINUM TOXICITY:
ALUMINUM UPTAKE BY NEUROBLASTOMA CELLS AND INHIBITION OF
INOSITOL PHOSPHATE FORMATION BY ALUMINUM IN NEUROBLASTOMA CELLS

By

Biao Shi

Aluminum is apparently involved in a broad spectrum of physiological disorders, e.g., in certain neurodegenerative diseases of humans; some of these disorders may originate from aluminum's primary interaction with a key target in cells. One possibility is that aluminum interferes with phosphoinositide signal transduction where an intracellular second messenger, inositol 1,4,5-triphosphate (IP_3) is generated which, in turn, signals intracellular Ca^{2+} release.

Employing murine neuroblastoma cells, labelled with [^{3}H]-myo-inositol, experimental results demonstrate that aluminum application drastically reduces inositol phosphate production stimulated by Gp protein activators, GTP[S] or fluoride, or the receptor agonist bradykinin. The inhibition principally affects

formation of IP_3, from hydrolysis of phosphatidylinositol 4,5-biphosphate (PIP_2), rather than downstream or upstream reactions distal to IP_3 formation along the signal transduction. When aluminum is prechelated with agents impermeable to the plasma membrane, aluminum-related inhibition is almost completely reversed in intact cells. The application of great excess of Mg^{2+}, GTP[S] and GTP reduces only partially or not all the inhibition of inositol phosphate formation by aluminum. In addition to Mg^{2+}/Gp protein-mediated PIP_2 hydrolysis, phospholipase C reaction can also be activated directly by applying increasing concentrations of Ca^{2+} in neuroblastoma cells. IP_3 production in both pathways is sensitive to aluminum, whereas Ca^{2+}-triggered IP_2 production is not affected by aluminum application. These findings suggest that aluminum inhibits inositol phosphate production through its putative interactions with the Gp protein and phospholipase C.

Employing atomic absorption spectroscopy, aluminum uptake by neuroblastoma cells was studied. At physiological pH, cells can protect themselves from incorporating toxic aluminum. As the medium pH decreases, cells accumulate large amounts of aluminum against the concentration gradient. At neutral pH, transferrin facilitates aluminum uptake, presumably via membrane receptors. Low molecular weight aluminum-chelating metabolites like citrate always act to inhibit aluminum internalization. Ca^{2+}, alleged to ameliorate aluminum toxicity, does not measurably inhibit aluminum uptake by neuroblastoma cells and aluminum binding onto the cellular surface.

To my parents, my wife and my daughter.

ACKNOWLEDGEMENTS

I would like to thank the following members of my dissertation committee for their advice, help and guidance: Dr. William Frantz, Dr. Alfred Haug, Dr. Patrick Oriel, Dr. Ronald Patterson, and Dr. James Tiedje.

I also wish to acknowledge Dr. Karen Chou, in Animal Science Department, for her concern and support.

And thanks to Li Chen, Harrie Koenraadt, Dr. Christopher Weis and Dr. Shixing Yuan for their friendship and help.

TABLE OF CONTENTS

LIST OF FIGURES

LIST OF TABLES

CHAPTER I

LITERATURE REVIEW

Aluminum Toxicity in Animals

Aluminum toxicity in plants was found first this century (Hartwell and Pember, 1918). In recent decades aluminum toxicity has drawn enhanced attention, since it creates serious problems in agricultural production and environmental protection. In vast subtropic and tropic areas, accounting for 40% of arable soils in the world, aluminum toxicity in plants cultivated on acidic soils constitutes a formidable barrier to food and biomass production (Osmond et al., 1980). The ecological impact of aluminum toxicity has been aggravated by environmental pollution. Brought about by acid rain causing acidification osoil and water bodies, the increasingly mobile aluminum ions are in part responsible for forest decline in European countries (Shortle and Smith, 1988) and the loss of fish population in lakes and streams in Canada and the northeastern U.S. (Godbold et al., 1988). As an ecological consequence, aluminum taken up by plants and aquatic organisms finally reaches the food chain for human and animals.

Until recently, the significance of aluminum toxicity in humans had been largely overlooked. Continual and unavoidable exposure to aluminum, slow accumulation and chronic toxicity by the metal have contributed to this indifference (Ganrot, 1986). In the past decade a considerable body of evidence has accumulated implicating aluminum in various diseases, particularly neurological disorders of humans. Aluminum toxicity is being recognized with

increasing frequency in patients with renal failure, leading to osteomalacia, anemia or encephalopathy (Levine et al., 1990). In these patients, tissue aluminum levels correlated directly with left ventricular mass and inversely sith the velocity of circumferential fiber shortening (London et al., 1989).

Several studies identified aluminum as a potential causative factor in the pathology of various types of dementia, especially Alzheimer's syndrome, which is a major health problem among the elderly (Martyn et al., 1989). In Britain, there are an estimated 600,000 people afflicted with these diseases, accounting for 5% of people over 65 years and 20% of those over 80%. Aluminum has been found in high concentrations on hippocampal neurons containing senile plaques and neurofibrillary tangles, which occur in the brain of subjects with Alzheimer's syndrome (Roskams and Connor, 1990). In cell culture, 70% of aluminum-treated human neuroblastoma cells reacted positively with antibody to tao protein and to paired helical filament, i.e., the changes resemble those seen in Alzheimer disease brain specimens (Guy et al., 1990).

Amyotropic lateral sclerosis (ALS)-Parkinson-dementia complex on Guam has been speculated to originate from a genetic disorder. However, Wisniewski et al. (1980) noticed that accumulation of aluminum in neurofilaments in perikarya and proximal axons shared some features with the neurolesions found in patients. Later, Hirano et al. (1984) confirmed that this abnormal structure closely resembled neuronal alterations in the early stages of ALS. Recently, employing X-ray microanalysis, Hirsch et al., (1991)

identified increased aluminum accumulation in the substantia nigra of patients with Parkinson's disease.

Experimentally, aluminum intoxication in neurological disorders has been well established in animal models. Intracranial administration of aluminum to animals produced a progressive encephalopathy with neurofibrillary degeneration of intermediate filaments (Selkoe et al., 1979). Abnormal neuronal axonal transport of neurofilament proteins has been reported in aluminum-intoxicated rabbits (Troncoso et al., 1985). This impaired transport is caused by aluminum-induced formation of protease-resistant high molecular weight complexes from neurofilamant protein (Nixon, et al., 1990).

Since contact and absorption of aluminum is unvoidable, everyday exposure to aluminum unlikely leads to pathological events of human neurodisorders. It is postulated that the onset of these neurodisorders may involve, besides aluminum itself, intrinsic factors like genetic lesions, aging and biological agents (Liss et al., 1989). Aluminum neurotoxicity is rarely expressed in a normal organism; it occurs only when the normal protective mechanisms are impaired or altered by intrinsic or extrinsic factors.

Chemical Properties of Aluminum

As the hardest trivalent metal element in the nature, aluminum has high ionic charge and small crystalline radius. Its high ratio of charge-over-radius ($z^2/r = 43.6C^2\ m^{-1} \times 10^{28}$) yields a reactivity unmatched by other soluble metals (Parker et al., 1989).

Therefore aluminum does not exist as a positive aquo ion, rather, the nonhydrated aluminum ion has a great tendency to polarize adjacent atoms, in particular ligands which contain small, hard negative oxygen donor groups (Martell and Motekaitis, 1987). In the aqueous solution, aluminum ion strongly polarizes O-H bonds of the water molecule, resulting in the dissociation of a proton from water molecule. With a small ionic volume and coordination number of 6, the hydrated aluminum ion is coordinated in its primary hydration shell by six water molecules in an octahedral configuration (Nordstrom and May, 1989), represented by $Al(H_2O)_6^{3+}$. Because of the high positive charge of aluminum ion, these water molecules form a tightly bound primary hydration shell.

The solvation of the aluminum ion largely depends on its concentration and the solution pH. Free Al^{3+} is the predominant species at low pH (< 5.2) solution. As the solution pH increases, the initially hydrated Al^{3+} undergoes stepwise hydrolysis, progressively losing its hydration shell proton to water molecules to maintain dissociation equilibrium, thus doubly and singly charged mononuclear species are formed: (Baes and Mesmer, 1976)

$$Al(H_2O)_6^{3+} + H_2O = Al(H_2O)_5(OH)^{2+} + H_3O^+$$

$$Al(H_2O)_5^{2+} + H_2O = Al(H_2O)_4(OH)_2^{+} + H_3O^+$$

$$Al(H_2O)_4^{2+} + H_2O = Al(H_2O)_3(OH)_3 + H_3O^+$$

Further pH increase in solution will lead to the formation of neutral and negatively charged species.

Aluminum chemistry is further complicated by a variety of complexation reactions. It tends to form electrostatic bonds preferentially with oxygen donor ligands. In biological systems, carboxylate and phosphate groups, inorganic phosphate, nucleotides, and polynucleotides meet this requirement (Martin, 1986). Therefore, carboxyl oxyanions of proteins and phosphate oxyanions of lipids provide targets for aluminum binding. Some polyhydroxy acid metabolites in biological systems like malate, tartrate and particularly citrate, are well-known aluminum chelators (Martell and Motekaitis, 1987). In citrate, carboxylate groups are arranged in a manner favorable for very strong chelation of the aluminum ion.

An important feature of aluminum ions is the slow rate of ligand exchange in and out of the coordination sphere. Ligand exchange rate for Al^{3+} is 10^5-fold slower than that for Mg^{2+} (Martin, 1986). This feature takes on special importance for aluminum toxicity, because the low ligand exchange rate makes aluminum useless as a metal at active sites on proteins and other cellular components. This low rate is partially due to the strict coordinate number 6 for aluminum. The ligand exchange generally occurs by a dissociative mechanism (Burgess, 1978), and the formation of a dissociative intermediate often requires a coordination number higher than 6.

With the complexity of solution and coordination chemistry, relationships between aluminum stress and biological responses have not yet been well established, e.g., the identity of aluminum's

toxic species. Among various aluminum species in solution, free ion Al^{3+} is generally believed to be the active form causing many aluminum effects (Zhang and Colombili, 1989), but aluminum toxicity sometimes can be ascribed to $Al(OH)^{2+}$, $Al(OH)_2^{+}$, or the sum of all mononuclear species activities (Parker et al., 1989). Under certain conditions, polynuclear hydroxy-aluminum is highly toxic (Wagatsuma and Kaneko, 1987). Furthermore, the possibility that certain aluminum-complexing ligands may be responsible for aluminum's adverse effects cannot be excluded. An example is given by aluminum-fluoride complex, which interferes with cellular signal transduction (Chabre, 1990).

Primary Cellular Lesions for Aluminum Toxicity

For plants, aluminum toxicity is a soilborne problem, and the major toxic reaction appears on the root surface (Akeson et al., 1989), where aluminum is taken up. Since the symptoms of aluminum stress in plants are those characteristic of deficiencies of several physiologically important ions including calcium, magnesium and phosphorus , it is generally agreed that aluminum injures plants mainly by interfering with the metabolism of those essential elements (Foy et al., 1978).

In human and animals, the mechanism of aluminum toxicity remains much more obscure. At the cellular level, a variety of organelles like chromatin (Walker et al., 1988), cytoskeleton (Oteiza et al., 1989), mitochondria (Dill et al.,1987) and plasma

membrane (Weis and Haug, 198) have been listed as potential primary injury site(s). At the molecular level, nucleic acids (Karlik et al., 1980), phospholipids (Deleers et al., 1986), polysaccharides (Moreno et al., 1985), and proteins are reported to be vulnerable to aluminum intoxication.

In in vitro experiments, aluminum inhibits various enzymes. In these cases, aluminum may inhibit enzyme through its substitution for physiological factors such as Mg^{2+}, or through its allosteric interaction with enzyme protein. (Macdonald and Martin, 1988). The first known example is hexokinase; the brain isomer is more sensitive to aluminum relative to muscle isomers. The aluminum--induced impairment of cerebral glucose utilization affects particularly the metabolism of acetylcholine and other neurotransmitters, which is typical of diseases associated clinically with dementia (Lai and Blass, 1984).

In the following sections, we will briefly review some current theories regarding the primary cellular lesions of aluminum.

1. Aluminum Interaction with Chromatin

Aluminum is reported to have high affinity to nucleic acid polymers, DNA and RNA. Besides phosphate oxygen, heterocyclic nitrogen and exocyclic carbonyl on purine and pyrimidine bases also provide potential binding sites, despite lower affinity for aluminum (Karlik et al., 1980). Investigations show chromatin being one of the cell structures most vulnerable to aluminum's action.

In experimental aluminum encephalopathies, aluminum accumulates rapidly upon DNA containing structures in the nucleus. and Al/DNA-P ratio in chromatin of the animal was found as high as 1.05% by weight (Crapper et al., 1980).

The interaction of aluminum with genetic machinery has not been investigated in depth. According to very limited information, at the replication level, DNA synthesis in osteoblast-like cells is substantially inhibited by micromolar aluminum, which in turn disturbs bone cell proliferation and differentiation (Kasai et al., 1991,). At the transcription level, the aluminum-induced condensation and aggregation of chromatin may prevent the formation and maintenance of a transcriptionally competent open structures, an important mechanism controlling gene expression, which allows RNA polymerase access to coding region of DNA. Walker et al. (1989) examined divalent and trivalent cations in terms of their ability to cause the compaction of chromatin from rat brain and liver, and found that aluminum, with its large ionic index Z^2/r and high covalent index, was the most reactive. Chromatin treated with aluminum in vivo and in vitro is less sensitive to DNase II digestion (Matsumoto, 1988), and coincidently Alzheimer chromatin was found to be less accessible to digestion by micrococcal nuclease. Employing a quantitative dot blot method, results showed that aluminum indeed had specific depression on some messenger RNA levels, which might be linked to the direct effect of aluminum on the transcription of genes. In aluminum-treated rabbit brain, level of calmodulin mRNA was reduced by 60 -70%, and the same magnitude

of reduction of these messengers was found in Alzheimer's rabbit brain (Crapper Maclachlan, 1989).

The actual binding sites of aluminum on chromatin are not known. One assumption is that aluminum might bind between the linker histones and DNA, based on the fact that dinucleosomes released from aluminum-treated cerebral cortex contained twice the content of linker histone H1 than that from the control (Crapper McLachlan, 1989). A potential site for aluminum's bridge may be provided by coordination at amino acid asp-98 and glu-99 of H1 and DNA phosphate. By anchoring H1 linker histone on DNA, aluminum may prevent the gene expression which only occurs on open euchromatin regions where H1 linker histones are depleted. Alternatively, aluminum may reside on a site on DNA which would be disruptive to the binding of associating cationic proteins (Record et al., 1978). In addition, aluminum may act as counterion to physiological cations, such as Mg^{2+}, Ca^{2+} or Zn^{2+}, required in gene expression, displacing them from their normal binding sites on chromatin (Garnot, 1986).

2. Effect of Aluminum on Cellular Calcium Metabolism

Calcium serves as a second messenger in bioregulation via various intracellular calcium trigger proteins. In response to a large variety of external stimuli, intracellular calcium transients are generated. Within the lifetime of these transients, Ca^{2+} binds to trigger proteins (signal input), causing conformational

changes. These changes play a key role in signal amplification and transmission (signal output) from the trigger protein to respective effector enzymes and structural elements. When Ca^{2+} coupled signal transduction is interrupted, severe repercussions on biological and physiological processes are expected to occur.

As an important biological messenger, Ca^{2+} is subjected to multiple cellular controls. Most cells have the capacity of regulating intracellular Ca^{2+} over a broad range by using diverse transport systems in endoplasmic reticulum, plasma membrane and mitochondria, as well as through Ca^{2+} binding proteins (Putney et al., 1989). Free Ca^{2+} concentration in cytosol thus reflects a balance between influx, efflux, and intracellular exchange and redistribution (Login et al., 1987).

It has been known that aluminum stress on plants always results in an interference with cellular Ca^{2+} metabolism (Zhao et al., 1987). In recent years, increasing evidence has emerged that Ca^{2+} regulation may also be a target for aluminum intoxication in animal cells. Application of aluminum to osteoblast-like cells inhibits Ca^{2+} accumulation in the cell matrix, which may underlie the development of aluminum-induced osteomalacia in certain patients (Ikeda et al., 1986). In laboratory rats, aluminum overload decreases sacroplasmic reticulum Ca^{2+} transport (Levine et al., 1990). Perturbation of free Ca^{2+} transients by aluminum was also reported in phenylephrine-stimulated hepatocytes (Scuofl et al., 1990).

One possible way by which aluminum manipulates intracellular Ca^{2+} metabolism is involved in the interaction of aluminum with intracellular Ca^{2+} regulator proteins. A well known example is calmodulin, which mediates a multitude of Ca^{2+}-dependent biochemical processes (Siegel and Haug, 1983). Calmodulin has a profound tendency to bind 4 Ca^{2+} in specific loci known as EF hands. As first two Ca^{2+} bind to the high-affinity binding sites III and IV, the protein undergoes conformational changes which expose a hydrophobic region serving as an interface for the interaction between calmodulin and target proteins. Aluminum is able to bind to calmudulin stoichiometrically at a molar ratio of 3:1. When bound on the protein, aluminum triggers a helix-coil transition concomitant with an increase in topographic surface (Yuan and Haug, 1988). The induced geometric rearrangement of calmodulin severely antagonizes its activity to stimulate effector proteins like calmodulin-dependent protein kinase which, in turn, controls Ca^{2+} channels on sarcoplasmic reticulum (Gasser et al., 1988).

In a newly-proposed approach, aluminum is suggested to downregulate intracellular Ca^{2+} through phosphoinositide signal transduction (Birchall and Chappell, 1988), in which second messenger molecule Ins(1,4,5)P^3, IP_3, is generated to signal Ca^{2+} release from intracellular stores (Berridge, 1983). Moreover, IP_3, together with its phosphorylation product Ins(1,3,4,5)P_4, presumably controls the entry of external

Ca^{2+} through second messenger-operated channels on the plasma membrane (Berridge and Irvine, 1989). This mechanism will be discussed in detail in later sections.

3. Substitution of aluminum for Mg^{2+}

A prevailing hypothesis regarding aluminum intoxication emphasizes the element's substitution for magnesium bound on crucial cellular components (Kraal et al., 1990). As a regulator in various biochemical processes, divalent cation Mg^{2+} is required for the functions of numerous enzymes and the maintenance of chromatin conformation (Wadrer 1980).

Al^{3+}/Mg^{2+} substitution theory has its solid chemical underpinning. It is known that size similarity, rather than charge identity, plays a key role in permitting metal ion substitution (Garnot, 1986). The ionic radii of Al^{3+} most closely resemble those of Mg^{2+}. In sixfold coordination, the radius is 0.54 A for Al^{3+} and 0.72 A for Mg^{2+} (MacDonald and Martin, 1988), respectively. With a slightly smaller ionic volume but much stronger ionic index, free Al^{3+} ion has enhanced association constants with many ligands, and is able to compete effectively for Mg^{2+} on binding sites in biological systems, even at Mg^{2+} molar concentrations 10^{7-8} fold higher than Al^{3+} (Miller et al., 1989).

In many cases of aluminum-mediated enzyme inhibition, replacement of aluminum for Mg^{2+} is implicated (MacDonald and

Martin, 1988). The Mg^{2+}-mediated enzymes vulnerable to aluminum include those involved in energy metabolism like hexokinase, glucose-6-phosphate dehydrogenase (Cho and Joshi, 1989), those involved in phosphate transfer reactions like 3',5'-cyclic nucleotide phosphodiesterase, acidic and alkaline phosphatases adenylate cyclase, and several carboxyl acid esterases like acetylcholine esterase (Macdonald and Martin, 1988).

The fundamental biochemical lesion effected by Al^{3+}/Mg^{2+} substitution is illustrated by aluminum's interaction with tubulin (Macdonald et al, 1987). Mg^{2+}, as the physiological mediator for assembly of tubulin, is thought to bind at the exchangeable guanine nucleotide (GTP or GDP) binding site (E site) of the protein. After the polymerization of Mg^{2+}-GTP bound tubulin monomers into microtubules, the bound GTP is hydrolyzed to GDP and dissociated from the tubulin, leading to the next cycle of microtubule assembly. Aluminum ion Al^{3+} at subnanomolar concentration competes effectively for E site with Mg^{2+} at 1 mM. Because of the extremely slow ligand exchange rate of Al^{3+}, the hydrolysis and dissociation of GTP is inhibited on Al^{3+}-bound GTP-tubulin, leading to aberrant microtubule assembly and disassembly.

4. Perturbation of Aluminum on Plasma Membrane

Plasma membranes manifest aluminum toxicity in two ways: serving as a primary lesion site or as a control of the access of

aluminum to intracellular targets. In either case, interaction of aluminum with plasma membrane would be an initial stage in aluminum intoxication.

Many components of plasma membrane may serve as targets for aluminum, but polar phospholipids are likely the prime candidates. The negatively charged phospholipids, phosphatidylserine (PS) and phosphatidylinositol (PI) especially have high affinities for aluminum binding, but they are mainly located on the cytoplasmic side of the plasma membrane. On the extracellular side, polar head regions of zwitterionic phospholipids, e.g., phosphatidylcholine (PC) and phosphatidylethanolamine (PE), are attractive ligands for aluminum binding. Such binding may cause drastical changes in membrane surface charge density and transmembrane potential (Akeson et al., 1989). With this electrostatic interaction, aluminum was reported to inhibit voltage gating of VADC channel on mitochondrial outer membrane by neutralizing the channel's sensor responsible for voltage dependence (Dill et al., 1987).

Aluminum crosslinking of the polar regions at the membrane surface was found to be translated deeply into the internal nonpolar regions, inducing a membrane phase separation, aggregation and membrane fusion (Deleers et al., 1985, Deleers et al., 1986). In human erythrocytes, the association of aluminum with plasma membranes results in an increased lipid order parameter and phase transition temperature, indicative of more rigid lipid packing (Weis and Haug, 1989). Such imposed changes in membrane structure and physical properties will influence membrane functions like

permeability. Zhao et al.,(1987) demonstrated that the perturbation of bulk lipid matrix, upon aluminum application, led to enhanced non-electrolyte transport across plasma membranes. In addition, the activity of some membrane-bound proteins might be also modified by the aluminum-induced changes in a lipid environment, particularly in the boundary lipid area. For instance, inhibition of membrane-bound K^+-ATPase by aluminum was found to correlate with the aluminum-induced decrease in membrane fluidity (Suhayda and Haug, 1986).

An interesting research area is the effect of aluminum on membrane lipid peroxidation, which is believed to be a culprit causing cellular aging. In vivo, the production of 2-thiobarbituric acid reactive substances (TBARS) was enhanced in brain and liver of mice after dietary aluminum intoxication (Fraga et al., 1990). In in in vitro experiments, aluminum was shown to facilitate iron-dependent peroxidation in erythrocyte membrane and liver microsomes (Quinlan et al., 1988). Due to its electronic configuration, aluminum is not able to interact directly with oxidative free radicals, therefore the observed acceleration of aluminum on lipid peroxidation more likely results from its interaction with lipid substrates. One interpretation is that binding of aluminum on membrane may cause a rearrangement of membrane phospholipid molecules, which renders lipids more accessible to the attack of free radicals (Fraga et al., 1990).

Aluminum Uptake and Intracellular Distribution

Since aluminum apparently does not have physiological importance, it is unlikely that there are specific cellular transport device for its entry. A major criticism of the aluminum hypothesis in neurodegenerative disorders is the postulated relative inaccessibility of the element. However, abnormally high accumulation of aluminum in the CNS argues against this notion. Because CNS neural cells are terminally differentiated, the aluminum transported to these cells will be accumulated unless specific systems are available to remove them. This is different from other tissues which have a set turnover rate, and thus aluminum accumulation over time would be less profound (Roskama and Connor, 1990).

In postmortem brain samples from patients with dialysis encephalopathy, aluminum concentration ranges from 100 - 800 uM (Garnot, 1986). In experimental intoxication, total brain aluminum concentration average about 100 uM and may reach 400 uM. Because of its nonuniform accumulation in different neurons, in vivo levels of aluminum in some neuronal populations may greatly exceed the 100 uM average (Nixon et al., 1990). Human neuroblastoma cells (IMR-32) were shown to accumulate 10-20 mM aluminum against 100 uM aluminum in the medium (Guy et al., 1990). The intracellular aluminum concentrations within this range were found in tangle-bearing

neurons of Guamanian patients with amyotropic lateral sclerosis or Parkinson's disease (Perl and Good, 1987).

How does aluminum enter mammalian cells? With limited experimental data, it is generally believed that mononuclear forms of aluminum are responsible for its transport across the plasma membrane. The hydrocarbon interior of the lipid membrane is not permeable to these aluminum ions, but the ionophoretic capacity of phospholipids may provide a means to translocate aluminum, e.g., by forming non-bilayer configurations like reversed vehicles or H_{II}. To illustrate, Al^{3+} adsorption by phosphatidylcholine was reportedly involved in aluminum uptake into cytoplasm (Akeson et al., 1989). In living cells, aluminum ions especially Al^{3+} is likely able to take advantage of co-transport or nonspecific transport machineries for metal cations.

In search of possible carriers for cellular uptake of aluminum, investigations have been focussed on two types of biological molecules: transporting protein, i.e., transferrin, and low molecular weight metabolites with capacity of chelating aluminum. Based on chemical study, the small aluminum-chelating metabolites like citrate have been suggested to provide an effective means for aluminum transport into cells (Martin, 1986). However, in most experiments, these little aluminum-chelating agents virtually protected animals and their cells by preventing aluminum internalization (Domingo et al., 1988, Guy et al., 1990). On the other hands, transferrin has been implicated in facilitating aluminum uptake by various mammalian cells including human

neuroblastoma cells (Morris et al., 1987) and cells in CNS (Rosskama and Connor, 1990), presumably through a transferrin receptor-mediated process.

Since it probably cannot be used physiologically, intracellular aluminum will possibly be bound on sites that are stronger than cytosolic pool chelators. At slightly acidic intracellular pH, at which cationic aluminum species are present, the prime candidates are membrane lipophosphates and phosphorylated proteins (Birchall and Chappell, 1988). The existence of such strong intracellular chelating pools for aluminum can partially explain how mammalian cells are able to establish high aluminum contents against low extracellular aluminum concentration.

Phosphoinositide Signal Transduction

Phosphoinositide signal transduction is a ubiquitous second messenger system in eukaryotic cells to regulate a large array of cellular processes including metabolism, secretion, contraction, neural activity and cell proliferation (Berridge and Irvine, 1989). In analogy with cAMP second messenger system, phosphoinositide signalling pathway consists of three components, viz., receptors, guanine nucleotide binding protein (Gp protein) and phospholipase C, residing in the plasma membrane. In neuronal cells, receptors on the cell surface detect extracellular stimuli like hormones or neurotransmitters, and transfer the signals to Gp protein. The activated G protein in turn triggers effector enzyme phospholipase

C, and the later cleaves phosphatidylinositol 4,5-biphosphate ($PtdIns(4,5)P_2$) into inositol 1,4,5 -triphosphate (IP_3) and diacylglycerol, which mobilizes intracellular Ca^{2+} or activates protein kinase C, respectively (Berridge, 1987).

In the last decade, a number of signal-mediating G proteins have been identified by the combination of classical biochemistry and DNA recombination technique. They are all heterotrimeric molecules, consisting of a distinct α subunit and identical β and γ subunits (Birnbaumer et al., 1990). α Subunit contains a high-affinity guanine nucleotide binding site and at least one high-affinity Mg^{2+} binding site. So far nine genes encoding α subunits have been identified, and 12 polypeptide products of these genes are known to be implicated in the activities (Freissmuth et al., 1989). The molecular process of G protein activation is briefly as following: after receiving the signal from the cell surface receptor, the G protein undergoes conformational change which facilitates the exchange of bound GDP for GTP, followed by dissociation of α subunit from $\beta\gamma$ subunits. After this dissociation, the GTP-bound α subunit becomes functional, its catalyzing center on the subunit activates phospholipase C. Concomitantly, GTPase activity of subunit hydrolyses the bound GTP, leading to association of α and $\beta\gamma$ subunits and inactivation of G_p protein (Freissmuth et al., 1989).

G protein was originally believed to be a ras oncogene product (Wakelam et al., 1986), since expression of $p21^{N\text{-}ras}$ in 3T3 cells responding to stimulus by growth factors led to a large increase in

inositol phosphate formation. Now it is known that there is a subset of "little" monomer GTP binding proteins with molecular masses 20-25 kDa. They include many factors controlling protein synthesis like the elongation factor, EF-Tu, and ras, rho, ral and rac gene products (Nozawa et al., 1991).

There is a multiplicity of phospholipases C (PLC) in mammalian tissues (Rhee et al., 1989). Four types of PLC isomers, assigned as α, β, γ and δ, have been identified. In cultured neuroblastoma cells, the major isomer is PLC_{r1}, accounting for 99% of total PLC activity. Cloning of the four types of PLC isoenzymes has revealed a surprisingly low degree of similarity in their primary structure, suggesting different roles and regulatory properties (Vicenti and Cattaneo, 1991). The activities of these PLC isomers are distinct in their respective compartmentation, substrate specificity and ligand requirement. The soluble phospholipase C apparently uses only PI as substrate, and is not able to reach the hormone-sensitive phosphoinositide pool residing in plasma membrane, while the Gp protein-mediated membrane-bound PLC activity is seemingly more specific to agonist-sensitive PIP and PIP_2 (Cockcroft, 1987). The PLC activity can also be activated directly by intracellular Ca^{2+} of increasing concentrations, bypassing receptor stimulation and Gp protein mediation (Cradle and Crews, 1990).

Phosphoinositide hydrolysis is followed by the extremely complicated inositol phosphate metabolism. In a bewildering array of phosphorylation and dephosphorylation reactions, dozens of

isomers of inositol mono-, bi-, tri-, tetraki-, penta-, hexaphosphates as well as cyclic derivatives are produced (Putney et al., 1989). Among them, only Ins(1,4,5)P_3 is firmly established as the primary signal to intracellular Ca^{2+} mobilization. It interacts with receptors on the endoplasmic reticulum and sarcoplasmic reticulum, and triggers the opening of Ca^{2+} channels on these organellar membranes, resulting in Ca^{2+} efflux from these intracellular stores. The depletion of IP_3-sensitive intracellular Ca^{2+} pools, in turn, signals Ca^{2+} entry mechanism, and extracellular Ca^{2+} is allowed to enter to refill the depleted Ca^{2+} pools (Berridge and Irvine, 1989).

Activation of Fluoroaluminate on Phosphoinositide Signal Transduction

Fluoride anions (F^-) have long been known to stimulate G protein-coupled transmembrane signalling. This activation process was later revealed to be dependent on trace amounts of aluminum (Sternweis and Gilman, 1982). In fluoride solutions, aluminum is able to form various soluble ionic complexes AlF_x^{x-3} (where x = 1 - 6) whose stoichiometry depends on the excess concentration of fluoride. These aluminum-fluoride complexes, most likely AlF_4^-, are proposed to stimulate G protein by acting as analogues of the terminal phosphate of GTP (Fain et al., 1988).

On the atomic and molecular bases, there are close similarities between aluminofluoride complex AlF_4^- and phosphate group PO_4^{3-}: here fluorine compares to oxygen, and aluminum to phosphorus. With the same size and valence orbitals as oxygen, fluorine has also the very strong electronegativity and thus a great capacity of forming hydrogen bonds. Fluorine in an ionic complex tends to bind to a hydrogen bond donor group on a protein. Moreover, an O-H..F is just slightly longer than O-H..O, and N-H..F and N-H..O are exactly in the same bond length. Like phosphorus, aluminum has coordinate number of 1 - 6, due to the possible hybridization of its outer shell 3p electrons with 3d orbitals. Furthermore, Al-F bond in aluminofluoride has the same length as a P-O bond in phosphate.

Because of these resemblances, Gp protein may erroneously take aluminofluoride as phosphate group. According to Chabre's model (Chabre, 1990), in a GTP-binding protein whose nucleotide site already contains a GDP, presumably AlF_4^- is tetrahedrally bound to four fluorides which are hydrogen-bound on the protein at or near the nucleotide site, then AlF_4^- exchanges one of its fluorides by binding ionically to the terminal oxygen of -phosphate of the bound GDP. However, unlike r-phosphate of GTP, the aluminofluoride bound to the GDP can not form the pentacoordinated bipyramidal structure which is required for GTP hydrolysis, thus it locks the catalytic center of G protein in the activated tetrahedral configuration. In other words, upon binding of aluminofluoride, G proteins are blocked at the active state as

with bound non-hydrolyzable GTP analogue GTP[S]. The similar structure changes in G proteins modified by aluminofluoride or by GTP[S] were reconsidered (Higashijima et al., 1987)

Objectives: Possible Impact of Aluminum on Phosphoinositide Signal Transduction and Cellular uptake of Aluminum.

Taken together, although knowledge has been built regarding the development of aluminum toxicity syndrome in human and animals, scant information is available on cellular and molecular mechanisms associated with aluminum intoxication. Fundamental questions that must be resolved are those of aluminum-caused primary cellular lesion(s) and aluminum uptake across the plasma membrane. The possible impact of aluminum on phosphoinositide signal transduction might be related to aluminum-caused neurodiorders. Furthermore, based in part on findings (Shi and Haug, 1988) in our laboratory we are therefore advancing the hypothesis that aluminum uptake by intact cells is dependent on medium pH and may also be interriorized by certain types of carrier-mediated mechanisms. To test these hypotheses I propose to pursue the following objectives:

OBJECTIVE I: Determine the effect of aluminum on inositol phosphate formation in phosphoinositide signal transduction pathway.

OBJECTIVE II: Determine aluminum uptake by viable neuroblastoma cells, by varying medium pH and employing potential carriers.

All experiments will be carried out on non-differential murine neuroblastoma cells, C1300, clone neuro-2A.

RATIONAL as to objective I:

1). Aluminum toxicity has been implicated in a broad spectrum of physiological disorders. This led to a proposal that aluminum's toxicity is a multigene-controlled syndrome. The ability of aluminum to bind nonspecifically to different cellular components offers the element opportunities to affect various cellular reactions (Ganrot, 1986). However, it is also possible that a group of these disorders originates from a single primary cellular lesion: aluminum interacts with a key target which is critical in cellular metabolism. What, at present, appear to be pleiotropic aluminum effects in mammalian cells, may in the end prove to emerge from a basic, underlying molecular mechanism. Phosphoinositide signal transduction could be one of such targets, because it is a ubiquitous system in eukaryotic cells to regulate many important cellular processes.

2). A major consequence of aluminum intoxication is the interference with cellular Ca^{2+} metabolism, which is known to be partially controlled by phosphoinositide signal transduction. Aluminum generally perturbs intracellular Ca^{2+} metabolism in an

inhibitory manner. This fact suggests that, apart from the activation mode in the presence of fluoride, aluminum may downregulate intracellular Ca^{2+} through signal transduction with a distinct mechanism.

3). Experimentally, aluminum has been reported to inhibit a number of signal-mediating G proteins like transducin in retinal rod outer segments (Miller et al., 1989), and G_s/G_i in cAMP signalling pathway (Mansour et al., 1983, Johnson, 1988,).

4). A principal mechanism toxicity expression is believed to be substitution by aluminum for Mg^{2+} at critical cellular site(s), and Mg^{2+} is a physiological ligand in G_p protein-coupled phosphoinositide signalling process. The replacement of Mg^{2+} by aluminum at the nucleotide binding center on Gp protein may result in the inactivation of Gp protein.

5). Aluminum is expected to be bound on vicinal phosphate groups on phosphoinositide in particular PIP_2 (Birchall and Chappel, 1989), leading to a depletion of hydrolyzable substrate pools. Alternately, aluminum may bind to IP_3 (Schofl et al., 1990), thereby altering IP_3 metabolic fate and/or IP_3 binding affinity to its receptor.

6). Finally, all key components of phosphoinositide signal transduction, i.e., receptors, G_p protein and phospholipase C, are residing in plasma membrane. Therefore, the perturbance of the membrane properties by aluminum may indirectly affect the phosphoinositide metabolism.

LIST OF REFERENCES

Akeson M.A., and Munns D.N. (1989) Lipid bilayer permeation by neutral citrate and by three hydroxy carboxylic acids. Biochim. Biophys. Acta. 984, 200-206.

Akeson M.A., Munns D.N. and Burau R.G. (1989) Adsorption of Al^{3+} to phosphatidylcholine vesicles. Biochim. Biophys. Acta. 986, 33-40.

Baes C.F. and Mesmer R.E. (1976) The Hydrolysis of Cations, pp. 112-113. J. Wiley & Sons, New York.

Berridge M.J., Dawson R.M.C., Downes C.P. and Irvine R.F. (1983) Changes in the levels of inositol phosphates after agonist -dependent hydrolysis of membrane phosphoinositides. Biochem. J. 212, 473-482.

Berridge M.J. (1987) Inositol triphosphate and diacylglycerol: two interacting second messengers. Annu. Rev. Biochem. 56, 159-193.

Berridge M.J. and Irvine R.F. (1989) Inositol phosphates and cell signalling. Nature. 341, 197-205.

Birchall J.D and Chappell J.S. (1988) Aluminium, chemical physiology, and Alzheimer's disease. The Lancet, Oct. 29, ii: 1008-1010.

Birnbaumer L., Abramowitz J. and Brown A.M. (1990) Receptor-effector coupling by G protein. Biochim. Biophys. Acta. 1031, 163-224.

Burgess, (1978) Chapter II, Kinetics and mechanisms: solvent exchange. In Metal Ions in Solution, pp 310-348

Chabre M. (1990) Aluminofluoride and beryllofluoride complexes: new phosphate analogs in enzymology. TIBS. 15, 6-10

Cho S.W. and Joshi J.G. (1989) Time-dependent inactivation of glucose-6-phosphate dehydrogenase from yeast by aluminum. Toxicol. Lett. 47, 215-219.

Cochran M., Coates J. and Neoh S. (1884) The competitive equilibrium between aluminum and ferric ions for the binding sites of transferrin. FEBS Lett. 176, 129-132.

Cockcroft S. (1987) Polyphosphoinositide phosphodiesterase: regulation by a novel guanine nucleotide binding protein, G_p. Trends Biochem. Sci. 2, 75-78.

Cotton F.A. and Wilkinson G. (1962) In Advanced Inorganic Chemistry. John Wiley & Sons.

Cradle L.J. and Crews F.T. (1990) Calcium- versus G protein-mediated phosphoinositide hydrolysis in rat cerebral cortical synaptoneurosomes. J. Neurochem. 55, 1022-1030.

Crapper Mclachlan D.R. (1989) Aluminum neurotoxicity: criteria for assigning a role in Alzheimer's disease, in Environmental Chemistry and Toxicology of Aluminum (Lewis T.E. ed), pp 299-315. Lewis Publ., Boca Raton, FL.

Crapper D.R., Quittkat S., Krishman S.S., Dalton A.J. and Deboni U. (1980) Intranuclear aluminum concert in Alzheimer's disease, dialysis encephalopathy, and experimental aluminum encephalopathy. Acta Neuropathol. 50, 19-24.

Deleers M., Servais J-P. and Wulfert E. (1985) Micromolar concentration of Al^{3+} induced phase separation, aggregation and dye release in phosphatidylserine-containing vesicles. Biochim. Biophys. Acta. 813, 195-200.

Deleers M., Servais J-P. and Wulfert E. (1986) Neurotoxic cations induce membrane rigidification and membrane fusion at micromolar concentrations. Biochim. Biophys. Acta. 855, 271-276.

Dill E.T., Holden M.J. and Colombini M. (1987) Voltage gating in VDAC is markedly inhibited by micromolar quantities of aluminum. J. Membrane Biol. 99, 187-196.

Domingo J.L., Gomes M., and Liobet J.M. (1988) Citric, malic and succinic acids as possible alternatives to deferroxamine in aluminum toxicity. Clin. Toxicol. 26, 67-79.

Fain J.N., Wallace M.A. and Wojcikiewicz R.J.H. (1988) Evidence for involvement of guanine nucleotide-binding regulatory proteins in the activation of phospholipases by hormones. FASEB J. 2, 2569-2574.

Fraga C.G., Oteiza P.I., Golub M.S., Gershwin M.E. and Keen C.L. (1990) Effects of aluminum on brain lipid peroxidation. Toxicol. Lett. 51, 213-219.

Freissmuth M., Casey, P.J. and Gilman A.G. (1989) G protein control diverse pathway of transmembrane signaling. FASEB J. 3, 2125-2131.

Foy C.C., Chaney R.L. and White M.C. (1978) The physiology of metal toxicity in plants. Ann. Rev. Plant Physiol. 29, 511-566.

Ganrot P.O. (1986) Metabolism and possible health effects of aluminum. Environm. Health Perspect. 65, 363-441.

Gasser J., Paganetti P. Carafoli E. and Chiesi. (1988) Heterogeneous distribution of calmodulin- and cAMP-dependent regulation of Ca^{2+} uptake in cardiac sarcoplasmic reticulum subfractions. Eur. J. Biochem. 176, 535.

Godbold D.L., Fritz E. and Huttermann A. (1988) Aluminum toxicity and forest decline. Proc. Natl. Acad. Sci. USA. 85, 3888-3892.

Guy S.P. Seabright P. and Itzhaki R.F. (1990) Uptake of aluminum by human neuroblastoma cells. J. Trace Elem. Electrolytes Health Dis. 4, 183-187.

Hartwell B.L. and Pember F.R. (1918) The presence of aluminum as a reason for the difference in the effect of so-called acid soil on barley and rye. Soil Sci. 6, 259-279.

Higashijima T., Ferguson K.M., Sternweis P.C., Ross E.M., Smigel M.D. and Gilman A.G. (1987) The effect of activating ligands on the intrinsic fluorescence of guanine nucleotide-binding regulatory proteins. J. Biol. Chem. 262, 752-756.

Hirano. A., Donnenfield H., Sasaki. S. and Nakano I. (1984) Fine structural observations of neurofilamentous changes in amyotrophic lateral sclerosis. J. Neuropathol. Exp. Neurol. 43, 461-470.

Hirsch E.C., Brandel J.-P., Galle F., Javoy-Agid F. and Agid Y. (1991) Iron and aluminum increase in the substantia nigra of patients with Parkinson's disease: an X-ray microanalysis. J. Neurochem. 56, 446-451.

Ikeda et al., (1986) Calif. Tissue Internat. 39, 319-323

Johnson G.V.W. (1988) The effects of aluminum on agonist-induced alterations in cyclic AMP and cyclic GMP concentrations in rat brain regions in vivo. Toxicol. 51, 299-308.

Karlic S.J., Eichhorn G.l. and Crapper Mclachlan D.R. (1988) Molecular interactions of aluminum with DNA. Neurotoxicol. 1, 83-88.

Kasai K., Hori, M.T. and Goodman W.G. (1991) Transferrin enhances the antiproliferative effect of aluminum on osteoblast-like cells. Am. J. Physiol. 260, E537-E543.

Klanzo I., Wisiniewski H. and Streicher E. (1965) Experimental production of neurofibrillary degeneration. J. Neuropathol. Exp. Neurol. 24, 187-199

Kraal B., de Graaf J.M., Mesters J.R., van Hoof P.M., Jacquet E. and Parmeggiani A. (1990) Fluoroaluminates do not affect the guanine- nucleotide binding centre of the peptide chain elongation factor EF-Tu. Eur. J. Biochem. 192, 305-309.

Lai J.C.K. and Blass J.B. (1984) Inhibition of brain glycolysis by aluminum. J. Neurochem. 42, 438-446.

Levine S.N., Sonnier G.B. and Abreo K. (1990) Effect of diabetes mellitus and aluminum toxicity on myocardial calcium transport. Toxicol. 65, 137-148.

Liss L., Long J. and Thornton D. (1989) Aluminum neurotoxicity, Alzheimer disease, and alcoholic encephalopathy. In Environmental Chemistry and Toxicology of Aluminum (Lewis T.E., ed) pp 317-325. Lewis Publ., Boca Raton, FL.

London G.M., de Vernejoul M.C., Fabiani F., Marchais S., Guerin A., Metivier F., Chappuis P. and Lilsch F. (1989) Association between aluminum accumulation and cardiac hypertrophy in hemodialyzed patients. Am. J. Kidney Dis. 13, 75

Login I.S., Judd A.M. and Macleod M. (1987) Activation of calcium channel by maitotoxin. Meth. Enzymol. 141, 63-79.

Macdonald T.L. and Martin R.B. (1988) Aluminum ion in biological system. Trends Biochem. Sci. 13, 15-19.

Macdonald T.L., Humphreys W.G. and Martin R.B. (1987) promotion of tubulin assembly by aluminum ions in vitro. Science. 236, 183-186.

Mansour J.M., Ehrlich A. and Mansour T.E. (1983) The dual effects of aluminum as activator and inhibitor of adenylate cyclase in the liver fluke Fasciola hepatica. Biochem. Biophys. Res. Comm. 112, 11-918.

Martell A.E. and Motekaitis R.J. (1989) Coordination chemistry and speciation of Al(III) in aqueous solution, in Environmental Chemistry and Toxicology of Aluminum (Lewis T.E., ed), pp. 3-17. Lewis Publ., Boca Raton, FL.

Martin R.B. (1986) The chemistry of aluminum as related to biology and medicine. Clin. Chem. 32, 1797-1806.

Matsumoto H. (1988) Changes of the structure of pea chromatin by aluminum. Plant Cell Physiol. 29, 281-287.

Mildevin A.S. and Loeb L.A. (1981) In Metal Ions in Genetic Information Transfer. (Eichhorn G.L. and Marzilli L.G. eds) pp. 103-123, Elsevier/North-Holland, New York.

Miller J.L., Hubbard C.M., Litman B.J. and Macdonald T.L. (1989) Inhibition of transducin activation and guanosine triphosphatase activity by aluminum ion. J. Biol. Chem. 264, 243-250.

Moreno C., Lifely M.R. and Esdaile J. (1985) Effect of aluminum ions on chemical and immunological properties of meningococcal group B polysaccharide. Infection and Immunity. 49, 587-592.

Morimura S. and Matsumoto H. (1978) Effect af aluminum on some properties and template activity of purified pea DNA. Plant Cell Physiol. 19, 429-436.

Morris C.M., Candy J.M., Court J.A., Whitford C.A. and Edwardson J.A. (1987) The role of transferrin in the uptake of aluminum and manganese by the IMR-32 neuroblastoma cell line. TIBS. 15, 498.

Martyn C.N., Barker D.J.P., Osmond C., Harris E.C., Edwardson J.A. and Lacey R.F. (1989) Geographical relation between Alzheimer's disease and aluminum in drinking water. Lancet. i, 59.

Nixon R.A., Clarke J.F., Logvinenko K.B., Tan M.K.H., Hoult M. and Grynspan F. (1990) Aluminum inhibits calpain-mediated proteolysis and induced human neurofilament proteins to form protease-resistant high molecular weight complexes. J. Neurochem. 55, 1950-1959.

Nordstroem D.K and May H.M. (1989) Chapter 2, Aqueous equilibrium data for mononuclear aluminum species. In Environ. Chem. of Aluminum (Sposito G. ed), pp 29-53. CRC Press, Boca Raton, FL.

Nozawa Y., Nakashima S. and Nagata K. (1991) Phospholipid-mediated signaling in receptor activation of human platelets. Biochim. Biophys. Acta. 1082, 219-238.

Osmond C.B., Bjorkman O. and Anderson D.J. (1980) In Physiological Processes in Plant Ecology. Springer-Verlag, Berlin.

Oteiza P.I., Golub M.S., Gershwin M.E., Donald J.M. and Keen C.L. (1989) The influence of high dietary aluminum on brain microtubule polymerization in mice. Toxicol. Lett. 47, 279-285.

Parker D.R., Zelany L.W. and Kinraide T.B. (1989) Chemical speciation and plant toxicity of aqueous aluminum. In Environmental Chemistry and Toxicology of Aluminum (Lewis T.E., ed), pp. 299-315. Lewis Publ., Boca Raton, FL.

Perl D.P. and Good P.F. (1987) The association of aluminum. Alzheimer's disease, and neurofibrillary tangles. J. Neurol. Transm. 24, 205-211.

Putney J.W., Takemura H., Hughes. A.R., Horstman D.A. and Thastrup O. (1989) How do inositol phosphates regulate calcium signaling? FASEB J. 3, 1899-1905.

Quinlan G.J., Halliwei B., Moorhouse C.P. and Gutteridge J.M.C. (1988) Action of lead(II) and aluminum(III) ions-stimulated lipid peroxidation in liposomes, erythrocytes and rat liver microsomal fractions. Biochim. Biophys. Acta. 962, 196-200.

Rhee S.G., Kim H., Suh P.G. and Choi W.C. (1991) Multiple forms of phosphoinositide-specific phospholipase C and different modes of activation. Biochem. Soc. Trans. 19, 337-341.

Record M.T.Jr., Anderson C.F. and Lohman T.M. (1978) Q. Rev. Biophys. 2, 103-178.

Rockams A.J. and Connor J.R. (1990) Aluminum access to the brain: A role for transferrin and its receptor. Proc. Natl. Acad. Sci. USA. 87, 9024-9027

Savoryet al., 1985, Clin. Endocrinol. Metab. 14, 681-702.

Schofl C., Sanchez-Bueuo A., Dixon C.J., Woods N.M., Lee J.A.C., Cuthbertson S.R., Cobbold P.H. and Birchall J.D. (1990) Aluminum perturbs oscillatory phosphoinositide-mediated calcium signalling in hormone-stimulated hepatocytes. Biochem. J. 269, 547-550.

Selkoe D.J., Liem R.K.H., Yen S.-H. and Shelanski M.L. (1979) Biological and immunological characterization of neurofibrillary degeneration by aluminum. Brain Res. 163, 235-252.

Shears S.B., Dawson., Loomis-Husselbee J.W. and Cullen P.J. (1990) The perturbation, by aluminum of receptor-generated calcium transients in hepatocytes is not due to effects of Ins(1,4,5)P_3--stimulated Ca^{2+} release or Ins(1,4,5)P_3 metabolism by the 5-phosphatase and 3-kinase. J. Biol. Chem. 270, 837.

Shi B. and Haug A. (1988) Uptake of aluminum by lipid vesicles. Toxicol. Environm. Chem. 17, 337-349.

Shortle W.C. and Smith K.T. (1988) Aluminum-induced calcium deficiency syndrome in declining red spruce. Science. 240, 1017-1018.

Siegel N. and Haug A. (1983) Aluminum interaction with calmodulin: evidence for altered structure and function from optical and enzymatic studies. Biochim. Biophys. Acta. 744, 36-45.

Sternweis P.C., and Gilman A.G (1982) Aluminum: a requirement for activation of the regulatory component of adenylate cyclase by fluoride. Proc. Natl. Acad. Sci. USA. 79, 4888-4891.

Suhayda C.G. and Haug. A. (1986) Organic acids reduce aluminum toxicity in maize root membrane. Physiol. Plantarum. 68, 189-195.

Terry R.D. and Pena C. (1965) Experimental production of neuro--fibrillary degeneration. 2. Electronmicroscopy, phosphatase histochemistry, and electron probe analysis. J. Neuropathol. Exp. Neuro. 24, 200-210.

Troncoso J.C., Hoffman P.N., Griffin J.W., Hess-Koslow K.M. and Price D.L. (1985) Aluminum neurotoxicity: a disorder of neurofilament transport in motor neurons. Brain Res., 342, 172-175

Vicentini L.M. and Cattaneo M.G. (1991) Are the multiple phospholipases C related by more than one mechanism? Pharmacological Res. 24, 1-4.

Wagatsuma T. and Kaneko M. (1987) High toxicity of hydroxy-aluminum polymer ions to plant roots. Soil Sci. Plant Nutr,. 33, 57-67

Walker P.R. LeBlanc J. and Sikorska M. (1989) Effect of aluminum and other cations on the structure of brain and liver chromatin. Biochem. 28, 3911- 3915.

Weis C. and Haug A. (1989) Aluminum-altered membrane dynamics in human red blood cell white ghosts. Thrombosis Res. 54, 141-149.

Winniewski H.M. Sturman J.A. and Shek J.W. (1980) aluminum chroride- induced neurofibrillary changes in the developing rabbit: a chronic animal model. (1980) Ann. Neuropathol. 8, 479-490.

Woolfitt A.R., Kellett G.L. and Hoggett J. G. (1988) Synergistic binding of glucose and aluminum-ATP to hexokinase from Saccharomyces cerevisiae. Biochim. Biophys. Acta. 955, 346-351.

Wuller L. and Wilhelm M. (1987) Uptake and distribution of aluminum in rat hepatocytes and its effect on enzyme leakage and lactate formation. Toxicol. 44, 203-212.

Yuan S. and Haug A. (1988) Frictional resistance to motions of bimane-labelled spinach calmodulin in responce to ligand binding. FEBS Lett. 234, 218-223.

Zhang D.W. and Colombini M. (1989) Inhibition by aluminum hydroxide of the voltage-dependent closure of the mitochondrial channel, VDAC. Biochim. Biophys. Acta. 991, 68-78.

Zhao X.J., Sucoff E. and Stadelmann J. (1987) Al^{3+} and Ca^{2+} alteration of membrane permeability of Quercus rubra root cortex cells. Plant Physiol. 83, 159-162.

CHAPTER II

ALUMINUM INTERFERES WITH INOSITOL PHOSPHATE PRODUCTION BY MURINE NEUROBLASTOMA CELLS

ABSTRACT

The effects of aluminum on inositol phosphate formation were examined in murine neuroblastoma N_2A cells labelled with [^{3}H]myo-inositol. In intact cells, aluminum reduced fluoride-induced inositol phosphate formation in a dose-dependent manner. In digitonin-permeabilized cells, GTP[S]-stimulated inositol phosphate formation was inhibited with increasing aluminum doses in a biphasic manner with an IC_{50} value of 20 uM. At 50 uM aluminum, the inositol phosphate level was reduced by about 2.5 - 3 fold. The inhibitory effect of aluminum (50 uM) could not be reversed by increasing GTP[S] concentrations up to 500 uM. Application of aluminum lowered the accumulation of inositol phosphates mainly by inhibiting IP_3 generation rather than by interfering with metabolic reactions after IP_3 formation. Pre-chelation of aluminum with citrate or EGTA completely abolished the inhibition of fluoride-induced inositol phosphate production by aluminum in intact cells, but had little effect on the inhibition of GTP[S]-induced inositol phosphate production in permeabilized cells. Applying aluminum prior to GTP[S] stimulation, turnover of PIP_2 and PIP became appreciably slower (30 - 45%). In addition of Mg^{2+}/G_p protein stimulation, phosphoinositide hydrolysis can be also evoked by increasing the intracellular Ca^{2+} concentration. When modulated by various divalent cations, inositol phosphate formation responded to aluminum stress differently. When Mg^{2+} was employed, formation of IP_3, IP_2 and IP was inhibited.

In Ca^{2+}-mediated production, however, only IP_3 release was appreciably depressed under aluminum stress; IP_2 level remained unaffected. Exposure of cells to aluminum also reduced bradykinin -triggered IP_3 production and intracellular Ca^{2+} release. These findings suggest that a primary lesion of aluminum toxicity may be related to the inhibition of inositol phosphate production through the metal's interaction with the phosphoinositide signal transduction pathway, presumably at Gp protein and phospholipase C.

INTRODUCTION

Aluminum has been implicated as a toxic agent in various neurodegenerative disorders, e.g., in certain types of senile dementia (Ganrot, 1986, Crapper MacLachlan, 1989). At this time, no single mechanism has been identified as causing a primary lesion in the aluminum toxicity syndrome.

Aluminum is apparently involved in a broad spectrum of physiological disorders. It is possible that a group of these disorders originates from the metal's interaction(s) with a key target in basic metabolic pathway(s). A major consequence of aluminum stress is known to result in a disturbance of cellular calcium metabolism (Marquis, 1989) which, in turn, is partially interrelated with signal transduction, involving polyphosphoinositide hydrolysis linked to a guanine nucleotide binding protein, named G_p protein (Berridge et al., 1983). Via this pathway, neural cells, in response to extracellular stimuli,

generate the intracellular messenger inositol-1,4,5-triphosphate (IP_3) to mobilize intracellular Ca^{2+} (Bansal and Majerus, 1990). In many types of cells, this signal transduction could be activated by fluoride in the presence of very low concentrations of aluminum (Gilman, 1987). Such activation is presumably accomplished by binding of fluoroaluminate complexes to the nucleotide center of Gp protein. Consequently, G_p protein is locked in GTP-bound activation conformation, thus preventing the effector enzyme from being switched off, leading to an elevated IP_3 formation (Chabre 1990).

However, aluminum stress generally interferes with cellular Ca^{2+} metabolism in an inhibitory manner (Levine et al., 1990), suggesting that aluminum may downregulate cellular Ca^{2+} levels via interference with phosphoinositide signal transduction by a mechanism different from the activation mode. Aluminum application indeed has been shown to cause profound negative effects on Ca^{2+} signalling in various types of cells like pancreatic acinar cells (Wakui et al., 1990). Application of aluminum to rat cortical slices reportedly depressed the release of inositol phosphate following stimulation of carbachol (Johnson and Jope, 1986) or fluoride (Jope, 1987). Moreover, aluminum was found to inhibit PIP_2 hydrolysis by phospholipase C from bovine heart (McDonald and Mamrack, 1988).

There are other possibilities for aluminum to interfere with IP_3/Ca^{2+} second messenger system, e.g., direct binding to IP_3 (Birchall and Chappell, 1988). In addition, key elements, namely

receptors, G_p protein and phospholipase C, of the signal transduction pathway are residing in the plasma membrane, and interaction of aluminum with membrane constituents may indirectly impact the regulation of the pathway.

Taken together, aluminum-induced changes in phosphoinositide signal transduction may provide a basis for understanding the mechanism whereby the toxic metal exerts its primary effect on neural cells. Hence, we decided to investigate the effect of aluminum on phosphoinositide hydrolysis, employing neuroblastoma cells. Our results demonstrate that application of aluminum inhibits inositol phosphate formation, presumably by interactions of the metal with G_p protein and phospholipase C.

MATERIALS AND METHODS

Materials

All tissue culture supplies were purchased from GIBCO Co.(Grand Island, NY). myo-[2-^{3}H]inositol (15.6 Ci/mmol) and [^{32}P]-orthophosphoric acid were obtained from New England Nuclear (Boston, MA). GTP[S] was bought from Boehringer Mannheim (Indianapolis, IN). Bradykinin was obtained from Sigma Chemical Co. (St. Louis, MO). All chemical reagents used were of high quality. Cleaning of plastic ware and the preparation of incubation buffers and solutions were performed as described (Shi and Haug, 1990).

Cell Culture

Cultures of C1300 mouse neuroblastoma cells, clone neuro-2A (American Type Culture Collection, Rockville, MD.), were grown as mentioned recently (Shi and Haug, 1990). The cells were used at confluence, 7-10 days after our first passage.

Measurement of Inositol Phosphate Formation

Neuroblastoma cells in 6-well multidishes were prelabelled for 24-30 h with 1.0 (for intact cells) or 2.0 uCi/ml (for permeabilized cell) of myo-[^{3}H]-inositol (15.6 uCi/mmol) in 2.0 ml Dulbecco Vogt's modified Eagle medium, DMEM. After labelling until equilibrium, the radioactive medium was removed, and cells of the monolayer (about 2.5 - 5 X 10^5/well) were washed twice with the incubation medium composed of 140 mM NaCl, 5 mM KCl, 10 mM $NaHCO_3$, 30 mM glucose, 5 mM $MgCl_2$; the medium was buffered to the desired pH values with 10 mM Tris, Hepes or Pipes.

Cells of monolayers were subjected to aluminum challenge in 1.0 ml incubation medium containing 10 mM LiCl, 2.5 mM ATP and 1.0 mM 2,3-diphospho-D-glycerate (Sigma, St. Louis, MO), prior to stimulation. The reaction was terminated by an addition of an ice-cold solution of trichloroacetic acid (TCA), final concentration 10%. Cells were extracted on ice for 10 min and then scraped off. The extracts were centrifuged at 1000 g for 5 min, and

supernatants and pellets were kept for the assay of inositol phosphates. The extraction procedure was carried out at 0 - 4°C.

A 1.0 ml volume of the supernatant solution was extracted with 2 ml solution of 1,1,2-trichloro-1,2,2-trifluoroethane and tri-n-octylamine (3 : 1) to remove TCA (Challiss et al., 1988). After removal of TCA, the upper phase solution was neutralized to pH 7.0 - 8.0 with 0.2 N NH_4OH. Inositol phosphate products in the solution were separated on a column containing AG 1-x8 (formate form, 200-400 mesh, Bio-Rad, Rockville Centre, NY), and [^{3}H]-inositol mono-, bis-, and triphosphates on the column were eluted stepwise (Figure 1) by using 0.1 M formic acid solution containing an increasing ammonium formate gradient (Berridge et al., 1983). The radioactivity of the fractions was counted by liquid scintillation spectrometry.

Permeabilizition of Neuroblastoma Cells

The permeabilization procedure followed basically that reported by Wojcikiewicz and Fain (1988): a monolayer of cells was cooled on ice for 10 min and DMEM culture medium was removed. After washing with incubation medium once, cells were incubated in an ice-cold medium resembling intracellular milieu (140 mM KCl, 20 mM NaCl, 10 mM glucose, 5 mM $MgCl_2$ and pH 7.4 buffers with 10 mM Hepes) containing 15 ug/ml digitonin for 10 min. Microscopic examination demonstrated that over 95% of cells fail to exclude trypan blue

Figure 1. Elution profiles of inositol phosphates by column chromatography. The water-soluble extracts of [^{3}H]inositol -labelled neuroblastoma cells, treated with 10 mM NaF/10 uM $AlCl_3$ (●) or with no NaF and $AlCl_3$ (○), were applied to AG 1-X8 column and eluted with: (A) water; (B) 5 mM sodium borate/60 mM sodium formate; (C) 0.1 M formic acid/0.2 M ammonium formate; (D) 0.1 M formic acid/ 0.4 M ammonium formate; (E) 0.1 M formic acid/1.0 M ammonium formate. Five peaks represent the metabolites eluted in the order (from left): free inositol, glycerophosphoinositol, IP, IP_2 and IP_3. The volume of each fraction was 1.0 ml.

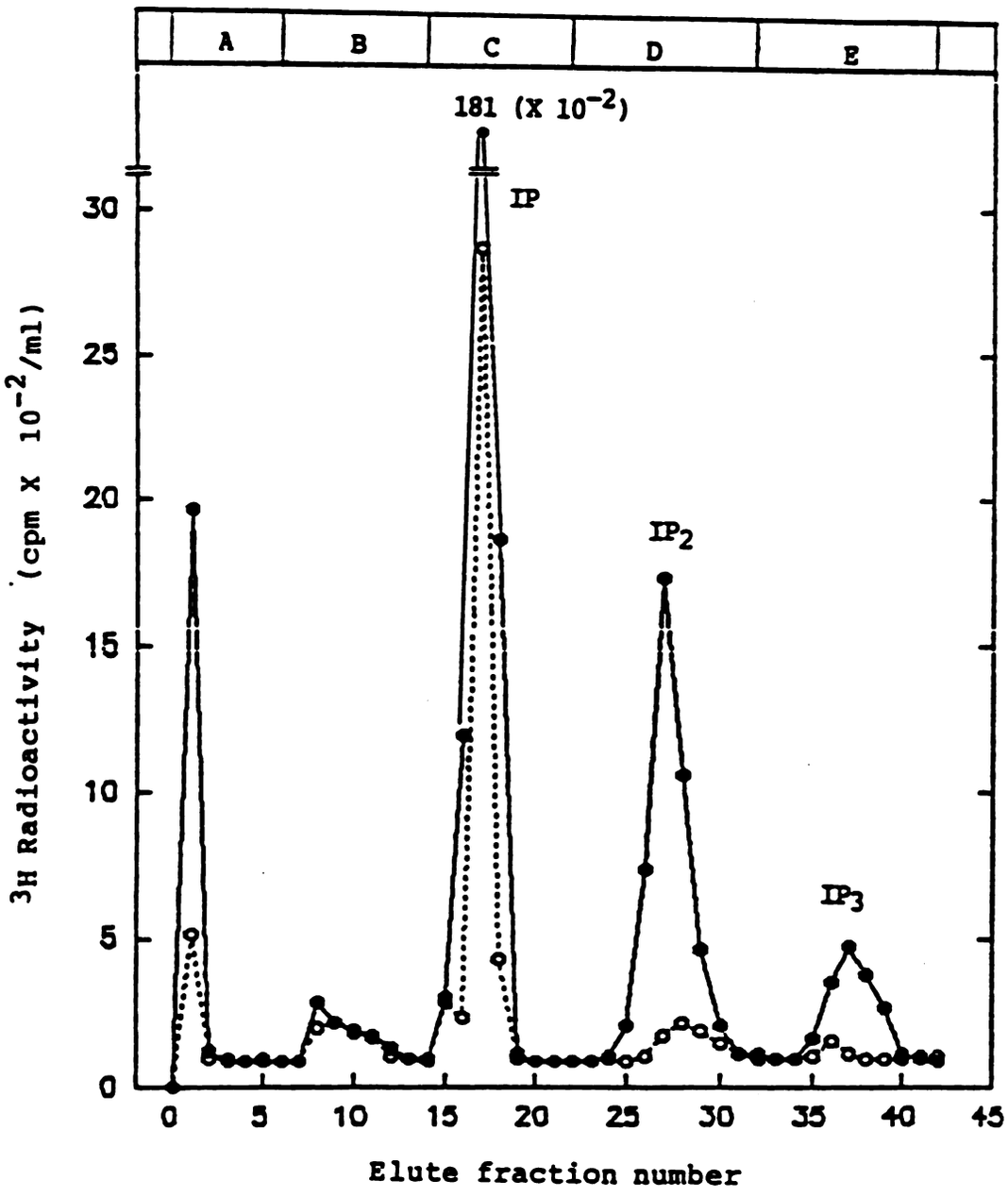

Figure 1. Elution profile of inositol phosphates by column chromatography.

after digitonin poration. Subsequently the permeabilized cells were washed once more in incubation medium for 5 min.

Measurement of Inositol Phospholipids

Except for minor modifications, lipids were extracted and separated as described (Horwitz and Perlman, 1987). In the case of [^{32}P]labelled cells, suspended cells, harvested from monolayers, were prelabelled with [^{32}P]orthophosphoric acid for 2 h in medium in 37° C water bath. [^{3}H]inositol (8.0 uCi/ml)- or [^{32}P]orthophosphoric acid (5.0 uCi/ml)-labelled cell pellets were dissolved in 1.0 ml of ice-cold solvent composed of chloroform /methanol /concentrated HCl (200/100/0.75, v/v/v). The mixture was allowed to stand in ice for 10 min, then was warmed to room temperature. After an addition of 0.2 ml of 0.6N HCl, the solution was centrifuged at 650 g for 5 min and the upper phase and middle flurry were discarded. The remaining lower phase was washed twice with 0.5 ml of an "upper phase-like solvent" chloroform/methanol/0.6 N HCl (3 : 48 : 47). The washed lower phase was completely dried under a nitrogen stream, and the residue was dissolved in chloroform/ methanol/H_2O (75:25:2) system.

Inositol phospholipids were separated by thin layer chromatography with a developing system of chloroform/ methanol/ H_2O/ammonium hydroxide (48:40:7:5). The labelled lipids were visualized by radioautography after incubation at -70° C, then scraped and extracted in $CHCl_3$/MTOH/0.2 M HCl (10 : 20 : 8).

After the addition of 0.5 ml $CHCl_3$ and 0.5 ml H_2O, the lower phase was dried and quantified by liquid scintillation counting.

Measurement of Intracellular Calcium

The intracellular free calcium concentration was determined as described (Zhou et al, 1990, Tojyo et al. 1991). Briefly, suspended cells (1.5 X 10^6/ml) were loaded with membrane-permeant, esterase-hydrolyzable acetoxy-methyl ester of fura-2 (2 uM/ml) for 1 h in DMEM, in a CO_2 incubator at 37°C. After washing twice, the fura-2/AM-loaded cells were resuspended in incubation buffer, at 5 X 10^5 cells/ml. Fluorescence measurement was performed at excitation wavelength 339 nm and emission wavelength 500 nm. Intracellular free Ca^{2+} concentration was calculated from the relation:

$$[Ca^{2+}] = K_d\ (F - F_{min})/(F_{max} - F)$$

where K_d = 224 nM (the dissociation constant of Ca^{2+} binding to fura-2).

RESULTS

For our neuroblastoma cells, equilibrium labelling was verified by monitoring the incorporation of [^{3}H]inositol into the phospholipid pool. Under our experimental conditions, 24 to 30 h were needed to attain equilibrium as demonstrated by stable inositol phosphate accumulation levels (Figure 2). Changes in

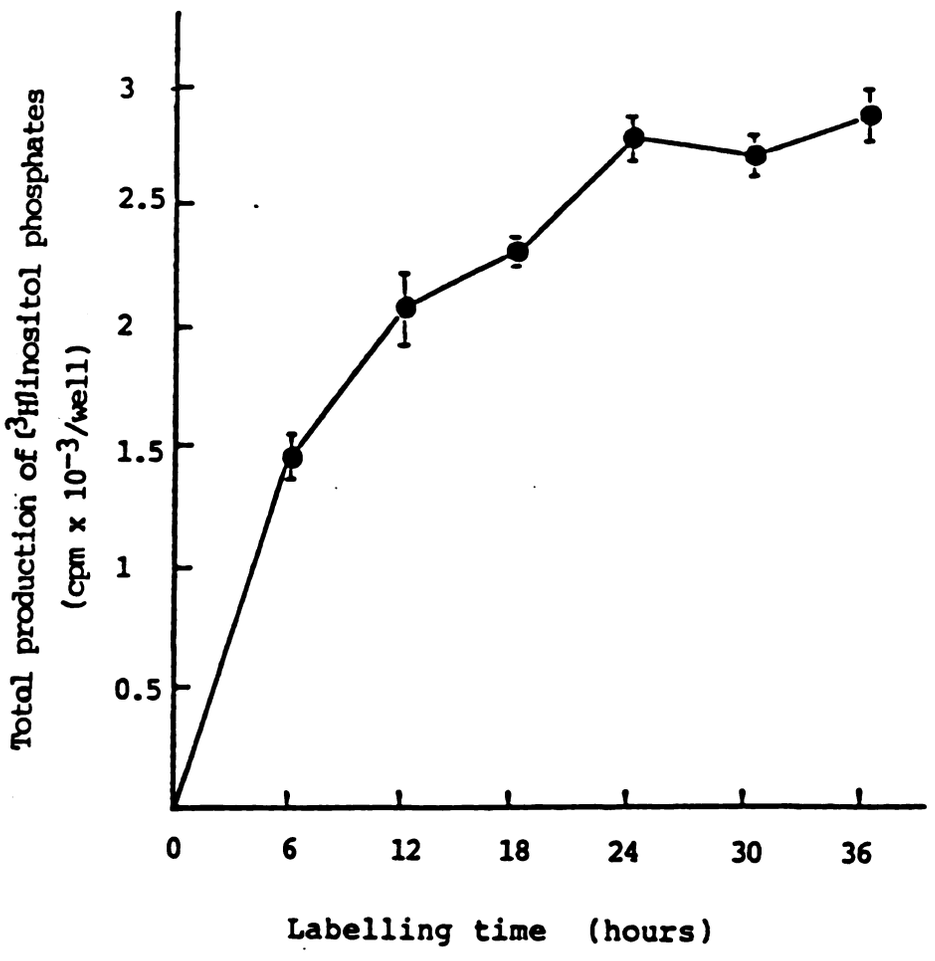

Figure 2. Incorporation of [^{3}H]myo-inositol into inositol phosphates in neuroblastoma cells. Cells of monolayers were grown in DMEM containing 2.0 uCi/ml [^{3}H]inositol for the times indicated. [^{3}H]inositol phosphates in samples were extracted and counted as described in Materials and Methods. The data points, representing the activities in total inositol phosphates, are means $\pm$ SEM of triplicate samples in a representative of two experiments.

concentration of [^{3}H]inositol phosphates are therefore indicative of changes in the amount of corresponding inositol phosphate (Dean and Beaven, 1989).

Activation of Fluoride on Phosphoinositide Hydrolysis

When neuroblastoma N_2A cells were treated with fluoride, enhanced turnover of phosphatidylinositol 4,5-biphosphate (PIP_2) and phosphatidylinositol 4-phosphate (PIP) was observed (Figure 3), similar to other cells tested (Gilman, 1987). With 10 mM fluoride added, [^{32}P]PIP_2 and [^{32}P]PIP counts in [^{32}P]ortho-phosphoric acid-labelled cells dropped by 50% and 30% from their control levels, respectively, whereas the [^{32}P]phosphatylinositol level was virtually not affected.

To determine whether the reduction of PIP_2 resulted from fluoride-stimulated PIP_2 hydrolysis, rather than from blocking upstream kinase reactions of phosphoinositides, the release of inositol phosphates, the hydrolytic products of phosphoinositide, was measured with [^{3}H]inositol-labelled cells. As expected, application of fluoride caused drastic elevation of inositol phosphate production. The fluoride-dose dependence of the induced inositol phosphate formation (Figure 4) was coincident with that of the induced PIP_2 and PIP depletion up to 10 mM fluoride,(Figure 3). All three major inositol phosphates, viz. IP_3, IP_2 and IP attained their peak values at 5 - 10 mM fluoride, and total inositol phosphate (IP_T = IP_3 + IP_2 + IP) production was

Figure 3. Effects of fluoride on [^{32}P]phosphoinositide turnover in neuroblastoma cells: PI (A), PIP (■ in B) and PIP_2 (● in B). Suspended cells, harvested from monolayers, were prelabelled with [^{32}P]orthophosphoric acid (5.0 uCi/ml) in incubation medium, 2 h, at 37 C in a water bath. The labelled cells were washed, then incubated with NaF at various concentrations for 30 min. After the termination of the reaction, lipid extraction and separation, radioactivity was counted; see description in Materials and Methods. Data are means ± SEM of duplicate samples. $^{*}P < 0.05$ and $^{**}P < 0.025$ vs. corresponding control (no NaF addition) by Student's test.

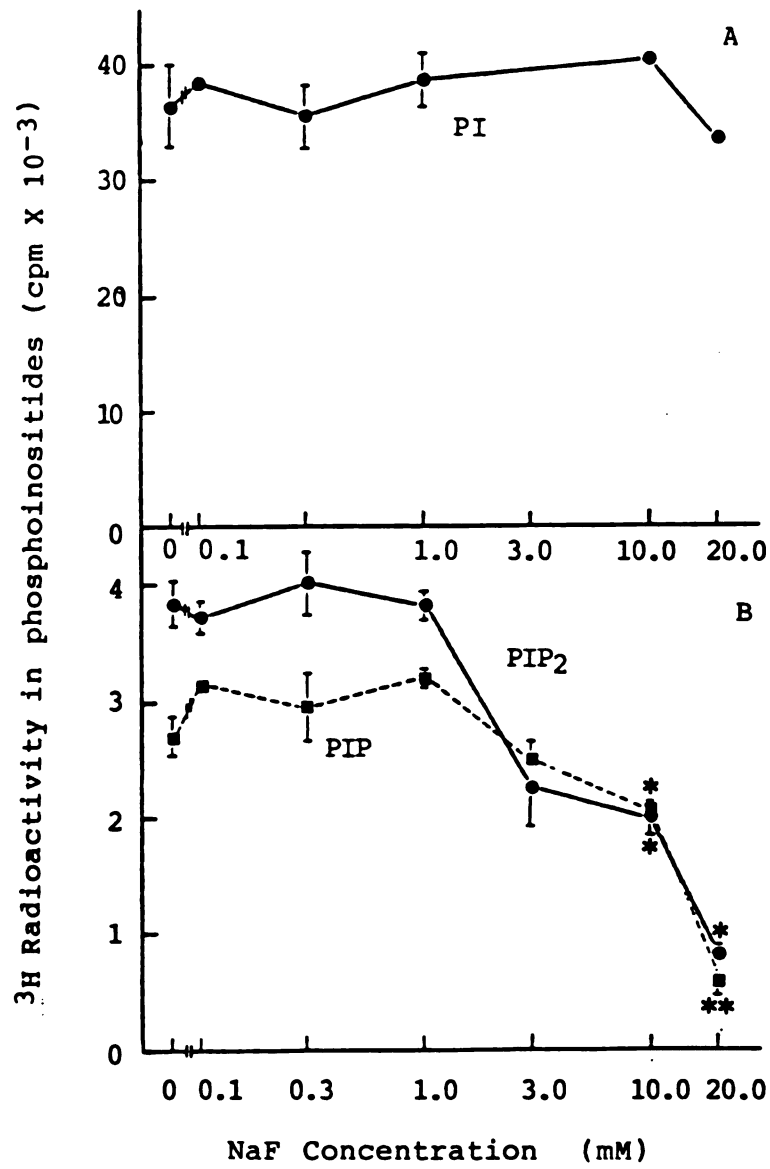

Figure 3. Effect of fluoride on [^{32}P]phosphoinositide turnover in neuroblastoma cells.

Figure 4. Dose-dependence of fluoride-induced inositol phosphate formation in neuroblastoma cells: IP (●), IP_2 (▲) and IP_3 (■). [^{3}H]inositol-labelled cells of monolayers were treated with 10 mM LiCl for 15 min, then incubated with NaF at various concentrations plus 10 $AlCl_3$, 30 min, in pH 6.8 incubation medium, in a 37 C CO_2 incubator. Data points with * represent the production in samples treated with 100 mM NaCl. Data are means ± SEM of duplicate samples. $^*P < 0.05$, $^{**}P < 0.025$ and $^{***}P < 0.01$ vs. corresponding control (no NaF addition).

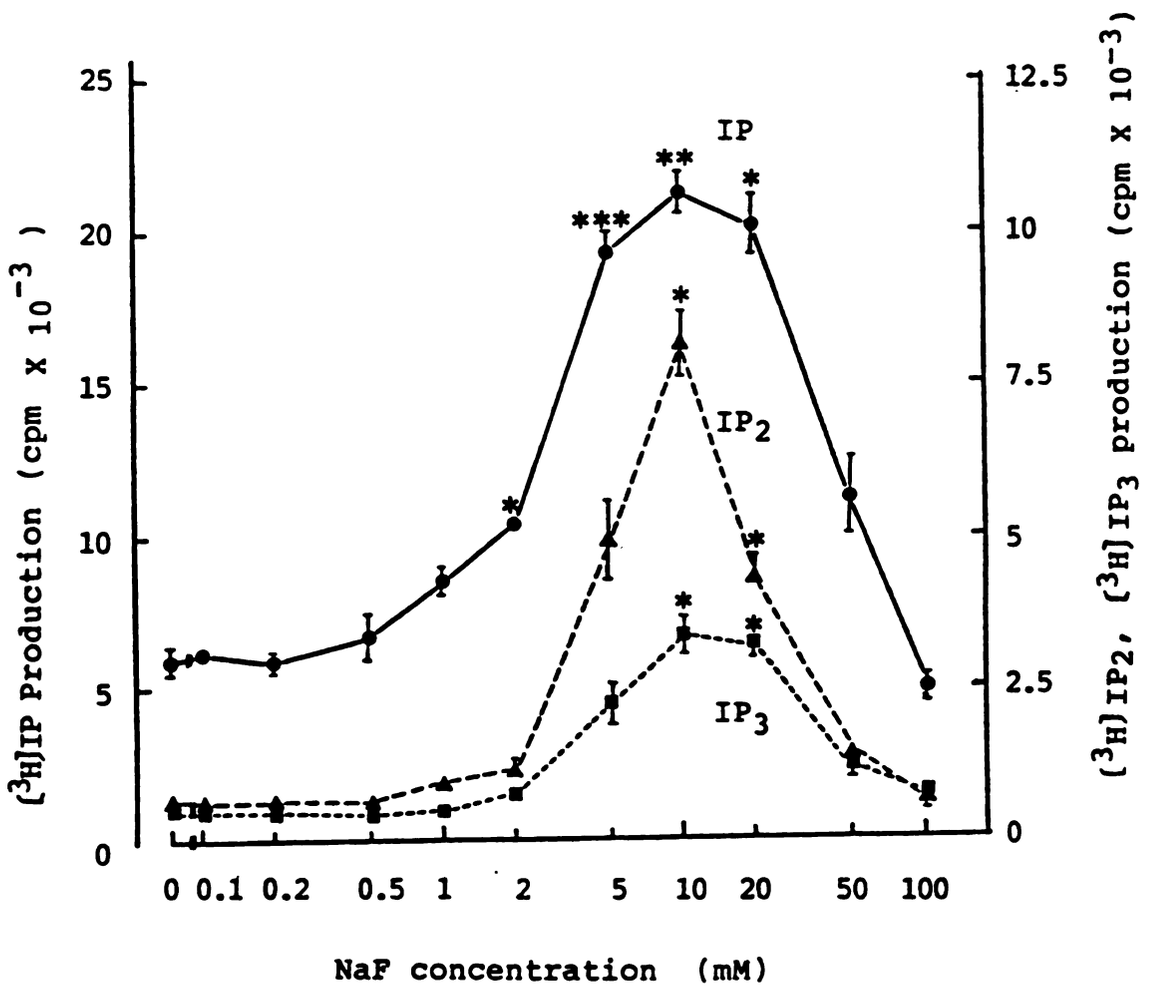

Figure 4. Dose-dependence of fluoride-induced inositol phosphate formation in neuroblastoma cells.

enhanced 4 to 5 fold compared with the basal level. With further increase in NaF concentration, inositol phosphate formation declined sharply. Since a similar reduction was also found if cells were treated with NaCl of the same concentration, it was obviously caused by high concentrations of Na^+.

The observed stimulation of inositol phosphate formation by fluoride was not or only marginally potentiated by application of aluminum. Presumably trace amounts of endogenous aluminum sufficed to form a fluoroaluminate complex capable of stimulating phosphoinositide hydrolysis (Cockcroft and Taylor, 1987). In cultured neuroblastoma cells, submicromolar aluminum always existed as contaminant (Shi and Haug, 1989).

Inhibition of Fluoride-Induced Inositol Phosphate Release by Aluminum

Fluoride-stimulated phosphoinositide hydrolysis was measured in the presence of increasing aluminum concentrations (Figure 5). At low concentrations of aluminum, the induced inositol phosphate formation was practically not affected. Above 50 uM of aluminum, inositol phosphate formation was inhibited in a dose-dependent manner with IC_{50} value of 250 uM aluminum. At 500 uM aluminum, the total inositol phosphate production decreased to about 30% of control value, close to that of the basal level. In the absence of added fluoride, basal production of inositol phosphates was also inhibited by aluminum, but significantly less.

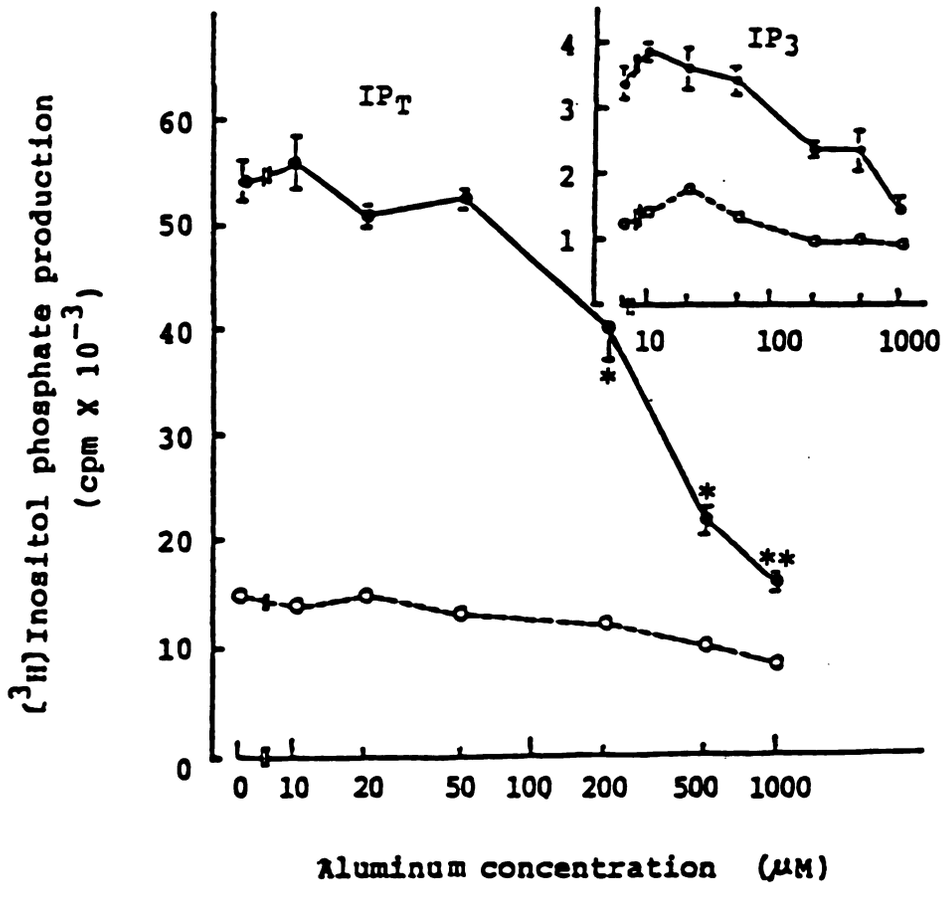

Figure 5. Aluminum-induced inhibition of fluoride-related total inositol phosphate and IP_3 (insert) formation. Following exposure to various aluminum doses for 30 min, intact neuroblastoma cells in monolayers were incubated an additional 45 min in an medium containing 5.0 mM NaF (●), or no NaF added (○), pH 6.8, 37 C, in a CO_2 incubator. The data are those of a typical experiment carried out in duplicate; three independent studies afforded similar results. $^*P < 0.05$ and $^{**}P < 0.01$ vs. control (no aluminum addition).

Similar data were obtained on rat cortical slices (Jope, 1988); application of 0.5 mM aluminum inhibited fluoride-related total inositol phosphate production by 45%. By monitoring accumulation of individual inositol phosphate, our results demonstrate that the formation of three inositol phosphates, IP_3, IP_2 and IP, was reduced in a similar pattern when neuroblastoma cells were exposed to aluminum prior to fluoride stimulation. In our system, IP_3 usually accounted for 5 - 10% of total inositol phosphate products. Given its short life (about 10 sec) and low level (Bansal and Majerus, 1990), determination of IP_3 was less accurate than that of IP. In the presence of lithium (10 mM), an inhibitor of inositol-1-phosphatase (Huckle and Conn, 1987), the predominant inositol phosphate species was IP, accounting for about 70 - 80% of total inositol phosphates. Assuming that most of IP was originating from IP_3, and that most IP_3 was converted to IP (Wojcikiewicz and Fain, 1988), the amount of total inositol phosphate accumulated, $[IP_T]$, where $IP_T = (IP + IP_2 + IP_3)$, appears to be a reasonable estimate of total IP_3 production within the experimental time frame; at any given time, the quantity of IP_3 measured appears to reflect the instant production of IP_3 at this moment.

Calculation indicates that the ratio of a specific inositol phosphate quantity over that of total inositol phosphates, viz., $[IP]/[IP_T]$, $[IP_2]/[IP_T]$ and $[IP_3]/[IP_T]$, was approximately constant irrespective of the presence of aluminum at various concentrations (Table 1). This fact suggests that aluminum

Table 1. Inhibition of GTP[S]-induced inositol phosphate formation by aluminum.

Al(uM)	Inositol phosphate production (cpm/well)			
	IP	IP_2	IP_3	IP_T
0	33840 (80.8)	5860 (14.0)	2210 (5.3)	41900
2	32380 (79.5)	5960 (14.7)	2360 (5,8)	40700
5	29080 (80.3)	5130 (14.2)	2010 (5.6)	36200
10	27500 (81.1)	4600 (13.6)	1830 (5.4)	33920
20	22700 (82.1)	3410 (12.3)	1410 (5.1)	27650
50	16110 (80.8)	2860 (14.3)	980 (4.9)	19950
200	14020 (81.6)	2450 (14.3)	720 (4.2)	17180
500	12460 (78.2)	2590 (16.3)	870 (5.5)	15940

Permeabilized cells were treated with aluminum, then incubated with 100 uM GTP[S] as in Fig.6. Numbers in parenthesis represent the fraction, in percentage, of individual inositol phosphate (i.e., IP, IP_2 and IP_3), elated to total inositol phosphate accumulation (IP_T), viz., IP/IP_T, IP_2/IP_T and IP_3/IP_T. Data are means of duplicate samples in a representative of three experiments.

did not interfere with the sequential kinase or phosphatase reactions after IP_3 formation. In other words, the primary action seemingly occurred at or prior to site(s) where IP_3 was generated.

In intact cells, inositol phosphate formation was determined as to its dependence on the duration of aluminum incubation (Figure 11B, curve e). Cells were exposed to aluminum for varying time periods, then washed with aluminum-chelating medium prior to fluoride treatment. A brief treatment of cells for less than 5 min was accompanied by slight decreases (< 10%) in phosphoinositide hydrolysis. Apart from that, inositol phosphate production was drastically reduced as the incubation time was lengthened to 60 min.

Inhibition of GTP[S]-induced Inositol Phosphate Formation by Aluminum

GTP[S], a nonhydrolyzable analogue of GTP, continually stimulates G_p protein and is widely used in investigations on signal transduction (Simonsson et al., 1991). Studies on GTP[S]-induced inositol phosphate formation were carried out with digitonin-permeabilized cells, since application of GTP[S] to intact cells failed to show significant impact. Under our experimental condition, incubation of monolayer cells in cytosol-like medium containing 15 ug/ml digitonin on ice yielded over 95% of cells porated, and maximal GTP[S] stimulation.

The saturation level of GTP[S]-evoked inositol phosphate formation was about 2.5 - 3 times higher than the basal level (Figure 6), i.e., less pronounced than fluoride-induced response, although GTP[S]-treated cells were labelled with 2.0 uCi/ml of [^{3}H]inositol, i.e., twofold that used for fluoride-treated cells. A similar observation was reported on rat cortical membranes (Li et al., 1990). Digitonin permeabilization did not cause leakage of inositol phosphates to the extracellular milieu since 85 - 90% of these compounds were found to be associated with cells.

Compared with fluoride-induced inositol phosphate formation, the GTP[S]-activated process was more responsive to aluminum's action. The onset of inhibition of aluminum on inositol phosphate release became distinct at an aluminum concentration as low as 2 to 5 uM, i.e., at concentrations usually employed in fluoroaluminate activation experiments; and IC_{50} shifted to 20 uM. This enhanced sensitivity is expected because digitonin-porated cells were fully accessible to aluminum. Moreover, in the absence of fluoride, aluminum lost its activation capability, and more free aluminum was available. In response to aluminum application, GTP[S]-induced inositol phosphate formation appeared to reflect a biphasic dependence: a sharp decrease between 0 - 50 mM and gradual decrease above 50 uM of aluminum.

When [^{3}H]inositol-labelled cells were stimulated with GTP[S] in the presence of 0.5 mM non-radioactive "cold" IP_3, an increase in [^{3}H]IP_3 formation was accompanied by an equivalent decrease in [^{3}H]IP accumulation regardless of aluminum stress. As shown in

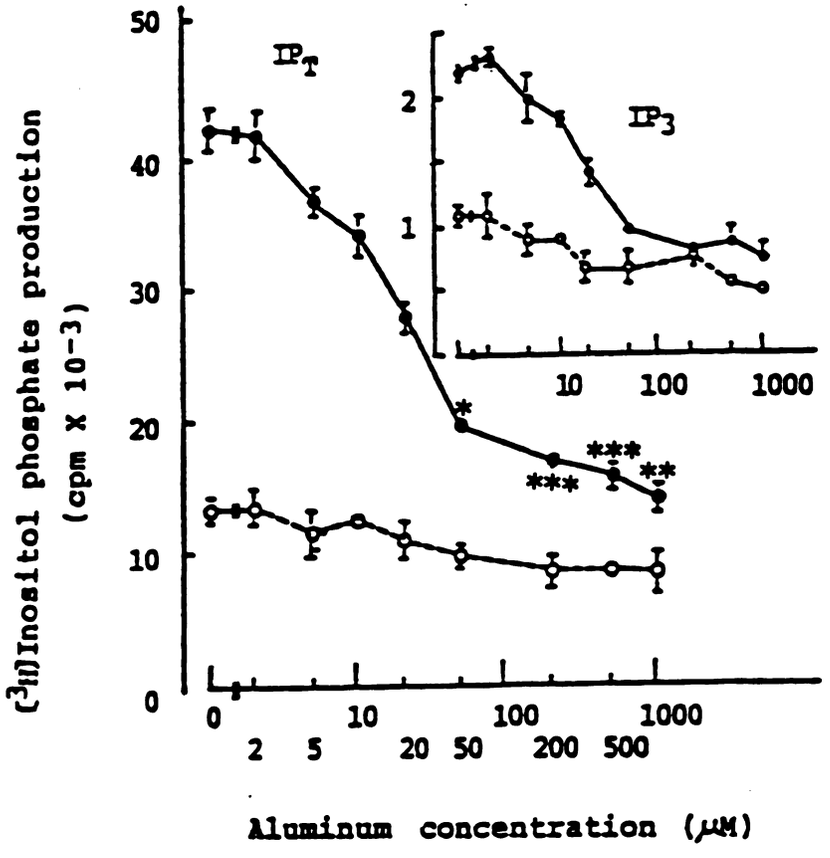

Figure 6. Aluminum-induced inhibition of GTP[S]-triggered total inositol phosphate and IP_3 (insert) formation. After exposure to various aluminum concentrations for 15 min, digitonin -permeabilized neuroblastoma cells were further incubated, 60 min, pH 7.4, in an incubation medium containing 100 uM GTP[S] (●), or no GTP[S] (○), 37 C, in a CO_2 incubator. Data are those of a typical experiment performed in duplicate; three independent studies afforded similar results. $^{*}P < 0.05$, $^{**}P < 0.025$ and $^{***}P < 0.01$ vs. control (no aluminum addition).

Figure 7, [^{3}H]IP_3 production in the absence of cold IP_3 was 25 -30 % that in the presence of cold IP_3, and [^{3}H]IP production in the presence of cold IP_3 was 35% of that in the absence of cold IP_3. Considering that radioactive IP_3 might not be diluted sufficiently by "cold" IP_3 employed, and that a certain amount of basal level IP_3 had been already accumulated prior to "cold" IP_3 introduction, the fraction of IP generated from IP_3 might have been larger. Nevertheless, these findings suggest: 1). IP accumulation observed in our system is not due to direct PI and PIP hydrolysis occurring independently from the G_p protein-mediated pathway, and 2). application of aluminum lowered inositol phosphate accumulation principally by inhibiting IP_3 formation.

To test whether the observed reduction of inositol phosphates resulted from aluminum interference with the chromatographic assay of these metabolites, in particular IP_3, experiments were performed whereby aluminum was added to samples after termination of reaction and removal of TCA. The results in figure 8 indicate that no interference with IP_3 and IP_2 production was detectable following such a "post"-incorporation of aluminum, even though a high concentration of aluminum (500 uM) was found to slow the elution rate. The radioactive counts of these compounds (bars B, C and D) were virtually identical to those from "negative" control (bar A), which had not been treated with aluminum; but were appreciably higher than those of "positive" controls (bars E, F and G) which had been exposed to the same aluminum concentration prior

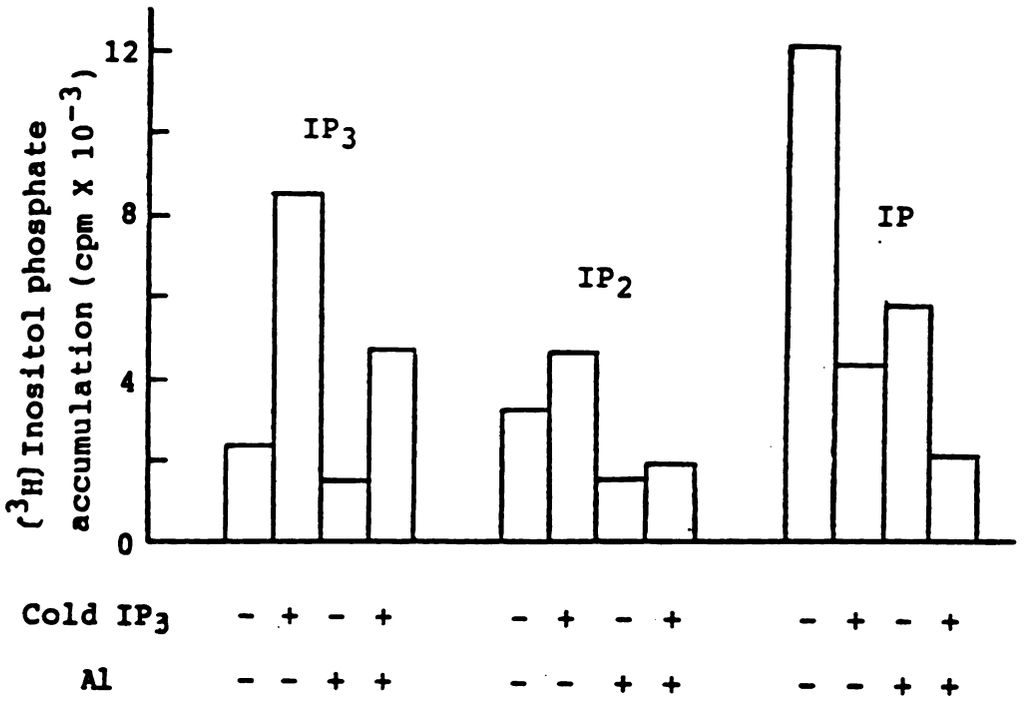

Figure 7. GTP[S]-induced [^{3}H]inositol phosphate formation in the presence of non-radioactive IP_3. Digitonin-permeabilized cells, either treated with 50 uM aluminum or with no aluminum, were incubated with 100 uM GTP[S] in the presence of 0.5 mM non-radioactive IP_3 or in the absence of non-radioactive IP_3 for 20 min.

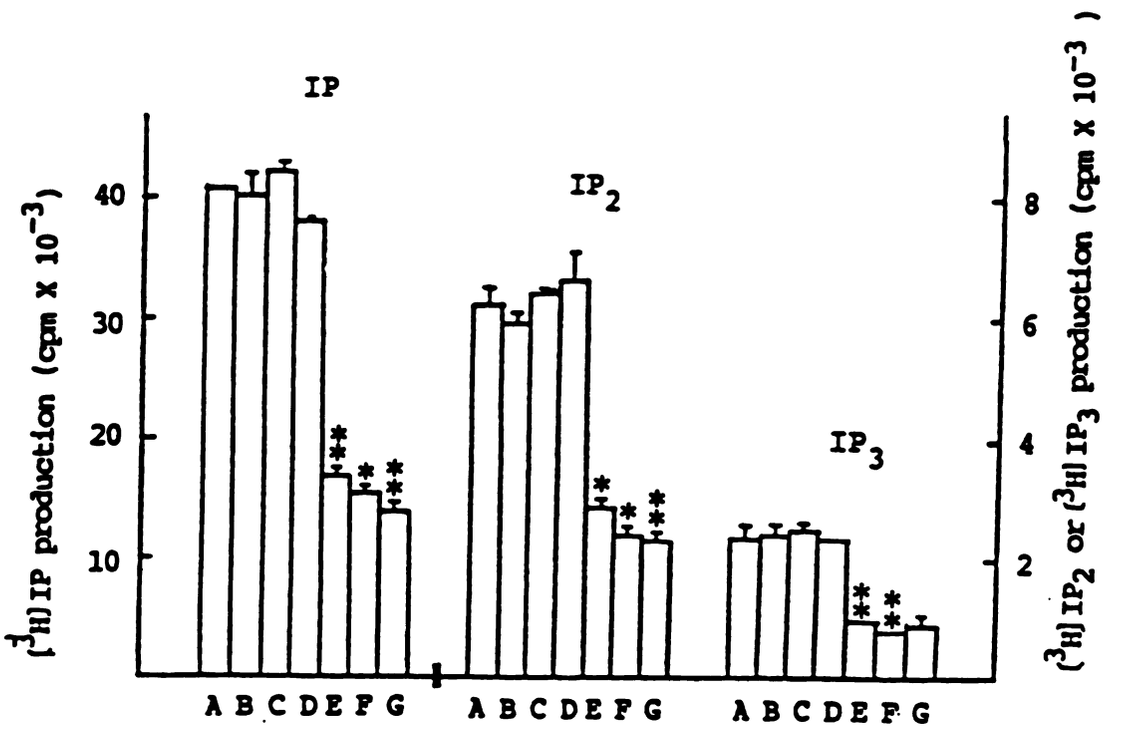

Figure 8. Effects of aluminum on the chromatographic assay of inositol phosphates in GTP[S]-stimulated permeabilized cells. "Pre-aluminum" samples were treated with aluminum doses of 50 (B), 200 (C), 500 (D) uM, prior to GTP[S] (100 uM) stimulation. "Post-aluminum" samples were treated with identical doses (E,F,G) after removal of trichloroacetic acid. Sample "A" is the control where aluminum was not administered, neither before nor after GTP[S] stimulation. Data are means ± SEM from a single experiment with duplicate samples. $^{*}P < 0.05$, $^{**}P < 0.025$ and $^{***}P < 0.01$ vs. corresponding control (sample A).

to GTP[S] stimulation. Quantitation of IP levels was also unaffected by "post"-addition of aluminum up to 200 uM, and it became slightly reduced (about 10%) at 500 uM aluminum (37840 cpm on bar D vs. 40140 cpm on bar A).

The effect of aluminum on inositol phosphate formation was examined in a GTP[S] dose-dependent manner (Figure 9). With no aluminum added, inositol phosphate production attained its plateau at 20 uM GTP[S], and EC_{50} value for GTP[S] was 2.5 uM. Following application of 50 uM aluminum, the saturation level was reached at 50 uM GTP[S], and EC_{50} shifted to the right slightly (5 uM). Apart from these, addition of aluminum did not change largely the graph depicting the relationship of the induced inositol phosphate formation vs. GTP[S] concentration, albeit aluminum reduced remarkably the inositol phosphate level at a given GTP[S] dose. In other words, the inhibitory effect of aluminum was not reversed by increasing GTP[S] dose up to 500 uM.

Similar results were obtained with GTP (in the presence of 100 uM GTP[S]). As shown in figure 10, application of GTP up to 5 mM (100 fold excess over aluminum) had practically no influence on aluminum -related inhibition of inositol phosphate formation. At 5 mM GTP, the production of inositol phosphates decreased at approximately the same degree in the absence and presence of aluminum, suggesting that the observed reduction was due to the dilution of GTP[S], a permanent G_p protein activator, by its analog GTP.

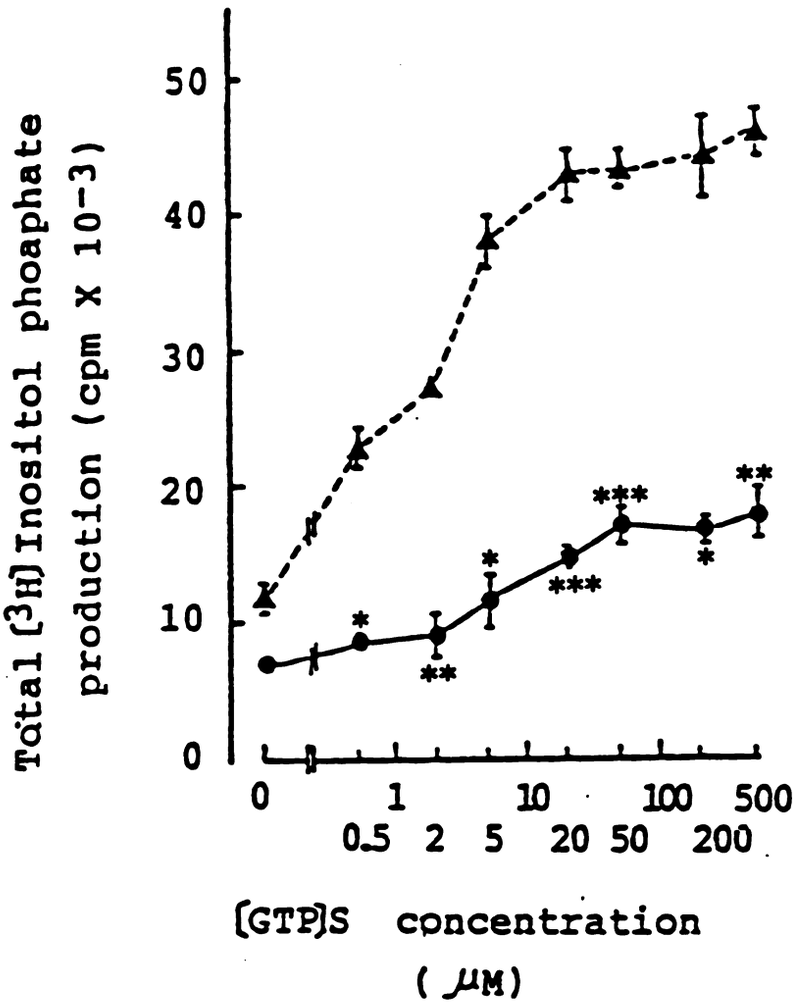

Figure 9. GTP[S] dose-dependence of inositol phosphate formation in permeabilized cells. Cells were preincubated in the presence of 50 uM aluminum (●) or in the absence of aluminum (▲) prior to stimulation of GTP[S] at various concentrations. Typical data of total inositol phosphate production are means ± SEM of duplicate samples; two independent experiments were performed. $^{*}P < 0.05$, $^{**}P < 0.025$ and $^{***}P < 0.01$ by paired test.

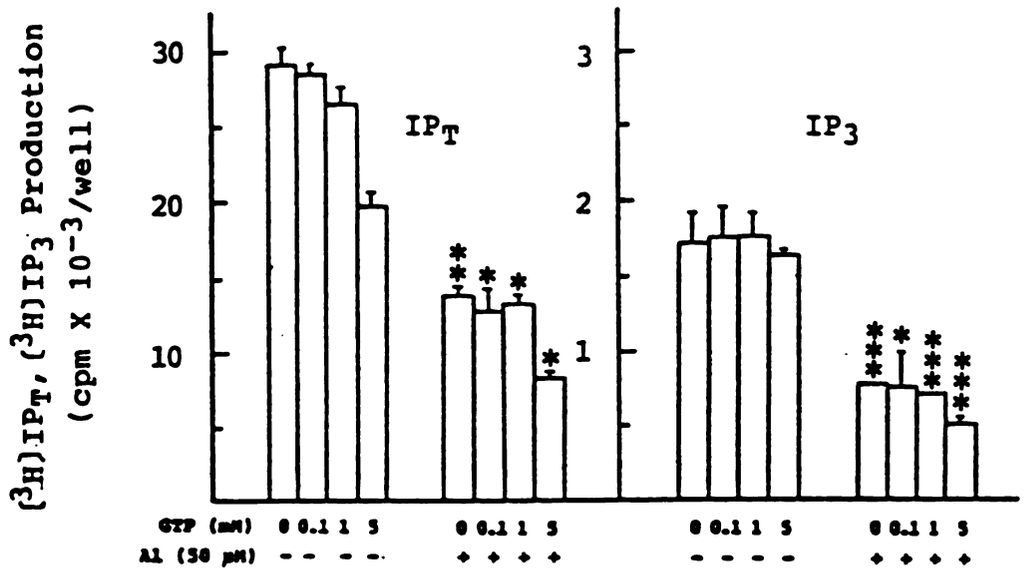

Figure 10. Inhibition of aluminum on inositol phosphate formation in the presence of exogenous GTP. Control or aluminum (50 um)- -treated permeabilized cells were stimulated with 100 uM GTP[S] in the presence of GTP of various concentrations in medium. Data are means ± SEM of duplicate samples. $^{*}P < 0.05$, $^{**}P < 0.025$ and $^{***}P < 0.01$ by paired t test.

Time Course of GTP[S]-induced Inositol Phosphate Formation in The Absence and Presence of Aluminum

At variance with stimulation of inositol phosphate formation by agonists, in which maximal IP_3 enhancement is seen within seconds (Figure 11), the response of inositol phosphate accumulation to GTP[S] was slower but lasting much longer (Figure 17). The lag in onset of the GTP[S] stimulation found here was also reported on other cells, and was attributed to the time required for GTP[S] to exchange with endogenous guanine nucleotide on G_p protein.

According to our time course experiments, the kinetics of inositol phosphate production followed basically the same pattern regardless of aluminum (50 uM) treatment. In both cases, responding to GTP[S] addition, IP_3 initially increased rapidly, attaining a plateau at 10 min, followed by elevation of IP_2 level, which reached its peak value at about 30 min, and IP gradually accumulated. At 1 h, IP_3 level began to decline, but IP was still increasing with time. The presence of aluminum attenuated inositol phosphate production at each time point, but the general shape of the time course curve remained unaltered compared with that of control cells. For example, IP_2 accumulations (Figure 11A) reached their plateau levels at about the same time regardless of aluminum administration, but the height (2800 cpm) in the presence of aluminum declined to 40% of the corresponding control values (6800 cpm).

Figure 11. Time course of GTP[S]-induced inositol phosphate formation in the absence or presence of aluminum. Time course of IP_T (B: ● ○), IP (B: ▲ △), IP_2 (A: ▲ △), and IP_3 (A: ● ○) production was measured in the presence of 250 uM aluminum (solid symbols), or in the absence of added aluminum (open symbols). After treatment with aluminum for 15 min, permeabilized cells were stimulated with 100 uM GTP[S] for various times. In panel A: The left ordinate refers to IP_2 (▲ △), the right ordinate to IP_3 formation (● ○). Typical data are means ± SEM of duplicate samples; three independent experiments were carried out. $^{*}P < 0.05$, $^{**}P < 0.025$ and $^{***}P < 0.01$ by paired test.

Temporal dependence of fluoride-induced total inositol phosphate formation in intact neuroblastoma cells on preincubation of cells with aluminum (B: curve e). Cells were preincubated with 200 uM aluminum for various times, then subjected to stimulation with 5 mM NaF for 45 min. Data are means ± SEM of duplicate sample from two independent experiments.

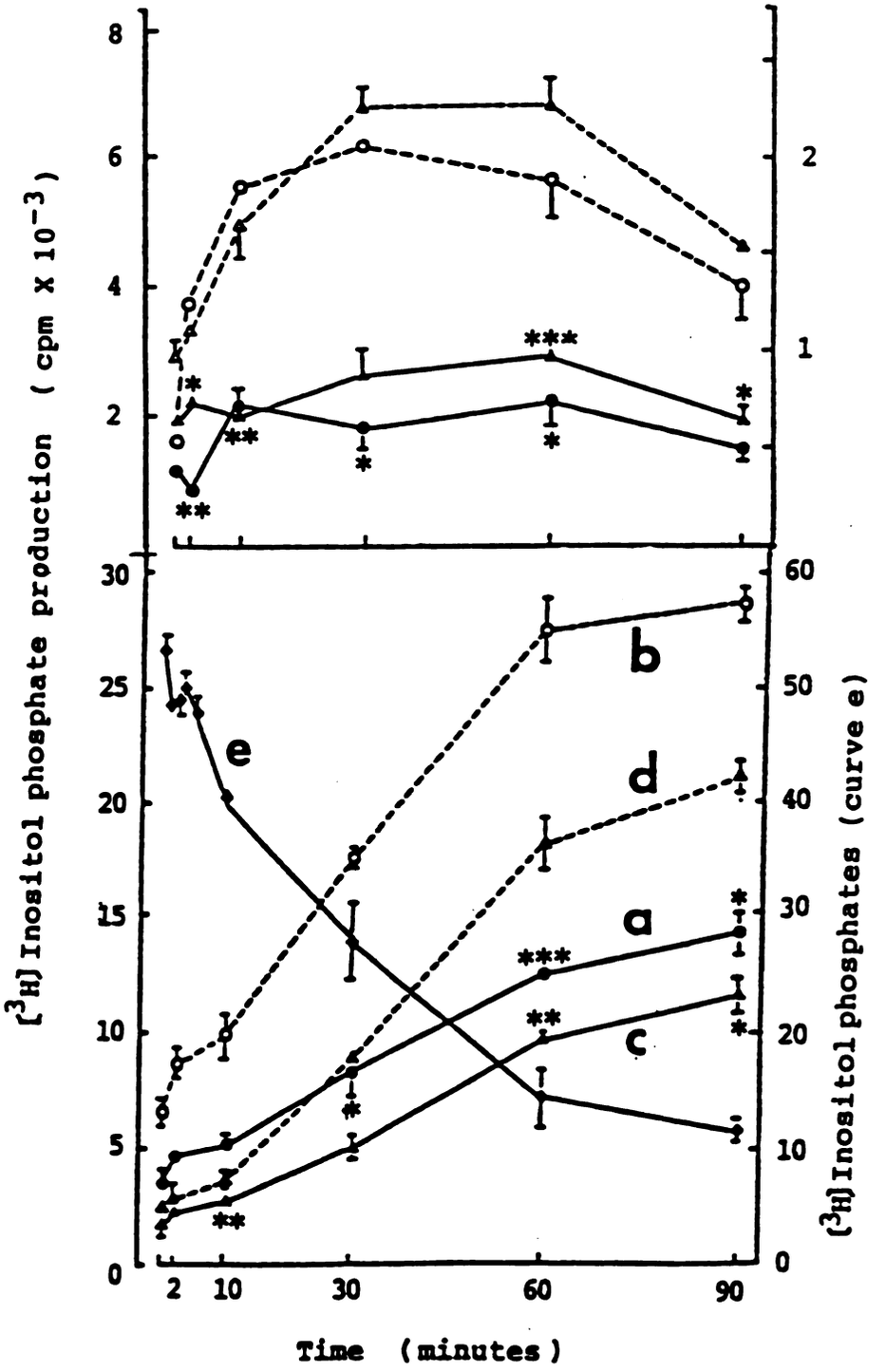

Figure 11. Time course of GTP[S]-induced inositol phosphate formation in the absence or presence of aluminum.

IP_T accumulated similarly to that of IP, increasing linearly within the time period of 10 to 60 min (Figure 11B). The time course curves in the absence and presence of aluminum had different slopes: 34000 cpm vs. 14000 cpm. The ratio of the slopes, i.e., the ratio of the estimated average IP_3 production in the absence of aluminum vs. that in the presence of aluminum is 2.4, similar to the ratio of instant IP_3 production, 2.8, calculated directly from the IP_3 levels in 10 - 60 min plateau. This finding with the temporal pattern of individual inositol phosphate formation, further support the notion that aluminum's inhibitory effect occurs at sites of IP_3 formation rather than at events after IP_3 formation.

Inhibition of Aluminum in The Presence of Chelating Agents

For experiments on intact cells (Figure 12B), aluminum was pre-mixed with chelating agents, EGTA or citrate, at a molar ratio of 1.1 (chelator/metal). Aluminum complexes of these chelators were found to be excluded from entering cells within the short time used (Shi and Haug, 1990, Guy et al., 1991). After removal of aluminum -containing medium, cells were washed with chelator-containing buffer, then plain buffer, and finally exposed to fluoride. When citrate (bar 3) or EGTA (bar 4) was present in the medium, phosphate inositol production was as high as that in the positive control (bar 0), i.e., in cells which had not been treated with aluminum. Examining cells pretreated with aluminum alone (bar 1),

Figure 12. Effects of aluminum-chelators on aluminum-induced inhibition of inositol phosphate formation. Aluminum-induced inhibition of fluoride-triggered, total inositol phosphate, IP_T, and IP_3 formation in intact neuroblastoma cells (B) and of GTP[S]-induced IP_T and IP_3 formation in permeabilized cells (A), in the absence, or presence of chelating agents. Bar 0 represents the respective control sample, i.e., without aluminum and without chelator. Intact cells (B) were preincubated, 30 min, with 500 uM aluminum (1 and 2), 500 uM aluminum + 550 uM citrate (3), 500 uM aluminum + 550 uM EGTA (4), 550 uM citrate (5), or 550 uM EGTA (6), then washed with incubation medium containing 5 mM citrate and plain buffer. Finally the washed cells were exposed to stimulation with 5 mM NaF, for 45 min, in the medium containing no aluminum except for samples 1 and 2, which were incubated in the medium containing 500 uM aluminum. Permeabilized cells (A) were treated with 200 uM aluminum (1), 200 uM aluminum + 220 uM citrate (3), 200 uM aluminum + 220 uM EGTA (4), 220 uM citrate (5), or 220 uM EGTA (6) prior to GTP[S] stimulation (100 uM). Typical data are means $\pm$ SEM of duplicate samples; two independent experiments were performed. $^{*}P < 0.05$, $^{**}P < 0.025$ and $^{***}P < 0.01$ vs. corresponding control (sample 0)

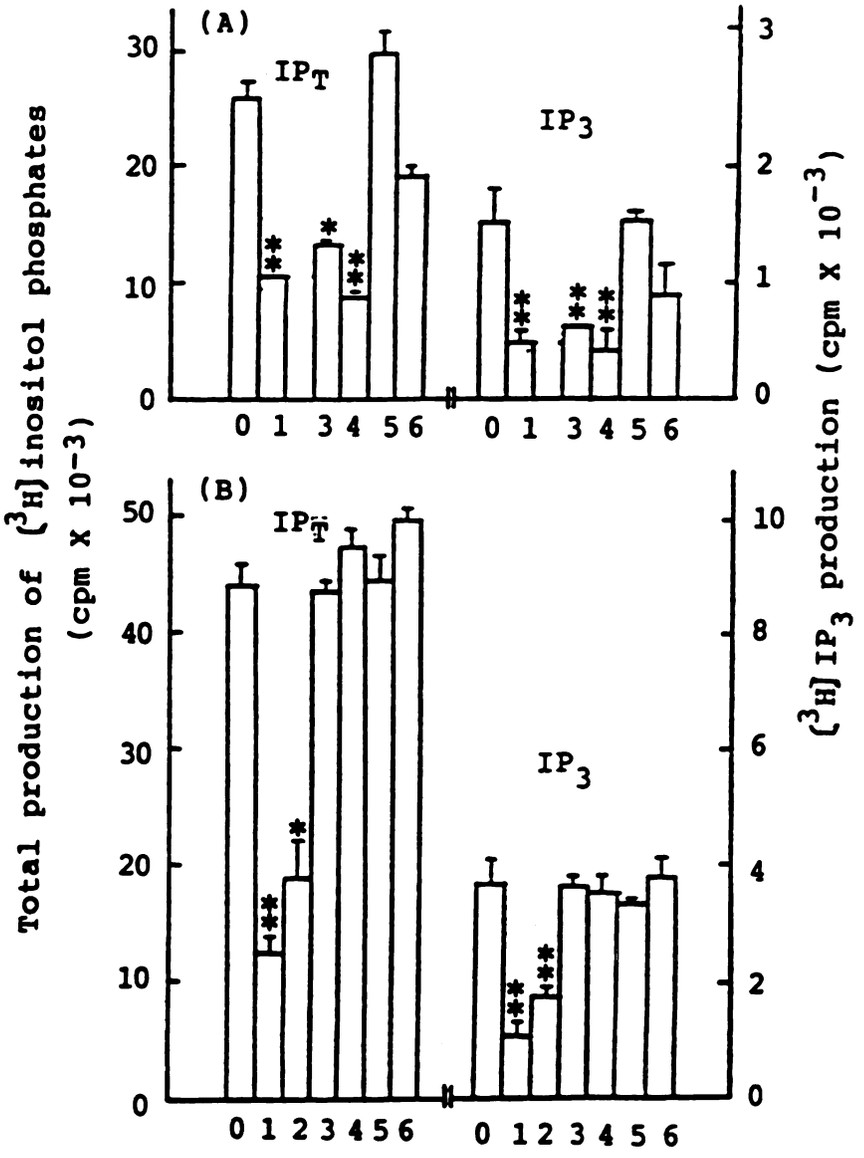

Figure 12. Effects of aluminum-chelators on aluminum-induced inhibition of inositol phosphate formation

inhibition persisted after washing cells with a chelator-containing medium: IP_T (12500 cpm/well) and IP_3 (1060 cpm/well) levels were about 30% of the respective control value (bar 0,44390 and 3720 cpm/well, respectively).

Conducting similar experiments on permeabilized cells (Figure 12A), cells were simply incubated with aluminum prechelated with EGTA or citrate prior to GTP[S] stimulation. The spectra of the aluminum's inhibition were different from those in intact cells. When citrate was employed (bar 3), inhibition of inositol phosphate formation by aluminum (bar 2) was only slightly reversed (13220 cpm on bar 3 vs. 10550 cpm on bar 2). This observation suggested that the chelating agents were eliminating the inhibitory effect by preventing aluminum's interiorization into intact cells. If aluminum was premixed with EGTA (bar 4), the inhibition of inositol phosphate release in the presence of aluminum (bar 2) was even potentiated (8600 cpm on bar 4 vs. 10500 cpm on bar 2). Such an EGTA-related reduction was also found in the absence of aluminum (19200 cpm on bar 6 vs. 25600 cpm on bar 0), it is apparently caused by chelation of physiological cations, like Mg^{2+} and Ca^{2+}, by EGTA. Unlike citrate, EGTA does not selectively chelate aluminum, and it has high affinity to bind various divalent cations, in particular Ca^{2+}.

Effect of Aluminum on Turnover of Inositol Phospholipids

To further examine aluminum's putative action site along the signal transduction pathway, the impact of aluminum on inositol phospholipid turnover was investigated (Figure 13). With no aluminum added, stimulation by GTP[S] (sample B) resulted in a 40% PIP_2 and 30% PIP loss, respectively. Thus, compared with GTP[S]-induced increase in inositol phosphate production, GTP[S]-induced PIP_2 and PIP turnover were significantly smaller. Similar data were reported in other systems like rat pituitary tumor cells (Wojcikiewicz and Fain, 1988) and mouse keratinocytes (Lee and Yuspa, 1991). This result is expected because only a portion of the phosphoinositide pool is hormone-sensitive (Berridge, 1987). The concomitant depletion of PI after GTP[S] stimulation was even less pronounced (about 10 %), probably because of a larger size of cellular PI pool, and mobilization of a small portion of PI appears sufficient to replenish the PIP_2 pool for hydrolysis.

Applying aluminum prior to GTP[S] stimulations, PIP_2 and PIP levels appreciably increased whereas the PI level was elevated marginally. At 50 uM aluminum (sample C), the levels of PIP and PIP_2 were reversed to the corresponding control levels. Above 200 uM aluminum (sample D and E), PIP_2 and PIP levels attained their respective plateau, about twice as high as their control values.

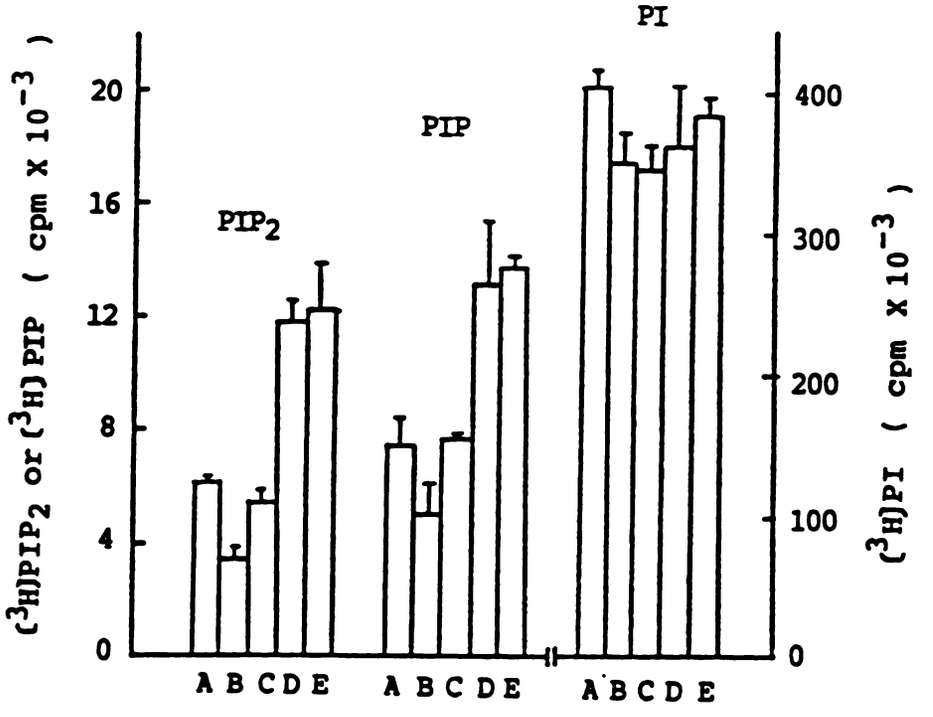

Figure 13. Effect of aluminum on GTP[S]-induced phosphoinositide turnover. Permeabilized cells were treated with 0 uM (A,B), 50 uM (C), 200 uM (D), and 500 uM (E) aluminum, for 15 min, then samples (B,C,D,E) were subsequently exposed to stimulation with GTP[S] (100 uM), for 60 min. Control A was not treated with GTP[S] during 60 min incubation. Extraction and analysis see description in Materials and Methods. Typical data are means ± SEM of duplicate samples; two independent experiments were performed.

Effects of Aluminum on Inositol Phosphate Formation Evoked by Various Divalent Cations

Application of divalent cations, Mg^{2+}, Ca^{2+} and Mn^{2+}, stimulated phosphoinositide hydrolysis in different ways (Figure 14). Mg^{2+} stimulation on inositol phosphate production was only observable in the presence of GTP[S] (bar 3), whereas effects of Ca^{2+} or Mn^{2+} appeared to be independent of G_p protein activator, i.e., enhanced formation occurred to approximately the same degree in the absence (Figure 13A) and presence (Figure 13B) of GTP[S]. Application of Mn^{2+} (bar 5) increased IP and IP_2 formation by a factor 2 - 3 but failed to elicit a detectable increase in IP_3 formation. This finding is in accord with reports that Mn^{2+} enhances phosphoinositide hydrolysis by stimulating inositol headgroup exchange in phosphatidylinositol (PI) in an agonist-insensitive pool, which is apparently inaccessible to PIP_2-specific phospholipase C (Schoepp, 1985). Addition of Ca^{2+} (bar 7) caused remarkable increases in IP_2 accumulation, accounting for 40% of total inositol phosphate, which is believed to be a characteristic of Ca^{2+}-stimulated phosphoinositide hydrolysis (Brammer et al., 1988).

Interestingly, when modulated by these cations, production of inositol phosphate responded to aluminum stress differentially (Figure 14). Upon Mg^{2+} stimulation, production of all three inositol phosphates was inhibited in a parallel manner in aluminum-stressed cells (Figure 14B, bar 4). The inhibition of

Figure 14. Effect of aluminum on Mg^{2+}-, Ca^{2+}-, or Mn^{2+}-mediated inositol phosphate formation in the presence (B), or absence (A) of GTP[S]. After pretreatment with 50 uM aluminum for 15 min, permeabilized cells were incubated with 5.0 mM Mg^{2+} (bar 3 and 4), or 5.0 mM Mn^{2+} (bar 5 and 6), or 0.5 mM Ca^{2+} (bar 7 and 8), or combinations of the respective cation with 100 uM GTP[S] (100 uM), for 60 min. Samples represented by even-numbered bars were treated with aluminum, as opposed to odd-numbered bars which were not treated with aluminum. Samples represented by bars 1 and 2 are the control, in which no divalent cation was administered. Typical data $\pm$ SEM of duplicate samples; two independent experiments were carried out.

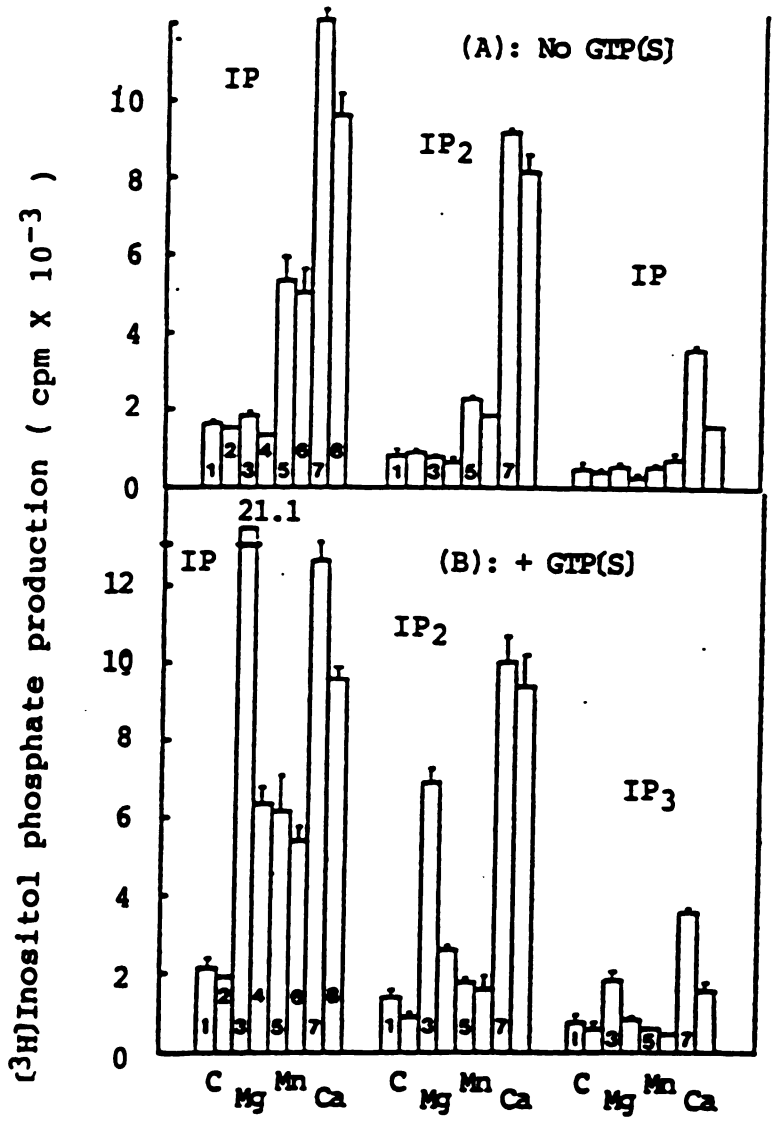

Figure 14. Effect of aluminum on Mg^{2+}-, Ca^{2+}- or Mn^{2+}-mediated inositol phosphate formation in the absence (A) or presence (B) of GTP[S].

Ca^{2+}-mediated inositol phosphate production by aluminum was found to be dependent on free Ca^{2+} concentration and inositol phosphate species. When 0.5 mM Ca^{2+} were applied (bar 8), IP_3 release was depressed more than 50% under aluminum stress. But IP_2 production decreased only 10%, and IP formation was reduced moderately (25 - 30%), and both were much less pronounced than inhibition of aluminum on Mg^{2+}/G_p-related inositol phosphate formation. This different response implies that a large proportion of Ca^{2+}-induced IP_2 was derived from other sources than dephosphorylation of IP_3, which is a major source for Mg^{2+}-related IP_2 and IP accumulation. Upon application of Mn^2, all three inositol phosphates are not all or at most marginally affected under aluminum stress (bar 6).

The different response of Ca^{2+}- and Mg^{2+}-mediated inositol phosphate formation to aluminum action was verified in cation dose-dependence experiments. To control free Ca^{2+} concentration in medium, Ca^{2+} (0 to 3.0 mM) was premixed with 3.0 mM EDTA, affording a calculated submicromolar concentrations of free Ca^{2+}. As shown in Figure 15, at 1 mM Ca^{2+} chelated with 3 mM EDTA, sharp increases in IP and IP_2 accumulation were accompanied by a concomitant IP_3 level increase, and all three species were sensitive to aluminum's inhibition, thus IP_2 and IP apparently originated from IP_3. As the Ca^{2+} dose added increased from 1 mM to 3 mM, IP_2 and IP levels were continuously enhanced, but IP_3 maintained its plateau level. Therefore, the observed increase in IP_2 and IP formation was likely derived from PIP hydrolysis.

Figure 15. Response of Ca^{2+}-mediated inositol phosphate formation to aluminum stress. After exposure to 50 uM aluminum, permeabilized cells were incubated for 60 min in an medium containing Ca^{2+} of various concentration; Ca^{2+} had been prechelated with 3.0 mM EDTA. A: IP_3 production in the absence (○) or presence (●) of aluminum. B: IP_2 (□■) and IP (○●) production in the absence (□ ○) or presence (■ ●) of aluminum. $^{*}P < 0.05$ and $^{*}P < 0.025$ by paired test.

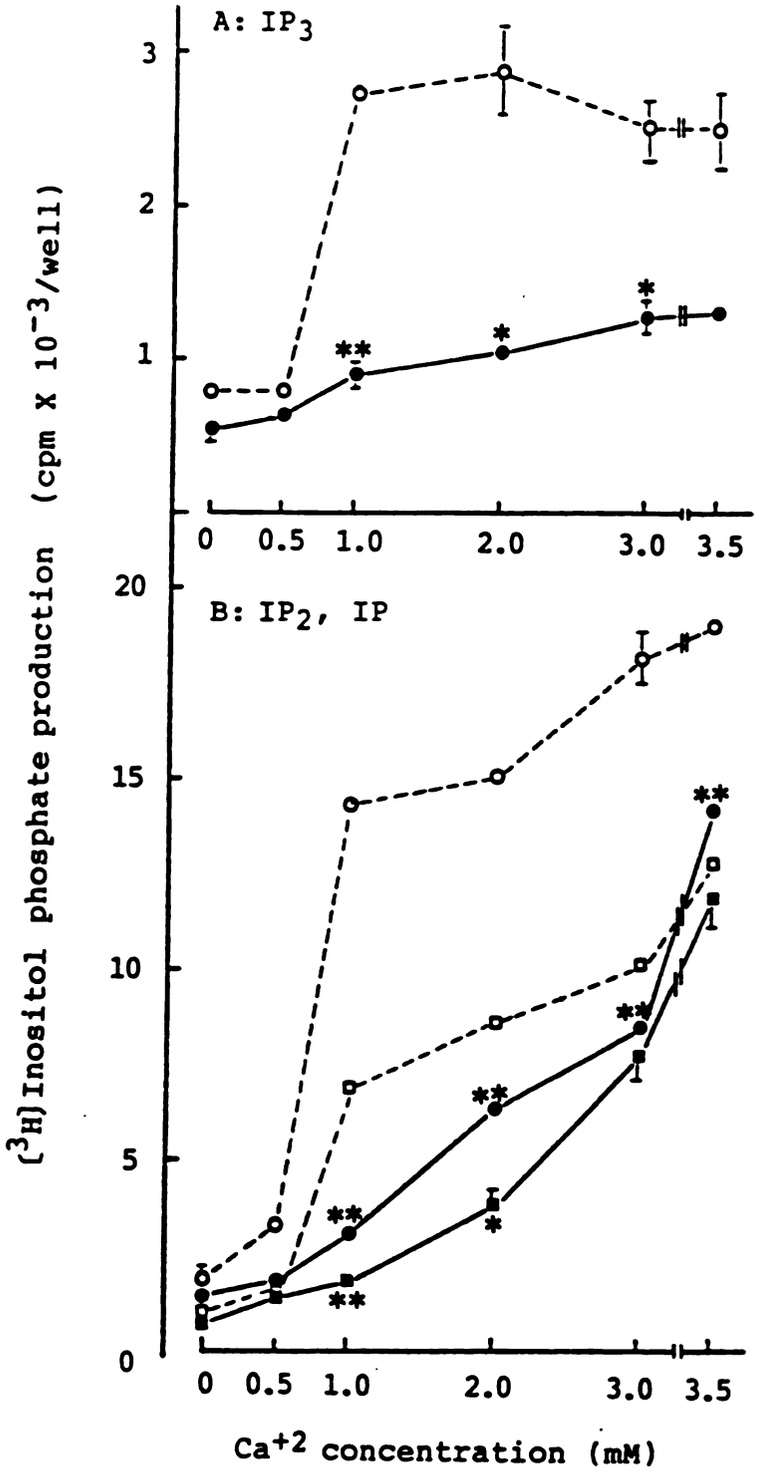

Figure 15. Response of Ca^{2+}-mediated inositol phosphate formation to aluminum stress.

In this Ca^{2+} concentration range, inhibition of IP_3 by aluminum was virtually not affected, but inhibition of IP_2 became less pronounced. Finally, when 3.5 mM Ca^{2+} were premixed with 3 mM EDTA, i.e., there were 0.5 mM non EDTA-chelated Ca^{2+} existing in the medium, inhibition of IP_2 production was almost completely eliminated. These facts suggest that Ca^{2+}-related PIP_2 hydrolysis is sensitive to aluminum's action, but Ca^{2+}-related PIP hydrolysis tends to resist aluminum inhibition, especially at high free Ca^{2+} concentrations (micromoles/ml).

The inhibition of aluminum on the Mg^{2+}/G_p protein-mediated inositol phosphate formation was affected by the Mg^{2+} dose in a differential manner (Figure 16). After the induced formation attained its maximal level at 4 mM Mg^{2+}, further increase in Mg^{2+} concentration only partially alleviated the aluminum-associated inhibition. Using the ratio of total inositol phosphate production, $(IP_T)_{+Al}$, in the presence of 50 uM aluminum over, that, $(IP_T)_{-Al}$, in the absence of aluminum as an estimate of inhibitory efficiency of aluminum. Calculation in Table 2 indicates a slightly negative correlation between Mg^{2+} concentration and aluminum's inhibiting ability. With an increase in Mg^{2+} dose from 4 mM to 8 mM, the aluminum-related reduction, $(IP_T)_{+Al}/(IP_T)_{-Al}$, increased from 0.34 to 0.50. Experiments could not be conducted at the high $[Mg^{2+}]$, where reduction of inositol phosphate formation was found.

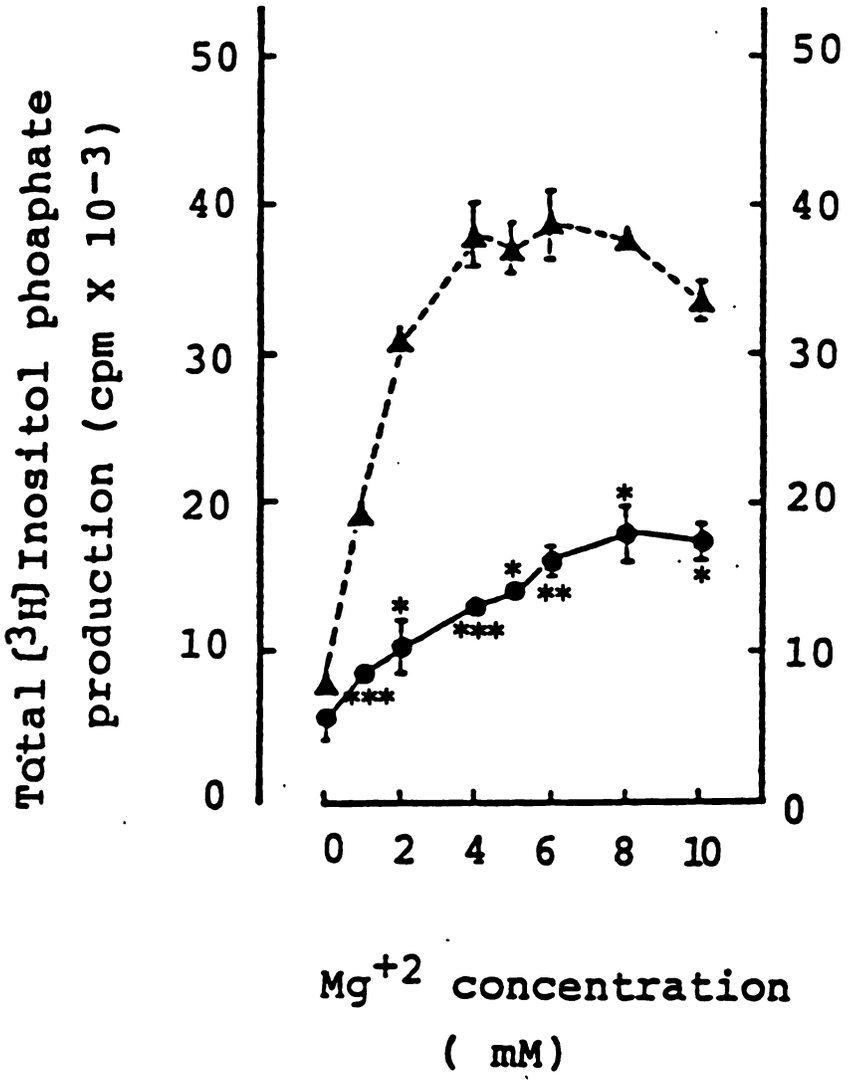

Figure 16. Mg^{2+}-dose dependence of GTP[S]-induced inositol phosphate formation. After preincubated with Mg^{2+} of various concentrations in the presence of 50 uM aluminum (●) or in the absence of aluminum (▲), permeabilized cells were treated with 100 uM GTP[S] for 1 hour. Typical data are means ± SEM of duplicate samples, two independent experiments were performed. $^{*}P < 0.05$, $^{**}P < 0.025$ and $^{***}P < 0.01$ by paired test.

Table 2. Mg^{2+}-dose dependence of aluminum-relatedinhibition of GTP[S]-stimulated inositol phosphate production

$[Mg^{2+}]$	Total inositol phosphate production (cpm/well)		
(mM)	$[IPs]_{-Al}$	$[IPs]_{+Al}$	$[IPs]_{+Al}/[IPs]_{-Al}$
0	7370 ± 170	5640 ± 290	0.76
1.0	19260 ± 680	8600 ± 30	0.45
2.0	30620 ± 1100	10110 ± 1550	0.33
4.0	38470 ± 1700	13010 ± 290	0.34
5.0	36890 ± 1670	14400 ± 0	0.39
6.0	38420 ± 2180	17450 ± 750	0.45
8.0	37380 ± 230	18650 ± 1550	0.50
10.0	33510 ± 280	17780 ± 1030	0.53

Data are derived from Fig.16. $[IP_T]_{-Al}$ represents total inositol phosphate production in the absence of aluminum; $[IP_T]_{+Al}$ represents that in the presence of 50 uM aluminum. Numbers in column 4 are the calculated ratios of values in column 3 over corresponding ones in column 2.

Effect of Aluminum on Bradykinin-mediated IP_3 Production and Intracellular Ca^{2+} Release

Stimulation of intact cells with bradykinin, a muscarinic receptor agonist, resulted in immediate increases in IP_3 formation and intracellular calcium release, in accord with previous findings (Takemura and Putney, 1989, Mouillac et al., 1989). Application of 20 uM bradykinin brought the IP_3 level to its maximal value of 4040 cpm compared with a basal level of 1090 cpm within 15 s (Figure 17A). The timing of increase in intracellular Ca^{2+} concentration (Figure 17B) resembled that of IP_3 level change; peak value of 142 $\pm$ 28 nM (n = 5) Ca^{2+} was obtained in 15 - 20 s (basal level 59 $\pm$ 13 nM).

The cell's ability to respond to bradykinin stimulation was however impaired by pre-exposure to aluminum. In aluminum-treated cells (Fig 17A and 17C), bradykinin-induced IP_3 level was lowered to 2170 nM and intracellular [Ca^{2+}] to 90 $\pm$ 18 nM (basal level 64 $\pm$ 8 nM, n = 5). After permeabilizition, cells became insensitive to bradykinin stimulation, presumably because the receptors on the cell surface were injured by digitonin treatment.

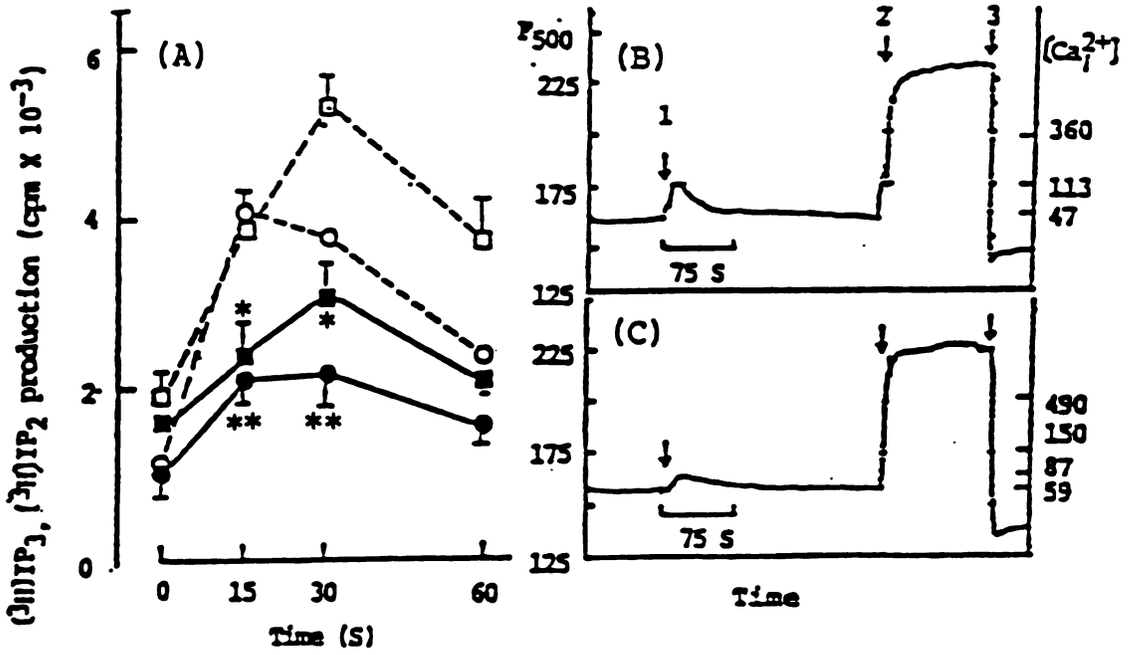

Figure 17. Inhibition of aluminum on bradykinin-triggered inositol phosphate formation (A) and intracellular Ca^{2+} release (B,C) in intact cells. A: Cells were treated with 200 uM aluminum (● ■) or with no aluminum (○ □), 30 min, followed by stimulation with 20 uM bradykinin. IP_3 (● ○) and IP_2 (■ □) production are shown. $^*P < 0.05$ and $^{**}P < 0.01$ by paired test. B and C: Fura-2 methyl ester-loaded cells were incubated with 200 uM aluminum, 30 min, then washed. For fluorescence studies at 500 nm (excitation at 339 nm), bradykinin of 10 uM final concentration was added into 3 ml cell suspension (5 x 10^5 cells/ ml). Stimulation and calibration are indicated by arrows: (1): 20 uM bradykinin, (2): 12 ug/ml digitonin, (3): 3.3 mM EGTA + 20 mM Tris.

DISCUSSION

Previous work had demonstrated that trace amounts of aluminum indeed activate G protein-mediated inositol phosphate production in the presence of fluoride (Gilman, 1987). The results from this study demonstrate for the first time at the cellular level that application of aluminum at higher concentrations reduces inositol phosphate formation. Our data suggest that the observed inhibition of inositol phosphate formation results from aluminum's interference with phosphoinositide signalling pathway, presumably at the primary targets Gp protein and phospholipase C.

In our studies, aluminum concentrations varied from 0 to 200 uM, within a range found in the brain after chronic administration to animals (Ganrot, 1986). In experimental intoxication, total brain aluminum concentrations average about 100 uM, and in some neuronal populations aluminum levels may reach 400 uM because of its nonuniform accumulation in different neurons (Nixon et al., 1990). In our system, ATP was used as a phosphate source as well as chelator to buffer aluminum. In the presence of 2.5 mM ATP, the total free Al^{3+} in the incubation medium was 10^{-10} - 10^{-12} M based on model calculation (Martin, 1986). Kinetics of aluminum exchange between various intracellular chelators is not clear. For instance, aluminum in the soluble hydrated form or other bound forms may be able to dissociate quickly enough to be available to interact with the target(s) in the signal transduction pathway.

Therefore we are here using as parameter the total aluminum dose added in the extracellular milieu.

Fluoride forms a series of aluminum-fluoride chelates (Martell and Motekaitis, 1989). Among the complexes, AlF_4^- is thought to be involved in activation of Gp protein (Gilman, 1987), leading to enhanced inositol phosphate formation. In the presence of milimolar fluoride and micromolar aluminum, AlF_4^- is apparently a major fluoroaluminate species. On first thought, the observed inhibition of inositol phosphate formation with increasing aluminum doses might be attributed to changes in speciation of fluoroaluminate complexes. Our results dispute such an explanation because the inhibition persisted despite the removal of external aluminum in the medium by washes with chelator-containing buffer, prior to fluoride addition (Figure 12B). More convincingly, in the absence of added fluoride, accumulation of inositol phosphates triggered by GTP[S] (Figure 6) or bradykinin (Figure 17) administration was also depressed in aluminum-stressed cells.

While lessening inositol phosphate production aluminum application slowed GTP[S]-stimulated PIP_2 turnover in neuroblastoma cells (Figure 13). Therefore, aluminum appears to block a site(s) responsible for PIP_2 hydrolysis along the signalling pathway, rather than upstream or downstream sites distal to PIP_2 hydrolysis. This notion is further supported by the following observations. Firstly, aluminum reduces the total inositol phosphate level principally by inhibiting IP_3 generation from PIP_2 hydrolysis. The observed lower IP and IP_2 levels in

the presence of aluminum seemed to originate from the reduction of IP_3 production rather than from depression of degradation of respective phospholipid precursors, PI and PIP. This was suggested by the temporal development of individual inositol phosphate products (Figure 11) and by the concomitant increase in [^{3}H]IP_3 level and decrease in [^{3}H]IP level following addition of "cold" IP_3 (Figure 7). PI and PIP may serve as hydrolysis substrates if Mg.ATP is not available. When ATP is added to maintain inositol lipids in the phosphorylated state, PIP_2 is reportedly the main substrate for hydrolysis (Cockcroft and Taylor, 1987). Secondly, aluminum failed to measurably interfere with Mn^{2+}- or Ca^{2+}-stimulated IP and IP_2 release, which are not coupled to G_p protein-mediated phosphoinositide hydrolysis (Figure 14).

The fact that aluminum reduces either fluoride-induced inositol phosphate formation in intact cells (Figure 5) or GTP[S]-induced inositol phosphate formation in permeabilized cells (Figure 6) suggests that the inhibition is apparently taking place at site(s) distal to receptors at the cellular surface. This notion is consistent with the finding that the aluminum-related inhibition of inositol phosphate formation was dependent on the metal's interiorization. Firstly, binding of aluminum onto the cellular surface is completed within a few minutes following aluminum treatment of cells (Shi and Haug, 1989). If aluminum acts on receptors at the cellular surface, its effect on inositol phosphate production would be seen immediately, similar to those of receptor

agonists or antagonists including metal cations (Smith et al., 1989); moreover, the inhibition should not be dependent on the preincubation time of cells with aluminum as long as surface-bound aluminum is removed. However, in our experiments, appreciably longer preincubation times were required for aluminum to become an effective inhibitor, and the extent of inhibition increased as the preincubation time was lengthened up to 60 min (curve e in Figure 11B). Secondly, inhibition of inositol phosphate formation by aluminum could be averted if cells had been preincubated with aluminum chelated to EGTA or citrate in media, thereby preventing surface binding and interiorization (Figure 12B, bar 3 and 4). Inhibition however persisted if cells were first treated with aluminum, then washed with a chelator-containing medium, in which only surface-bound aluminum was removable (Figure 12B, bar 1 and 2). Moreover, when permeabilized cells were employed, the reversion of aluminum-related inhibition by citrate- or EGTA-chelation was hardly or no longer observed (Figure 12A).

A putative target for aluminum interaction is membrane-bound Gp protein coupled to phospholipase C, whose activation is thought to be the rate-limiting step in phosphoinositide signal transduction (Gilman, 1987). Within our knowledge there has been no direct evidence for inactivation of G_p protein by aluminum, but a similar mechanism has been reported on other signal-mediating G proteins like transducin (Miller et al., 1989), and small molecular weight GTP binding proteins like tubulin (Macdonald et al, 1987).

The molecular nature regarding inactivation of G protein by aluminum is not known. Our data suggest that aluminum does not bind directly to GTP[S], because addition of GTP[S] in tenfold excess over aluminum could not reduce the aluminum-related reduction of inositol phosphate release (Figure 9). Compared with phosphate, the sulfur atom of the phosphorothioate is more nucleophilic towards "soft" ligands (Eckstein, 1985). Therefore, the "hard" aluminum aquo ion (Hartley et al., 1980) is probably only weakly bound (or not at all) to the substituent in the gamma position of GTP[S]. In addition, the probability of aluminum binding to GTP was drastically reduced since our experiments were conducted in the presence of a great excess of ATP. Moreover, when GTP was added in 20 - 100 times higher concentrations than aluminum, the aluminum -induced inhibition could not be reversed at all (Figure 10). Therefore, aluminum inhibits Gp protein-related inositol phosphate formation apparently not by forming a unusable Al-GTP complex, which would lead to depletion of the GTP pool required for Gp protein function. More likely, aluminum occupies a site at or near the nucleotide binding center on G_p protein, the formation of aluminum-liganded Gp protein hinders binding of Mg^{2+} or/and GTP on Gp protein, or prevents activation of G_p protein in response to Mg^{2+} or/and GTP binding.

As a physiological ligand for the formation of the functional GTP-bound Gp protein, Mg^{2+} is crucially involved in the regulatory cycle of G_p protein-coupled signal transduction (Freissmuth et al., 1989). Having similar ionic radii (Haug and

Weis, 1986) aluminum may compete for the binding site of Mg^{2+}. Because the ligand exchange rate of hydrated aluminum is about 10^5-fold lower than that of hydrated Mg^{2+} (Haug and Weis, 1986), kinetic features of G_p protein regulation are expected to be altered dramatically if Mg^{2+} is displaced by aluminum ion. This is illustrated by findings that aluminum inhibited the intrinsic GTPase activity of tubulin through Al^{3+}/Mg^{2+} exchange at the E site of the protein (Macdonald et al., 1987). The inactivation of transducin by aluminum was also reportedly due to aluminum's competition with Mg^{2+} on the metal-free transducin-guanine nucleotide complex (Miller et al. 1989). In our system, when GTP (5 mM) was added together with Mg^{2+} (5 mM) in excess over aluminum (50 uM), the aluminum-related inhibition could not be reversed (Figure 10). Therefore, the observed inhibition is apparently not due to the competition of two metals for GTP but for the binding site on G_p protein. The verification of the putative aluminum/Gp protein interaction requires investigations on purified Gp protein which has not been available in any system.

Inhibition of inositol phosphate formation by aluminum was only partially abolished with increasing Mg^{2+} dose (Figure 16 and Table 2). This observation might be explained by the fact that Mg^{2+} application up to 10 mM was perhaps inefficient in displacing aluminum bound on high affinity sites on the metal-Gp protein-nucleotide complex. This notion is in accord with data that the association constant for aluminum in metal-GTP-tubulin complex is approximately 10^7 times higher than that of Mg^{2+}

(Macdonald et al., 1987). Another possibility is that aluminum may have, besides Gp protein, an additional target along the phosphoinositide signal pathway.

This multitarget hypothesis is further supported by our findings that aluminum also interferes with Ca^{2+}-induced inositol phosphate production. Two separate pathways have been implicated in stimulating phosphoinositide hydrolysis (Chandler and Crews, 1990). They apparently employ distinct phospholipase C isozymes having different substrate specificity (e.g., PIP_2 vs. PIP) and Ca^{2+} sensitivity (Rhee et al. 1989). Besides the Mg/G_p protein-mediated classical pathway, phosphoinositide hydrolysis can be also stimulated directly by an increase in intracellular Ca^{2+} concentration, thus bypassing receptor and Gp protein involvement (Eberhard and Holz, 1991). Our experiments indeed corroborate the existence of these two pathways in neuroblastoma N_2A cells.

According to our data (Figure 14 and Figure 15), the substrate preference of phospholipase C activity in the Ca^{2+}-mediated pathways is seemingly dependent on intracellular free Ca^{2+} concentrations; PIP hydrolysis becomes more pronounced at high Ca^{2+} concentration (micromoles/l). It is not known whether both PIP_2- and PIP-hydrolysis activities reside in a single enzyme protein, or whether there are actually different isomers of phospholipase C involved. The dependence of PIP_2 and PIP hydrolytic rates on Ca^{2+} concentration may have its physiological significance. At high Ca^{2+} concentration, cells can

employ PIP-specific phospholipase C activity to generate DAG, a messenger signalling protein kinase C activation, without formation of unnecessary IP_3 and expenditure of an additional ATP. The inhibitory action of aluminum apparently is inclined towards PIP_2 hydrolysis over PIP hydrolysis; at micromolar free Ca^{2+}, PIP hydrolysis remains either unaffected or even slightly enhanced in the presence of aluminum.

Nevertheless, in our neuroblastoma cells, PIP_2 hydrolysis in both Mg^{2+}/G_p protein- and Ca^{2+}-mediated pathways are susceptible to aluminum inhibition. Therefore the PIP_2-specific phospholipase C reaction appears to be a likely target for aluminum. We postulate that the biphasic inhibition curve of GTP[S]-mediated inositol phosphate production (Figure 6) may represent the events occurring on these two sites. Presumably, inhibition at low aluminum concentrations (< 50 mM) is caused by inactivation of the G_p protein which is seemingly a more vulnerable, and at high concentrations by direct inhibition of phospholipase C reaction by aluminum. Here we do not rule out other means by which aluminum disturbs Ca^{2+}-mediated inositol phosphate release. For instance, aluminum may impair Ca^{2+}-calmodulin-dependent phospholipase C activity (Levine et al. 1990,) by inducing structural changes in calmodulin (Yuan and Haug, 1988).

The putative manipulation of aluminum on phospholipase C reaction may operate a different mechanism. At substrate level, theoretical evidence predicts an avid binding of aluminum to PIP_2 on 4′- and 5′-phosphate groups (Birchall and Chapell, 1988),

This aluminum-liganded PIP_2 might be less vulnerable for enzyme digestion. Such aluminum-phosphoinositide interaction was reportedly related to aluminum-caused inhibition of PIP_2 hydrolysis by purified phospholipase C from bovine heart (McDonald and Mamrack, 1988). At the enzymatic protein level, aluminum may interact directly with phospholipase C, or indirectly through its perturbation of membrane lipid environment. The hydrolyzing efficacy of phospholipases is known to be in part dependent on physico-chemical properties of their microenvironmental lipid milieu (Dennis, 1983).

The presence of aluminum up to 500 uM showed no effect on the inositol phosphate assay in column chromatography (Figure 8). This does not necessarily mean aluminum does not bind to these metabolites, particularly IP_3, in vivo. Some investigators predicted that such binding would alter the kinetics of IP_3 metabolism and the binding of IP_3 to its receptors. For instance, a prolonged half-life of aluminum-bound IP_3 may potentiate the ability of IP_3 to release Ca^{2+} from the stores (Schofl et al., 1990). But in our study, aluminum stress virtually diminished the bradykinin-induced intracellular Ca^{2+} release while reducing the bradykinin-triggered IP_3 production (Figure 17). Also, the inhibition of the 3-kinase or 5-phosphatase reaction of IP_3 by aluminum was not observed in our neuroblastoma cells and other cell systems (Shears et al., 1990).

Summing up, regarding adverse effects of aluminum in neuroblastoma cells, our data demonstrate that application of aluminum reduces inositol phosphate formation possibly through interactions with elements of phosphoinositide signal transduction. This aluminum-triggered malfunction of the universal signalling pathway in eukaryotic cells may be related to primary manifestations of aluminum toxicity by impairing the cell's ability to properly respond to diverse stimuli.

LIST OF REFERENCES

Bansal V.S. and Majerus P.W. (1990) Phosphatidylinositol-derived precursors and signals. Annu. Rev. Cell Biol. 6, 41-67.

Berridge M.J., Dawson R.M.C., Downes C.P., Heslop J.P., and Irvine R.F.(1983) Changes in the levels of inositol phosphates after agonist-dependent hydrolysis of membrane phosphoinositides. Biochem. J. 212, 473-482.

Berridge M.J. (1987) Inositol triphosphate and diacyl glycerol: two interacting second messengers. Annu. Rev. Biochem. 56, 159-193.

Birchall J.D. and Chappell J.S. (1988) Aluminium, chemical physiology, and Alzheimer's disease. Lancet, Oct. 29, ii:1008-1010.

Brammer J.B., Hajimohammadreza I., Sardiwal S and Weaver K. Is inositol bisphosphate the products of A23187 and carbachol -mediated polyphosphoinositide breakdown in synaptosomes? (1988) J. Neurochem. 51, 514-521.

Chabre M. (1990) Aluminofluoride and beryllofluoride complexes: new phosphate analogs in enzymology. TIBS 15, 6-10.

Challiss R.A.J., Batty I.H., and Nahorsky S.R. (1988) Mass measurements of inositol (1,4,5)-triphosphate in rat cerebral cortex slices using a radioreceptor assay: Effects of neurotransmitters and depolarization. Biochem. Biophys. Res. Comm. 157, 684-691.

Chandler L.J. and Crews F.T. (1990) Calcium- versus G protein--mediated phosphoinositide hydrolysis in rat cerebral cortical synaptoneurosomes. J. Neurochem. 55, 1022-1030.

Cockcroft S. and Taylor J.A. (1987) Fluoroaluminates mimic guanosine 5'-[gamma-thio]triphosphate in activating the polyphosphoinositide phosphodiesterase of hepatocyte membranes. Biochem. J. 241, 409-414.

Crapper McLachlan D.R. (1989) Aluminum neurotoxicity: criteria for assigning a role in Alzheimer's disease, in Environmental Chemistry and Toxicology of Aluminum (Lewis T.E., ed), pp. 299-315. Lewis Publ., Boca Raton, FL.

Dean N.M. and Beaven M.A. (1989) Methods for the analysis of inositol phosphates. Anal. Biochem. 183, 199-209.

Dennis E.A., Rhee S.G., Billah, M.M., and Hannum, Y.A. (1991) Role of phospholipases in generating lipid second messengers in signal transduction. FASEB J. 5, 2068-2077.

Dennis E.A. (1983) Phospholipases, in The Enzymes, vol. 16 (Boyer P.D., ed), pp. 307-353. Academic Press, New York.

Eberhard A and Holz R.W. (1991) Calcium promotes the accumulation of polyphosphoinositide in intact and permeabilized bovine adrenal chromaffin cells. Cellular and Molecular Neurobiol. 11, 357-379.

Eckstein F. (1985) Nucleoside phosphorothioates. Annu. Rev. Biochem. 54, 367-402.

Freissmuth M., Casey P.J., and Gilman A.G. (1989) G proteins control diverse pathways of transmembrane signaling. FASEB J. 3, 2125-2131.

Ganrot P.O. (1986) Metabolism and possible health effects of aluminum. Environm. Health Perspect. 65, 363-441.

Gilman A.G. (1987) G proteins: Transducers of receptor-generated signals. Annu. Rev. Biochem. 56, 615-649.

Guy S.P., Seabright P., Day J.P., and Itzhaki R.F. (1990) Uptake of aluminum by human neuroblastoma cells. J. Trace Elem. Electrolytes Health Dis. 4, 183-187.

Hartley F.R., Burgess C., and Alcock R.M. (1980) Solution Equilibria, pp. 249-274. John Wiley & Sons, New York, NY.

Haug A., and Weis C. (1986) Aluminum-induced changes in calmodulin, in Molecular and Cellular Aspects of Calcium in Plant Development (Trewavas A.J., ed), pp. 19-26. Plenum Press, New York.

Huckle W.R. and Conn P.M. (1987) Use of lithium ion in measurement of stimulated pituitary inositol phospholipid turnover. Meth. Enzymol. 141, 149-155.

Horwitz J. and Perlman R.L. (1987) Measurement of inositol phospholipid metabolism in PC12 pheochromocytoma cells. Meth. Enzymol. 141, 169-175.

Johnson G.V.W. and Jope R.S. (1986) Aluminum impairs glucose utilization and cholinergic activity in rat brain in vitro. Toxicol. 40, 93-102.

Jope R.S. (1988) Modulation of phosphoinositide hydrolysis by NaF and aluminum in rat cortical slices. J. Neurochem. 51, 1731-1736.

Lee E. and Yupsa S.H. (1991) Aluminum fluoride stimulates inositol phosphate metabolism and inhibits expression of differentiation markers in mouse keratinocytes. J. Cell. Physiol. 148, 106-115.

Levine S.N., Sonnier G.B. and Abroe K. (1990) Effects of diabetes mellitus and aluminum toxicity on myocardial calcium transport. Toxicol. 65, 137-148.

Li P.P., Sibony D. and Warsh J.J. (1990) Guanosine 5'-o-thio-triphosphate and sodium fluoride activate polyphosphoinositide hydrolysis in rat cortical membranes by distinct mechanisms. J. Neurochem. 54, 1426-1432.

Loomis-Husselbee J.W., Cullen P.J., Irvine R.F. and Dawson A.P. (1991) Electroporation can cause artefacts due to solubilization of cations from electrode plates. Biochem. J. 277, 883-885.

Macdonald T.L., Humphreys W.G. and Martin R.B. (1987) Promotion of tubulin assembly by aluminum ion. Science 236, 183-186.

Marquis J.K. (1989) Neurotoxicity of aluminum, in Environmental Chemistry and Toxicology of Aluminum (Lewis T.E., ed), pp. 289-298. Lewis Publ., Boca Raton, FL.

Martell A.E. and Motekaitis R.J. (1989) Coordination chemistry and speciation of Al(III) in aqueous solution, in Environmental Chemistry and Toxicology of Aluminum (Lewis T.E., ed), pp. 3-17. Lewis Publ., Boca Raton, FL.

Martin R.B. (1986) The chemistry of aluminum as related to biology and medicine. Clin. Chem. 32, 1797-1806.

McDonald J.J. and Mamrack M.D. (1988) Aluminum affects phospho-inositide hydrolysis by phosphoinositidase C. Biochim. Biophys. Res. Comm. 155, 203-208.

Miller J.L., Hubbard C.M., Litman B.J. and Macdonald T.L. (1989) Inhibition of transducin activation and guanosine triphosphatase activity by aluminum ion. J. Biol. Chem. 264, 243-250.

Mouillac B., Balestre M.N. and Guillon G. (1989) Transient inositol (1,4,5)triphosphate accumulation under vasopressin stimulation in WRK_1 cells: correlation with intracellular calcium mobilization. Biochem. Biophys. Res. Comm. 159, 953-960.

Nixon R.A., Clarke J.F., Logvinenko K.B., Tan M.K.H., Hoult M. and Grynspan F. (1990) Aluminum inhibits calpain-mediated proteolysis and induces human neurofilament proteins to form protease-resistant high molecular weight complexes. J. Neurochem. 55, 1950-1959.

Rhee S.G., Kim H., Suh P.G. and Choi W.C. (1991) Multiple forms of phosphoinositide-specific phospholipase C and different modes of activation. Biochem. Soc. Trans. 19, 337-341.

Schoepp D.D. (1985) Manganese stimulates the incorporation of [^{3}H] inositol into a pool of phosphatidylinositol in brain that is not coupled to agonist-induced hydrolysis. J. Neurochem. 45, 1481-1486.

Schofl C., Sanchez-Bueno A., Dixon C.J., Woods N.M., Lee J.A.C., Cuthbertson K.S.R., Cobbold P.H. and Birchall J.D. (1990) Aluminum perturbs oscillatory phosphoinositide-mediated calcium signalling in hormone-stimulated hepatoctes. Biochem. J. 269, 547-550.

Shi B. and Haug A.(1990) Aluminum uptake by neuroblastoma cells. J. Neurochem. 55, 551-558.

Simonsson P., Rodriguez F.D., Loman N. and Alling C. (1991) G protein coupled to phospholipase C: molecular targets of long-term ethanol exposure. J. Neurochem. 56, 2018-2026.

Smith J.B., Dwyer S.D. and Smith L., (1989) Cadmium evokes inositol polyphosphate formation and calcium mobilization. J. Biol. Chem. 264, 7115-7118.

Takemura H. and Putney J.W. (1989) Capacitive calcium entry in parotid acinar cells. Biochem. J. 258, 409-412.

Tojyo Y., Tanimura A., Matsui S., Matsumoto Y., Sugiya H. and Furuyama S. (1991) NaF-induced amylase release from rat parotid cells is mediated by PI breakdown leading to Ca^{2+} mobilization. Am. J. Physiol. 260, C194-C200.

Weis C. and Haug A. (1989) Aluminum-altered membrane dynamics in human red blood cell white ghosts. Thrombosis Res. 54, 141-149.

Wojcikiewicz J.H. and Fain J.N. (1988) Polyamines inhibit phospholipase C-catalyzed polyphosphoinositide hydrolysis. Biochem. J. 255, 1015-1021.

Woods N.M., Dixon C.J., Cuthbertson K.S.R., and Cobbold P.H. (1990) Fluoroaluminate mimics agonist application in single rat hepatocytes. Biochem. J. 265, 613-615.

Wakui M., Itaya K., Birchall D. and Petersen O.H. (1990) Intracellular aluminum inhibits acetylcholine- and caffeine-evoked Ca^{2+} mobilization. FEBS Lett. 267, 301-304

Yuan S. and Haug A. (1988) Frictional resistance to motions of bimane-labelled spinach calmodulin in response to ligand binding. FEBS Lettr. 234, 218-223.

Zhou R., Shi B., Chou K.C.K., Oswalt M.D., and Haug A. (1990) Changes in intracellular calcium of porcine sperm during in vitro incubation with seminal plasma and a capacitating medium. Biochem. Biophys. Res. Comm. 172, 47-53.

CHAPTER III

ALUMINUM UPTAKE BY MURINE NEUROBLASTOMA CELLS

Biao Shi and Alfred Haug

J. Neurochem. 55, 551-558

1990

ABSTRACT

Aluminum uptake in viable neuroblastoma cells was largely dependent on the medium pH. At physiological pH, cells were apparently unable to incorporate detectable amounts of aluminum in the absence of proper mediators. Aluminum uptake increased as the pH decreased, attaining a plateau at about pH 6.0. Performing experiments on 2 x 10^6 cells/ml, pH 6.0, and 25 uM aluminum in the medium, aluminum incorporation reached saturation at 5 nmol aluminum/ mg cellular protein, accounting for 60-70% of aluminum added. At pH 6.0, cells showed a large capacity of accumulating aluminum; about 70% of intracellular aluminum was associated with the postmitochondrial fraction. At neutral pH, application of transferrin seemed to facilitate aluminum translocation into cells via transferrin - transferrin receptor routes. Fatty acids were also capable of mediating aluminum uptake at neutral pH, probably by forming aluminum-fatty acid complexes. Low molecular weight aluminum chelators, like citrate, inhibited aluminum uptake with different efficiency, whereas Ca^{2+} failed to alleviate aluminum intoxication by inhibiting either aluminum incorporation into cells or aluminum superficial binding onto the cellular surface. Treatment of cells with energy metabolism inhibitors had virtually no influence on aluminum uptake, indicative of passive mechanisms. The results suggest that aluminum uptake occurs via different modes dependent on growth conditions such as medium pH.

INTRODUCTION

Aluminum toxicity in plants has been known for a long time, while its toxic effects on humans and animals have only recently been recognized. Brain and central neural systems are known as major targets of toxic aluminum, and high level accumulation of the metal in these tissues has been implicated in a number of neural diseases like dialysis encephalopathy, Alzheimer syndrome and Parkinson syndrome (Ganrot, 1986; Crapper McLachlan and De Boni, 1980).

Although aluminum is apparently involved in a broad spectrum of physiological disorders, mechanisms of its toxicity remain largely unknown. Two general hypotheses have been advanced in terms of primary injury sites. According to the extracellular lesion model, the plasma membrane is believed to play a role as the primary target. As to the intracellular lesion model, different organelles and macromolecules, e.g., chromatin (Walker et al., 1989), cytoskeleton (Macdonald et al., 1987), enzymatic proteins like hexokinase (Lai and Blass, 1984), and regulatory proteins like calmodulin (Siegel and Haug, 1983) are potential targets for aluminum intoxication. In this case the plasma membrane plays a role in the manifestation of aluminum toxicity by controlling aluminum entry. In either case, the interaction of aluminum with the plasma membrane represents the first stage of aluminum cytotoxicity. Therefore, irrespective of the target site, detailed

information about aluminum uptake by living cells is important for understanding mechanisms of aluminum toxicity.

Aluminum uptake in plants has been extensively studied, and there have been a number of reports on aluminum accumulation in human and animal model (Slanina, et al., 1986, Domingo et al., 1988). But until recently few attempts have been made regarding aluminum uptake at the cellular level partly because of technique difficulties, thus only scant data are available on cellular and molecular processes of aluminum uptake and transport, e.g., the translocatable aluminum species, potential carriers, cell's capacity of accumulating aluminum and intracellular aluminum compartmentation. In this article, we are therefore reporting results, obtained by atomic absorption spectroscopy, on aluminum uptake by murine neuroblastoma cells. Neuroblastoma cells were selected as the biological model because elevated aluminum is found in neural tissues of patients with neurological disorders (Forrester and Yokel, 1985), and because neuroblastoma cells express many of the characteristics found in normal differentiated neurons (de Laat et al., 1984).

MATERIALS AND METHODS

Chemicals

All tissue culture supplies were obtained from Gibco Co.(Grand Island, NY). Chemical reagents used were all of the highest quality available. Plastic ware, washed with diluted nitric acid and then with redistilled water, was employed to prevent aluminum contamination from the usage of glassware. All buffers and solutions were prepared from redistilled water which had been passed through a Chelex-100 column to remove residual aluminum.

Cell Culture

C1300 mouse neuroblastoma cells, clone Neuro-2A, were obtained from the American Type Culture Collection (Rockville, MD). Cells were cultured in Dulbecco-Vogt's Modified Eagle Medium (DMEM) supplemented with 5% (v/v) fetal bovine serum. Cells were grown in a humidified atmosphere of 10% CO_2/90% air at 37°C.

Monolayers of neuroblastoma cells were washed with Spiner salt solution and subsequently treated with a 0.2% trypsin solution. The trypsinized cells were removed by aspiration of incubation buffer, followed by centrifugation at 100 g for 5 min. The sedimented cells were resuspended in and washed with the incubation buffer three times, and were then available for experimental use.

Cell viability was examined by using a vital stain, viz., trypan blue. The initial viability of cells was about 95%. Prior to aluminum uptake experiments, the effect of a given experimental condition (e.g., pH, fatty acids, energy inhibitors) on cell viability was evaluated. Conditions were selected whereby viability of treated cells resembled that for untreated cells.

Measurement of Aluminum Uptake

The following standard procedure was applied for measuring aluminum uptake into cells except where indicated otherwise (Figure 1). Employing an incubation medium consisting of 140 mM NaCl, 5 mM KCl, 1 mM $CaCl_2$, 10 mM $NaHCO_3$, and 30 mM glucose, and buffered with 10 mM Tris, MES, or HEPES, depending on the desired pH range, neuroblastoma cells were resuspended to afford a cell titer of about 2×10^6/ml. The suspended cells were stressed with aluminum from a freshly prepared $AlCl_3$ stock solution, and were then incubated in a 37°C water bath with gentle shaking for the desired period of time. The final concentration of aluminum was 25 uM unless specifically indicated. Each sample was replicated four times.

To remove aluminum bound on cellular surfaces, the cell suspension was washed with citrate or EDTA. The reaction system was allowed to stand for 5 min, followed by centrifugation. The pellet was washed 1 to 2 times more with the chelator solution. Supernatants from the washes were used for the determination of the

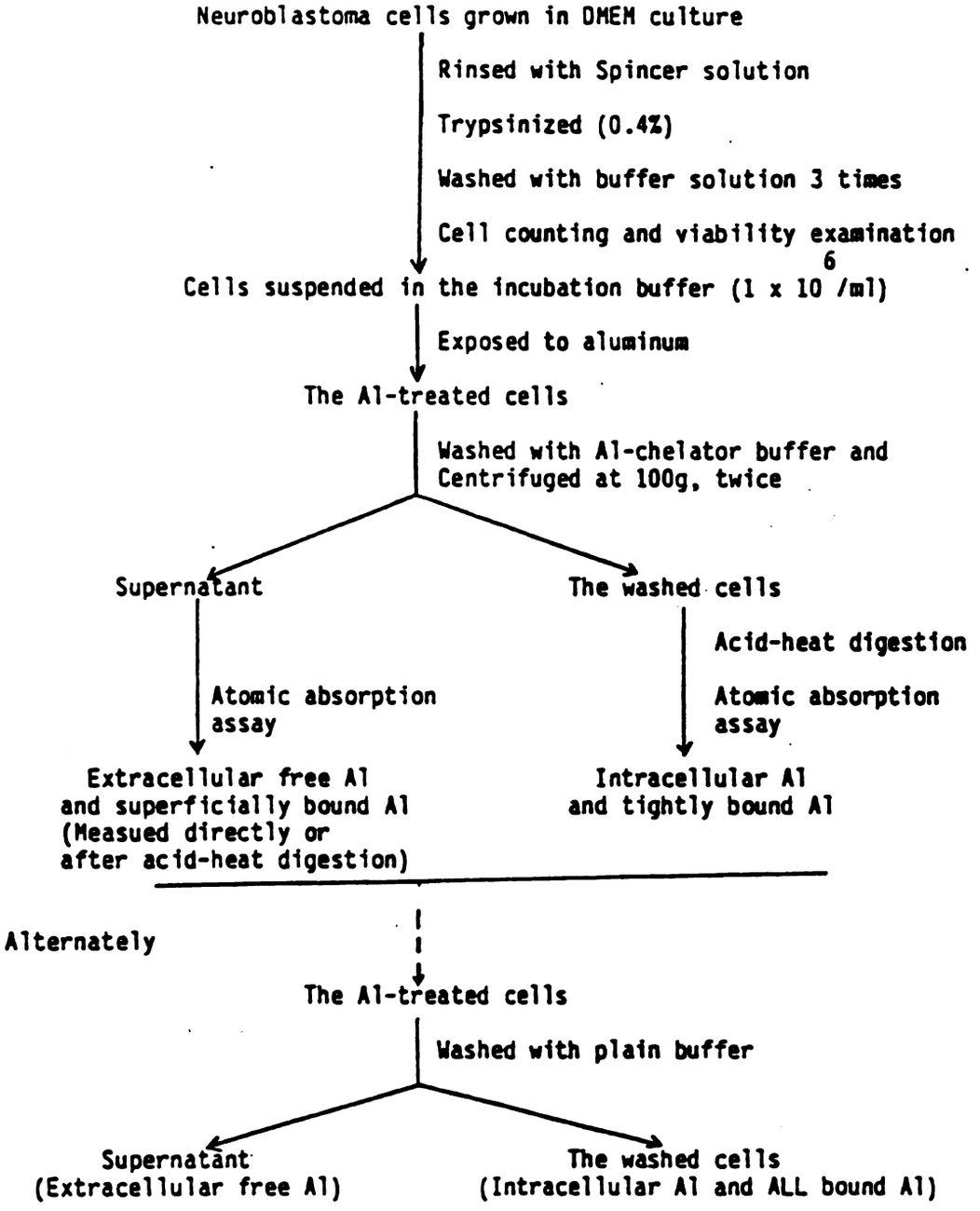

Figure 1. Experimental procedure for aluminum uptake.

aluminum fraction which had remained outside the cells. This washing procedure removed virtually all superficially bound aluminum from the cell surface, which was further verified by additional washes with chelator buffer (Table 1). Therefore, the amount of intracellular aluminum could be determined indirectly. In some cases intracellular aluminum was also determined directly by washing cell pellets 2 - 3 times with citrate or EDTA solution, followed by hot acid digestion (Pettersson et al., 1986). Within experimental errors both methods yielded the same result.

Aluminum Assay

The aluminum content was quantitatively assayed by furnace atomic absorption spectrophotometry. The samples were analyzed on a Hitachi polarized Zeeman spectrophotometer (model 108-80) employing a wavelength of 309.3 nm. Performing pre-experiments, the optimal furnace program was established by modifying a procedure described (Krishnan, et al., 1976).

TABLE 1. Recovery of aluminum by washing procedures

pH	wash agent	1st wash (ug/ml)	2nd wash (ug/ml)	3rd wash (ug/ml)	pellet (ug/ml)	total (ug/ml)	recovery (%)
7.4	citrate	630±45	25±2	18±0	43±6 (6.0%)	716	106.1
	EDTA	633±8	8±3	3±3	53±8 (7.6%)	697	103.3
6.0	citrate	253±13	48±11	25±4	335±23 (51.1%)	656	97.2
	EDTA	205±20	65±9	33±7	412±8 (57.2%)	720	106.7

Neuroblastoma cells were suspended in pH 7.4 or 6.0 incubation buffer containing 25 uM (i.e., 675 ug/ml) aluminum for 1 h. The *ashes were performed in the presence of 5 mM washing agents and the aluminum measured is listed in ug/ml. The pellets were subjected to hot acid digestion. The numbers in parenthesis under the pellet fraction represent internalized aluminum, i.e., the fraction of aluminum coprecipitated with the cell pellet relative to total aluminum measured. Recovery is calculated by dividing total aluminum measured by aluminum added (675 ug/ml).

RESULTS

Microscopic examination of cells stained with trypan blue showed that cell viability slightly declined at either pH 7.4, or pH 5.5, during 4 h incubation, but the viability was not affected by 50 uM aluminum stress (Table 2). As a control, all cells died within a few min following exposure to 1 uM $HgCl_2$. Thus, aluminum apparently exerted its toxic effects rather slowly, which is in accord with findings on neuroblastoma cells NIE-115 where aluminum toxicity became manifest only after 24 - 48 h (Roll et al., 1989).

pH Effects

In pH titration experiments, cells were washed 2 - 3 times with incubation buffers of various pH; the initial pH of cell suspension was carefully adjusted. The sample's pH was also checked at the end of the incubation period. The difference between the initial and final pH usually did not exceed 0.1 unit, and only these samples were considered in the studies.

In the physiological pH region (7.0 - 7.5), and also at pH 7.5 - 8.0, neuroblastoma cells apparently did not take up aluminum measurably, and after 1 h incubation, the intracellular aluminum content was usually less than 10% of total aluminum (25 uM) added. pH titration experiments (Figure 2) indicated that aluminum uptake by cells was enhanced dramatically when the pH was changed from pH

Table 2. Viability of neuroblastoma cells following incubation with aluminum for several hours. Viability was assayed by the trypan blue method.

Incubation pH	Al added (uM)	Viability (%) 0 h	2 h	4 h
7.4	0	93.0 ± 1.4	89.8 ± 1.2	87.0 ± 2.6
	50		90.0 ± 3.4	88.0 ± 1.2
5.5	0	94.1 ± 1.1	90.7 ± 0.9	82.7 ± 4.3
	50		85.6 ± 2.4	84.0 ± 1.3

Figure 2. pH-dependence of aluminum uptake. (a) neuroblastoma cells were twice washed with incubation buffer of various pH, then resuspended and incubated with 25 uM aluminum in buffers for 1 h. (b) cells were first incubated at the pH value indicated, in the absence of aluminum, then resuspended and incubated with 25 uM aluminum for 1 h, in pH 7.4 incu- bation buffer. (c) same as (a), except cells were incubated in buffer containing 25 uM aluminum and 3.0 uM apotransferrin. (d) net transferrin-associated aluminum uptake in the neutral pH range, obtained by subtracting data (a) from data (c). (e) Superficial binding of aluminum onto the cell surface; after incubation with aluminum for 10 min, cells were centrifuged without wash.

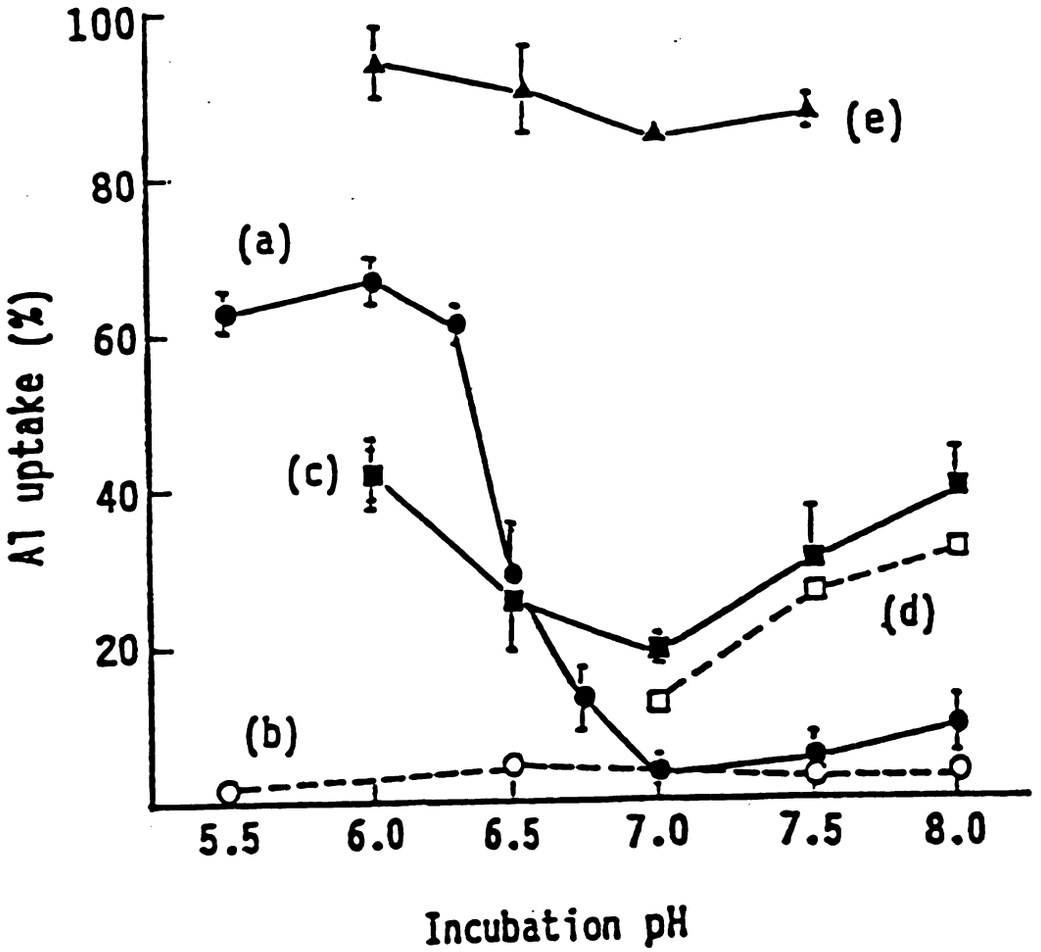

Figure 2. pH-dependence of aluminum uptake.

7.0 to 6.25. The enhanced aluminum uptake cannot be attributed to differences in washing efficiency as the pH is lowered, because the stability constants for the aluminum chelates with citrate or EDTA remained practically constant (Rajan et al., 1981), within the pH region tested. Furthermore, at a slight excess of citrate or EDTA, aluminum incorporation by the cell was prevented regardless of the medium pH. Maximal aluminum uptake reached a plateau which was maintained up to pH 5.5; beyond this value experiments were not conducted because more and more cells died. Our results are roughly consistent with other findings. Muller and Wilhelm (1987) reported that about 14% of added aluminum (100 uM, 1 h incubation) was taken up by rat hepatocytes ($5 - 6 \times 10^6$/ml), at pH 7.4.

To further investigate the pH dependence of aluminum uptake, neuroblastoma cells were first incubated in buffers of various pH, for 30 min, in the absence of aluminum. Then cells were transferred to pH 7.4 buffer and challenged with aluminum. The experimental results showed that aluminum was apparently unable to enter cells at pH 7.4, regardless of the original pH treatment (Figure 2).

Time Course and Intracellular Subdistribution

To measure kinetics of superficial binding and internalization of aluminum, aluminum-stressed neuroblastoma cells were washed with incubation buffer containing citrate, or containing no washing agent, respectively. Aluminum binding to the cell surface appeared to occur very rapidly. Within a few minutes, about 90% of added

aluminum was adsorbed onto the cellular surface (Figure 3). Unlike aluminum internalization, this superficial binding was largely pH-independent in the tested pH range (curve e in Figure 2). On the other hand, assuming a biphasic uptake process, the initial rate of aluminum uptake was estimated as 0.3 nmol aluminum/mg cellular protein/min (inner panel in Figure 3). Following this initial (about 20 min) process, the rate of uptake decreased remarkably with time. After about 1 h, metal uptake nearly attained a plateau, which in turn was accompanied by a slight increase in intracellular metal content. Under our standard experimental conditions (2 x 10^6 cells/ml, 25.0 uM Al, and 1 h incubation, at 37°C), the aluminum uptake reached saturation at about 5 nmol intracellular Al/mg cellular protein,accounting for about 60 - 70% of the metal initially applied to the medium. In control cells, incubated in aluminum-free saline, the background level of aluminum was found to be less than 0.2 uM, indicating that the aluminum uptake measured was not interfered with by metal contamination during growth and manipulation of the cells. At pH 7.4, aluminum uptake was not measurable within a monitoring period of 4 h.

The intracellular aluminum distribution (Table 3) was determined following slightly modified methods recently described (Muller and Wilhelm, 1987): after homogenization and differential centrifugation, the heat-acid digests of the cellular fractions were assayed for aluminum. After 2 h incubation, a great proportion (70%) of intra-cellular aluminum coprecipitated with post-mitochondrial components, consisting of endoplasmic reticulum,

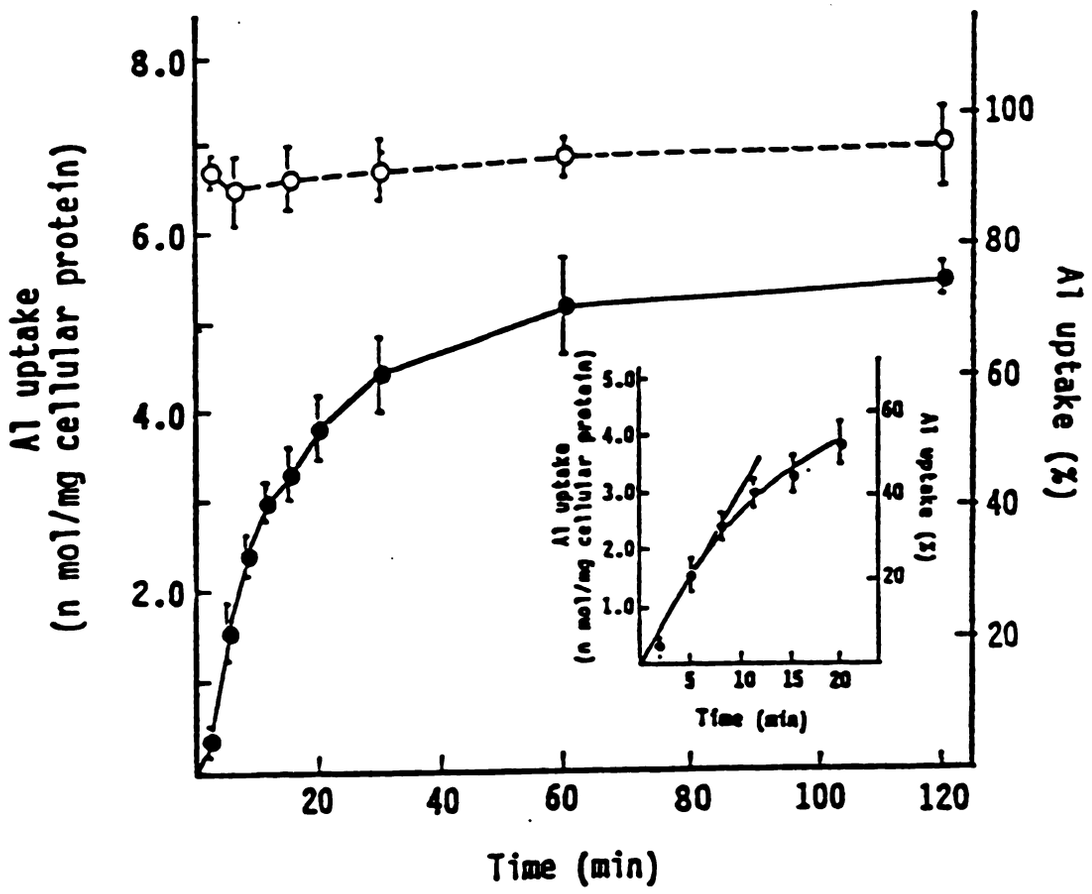

Figure 3. Time course of superficial binding of aluminum on and incorporation of aluminum in neuroblastoma cells. Incubated with 25 uM aluminum in pH 6.0 MES incubation buffer, cells were removed for aluminum assay at various times. Cells were washed with buffer containing 5.0 mM citrate to ascertain internalized aluminum (●), and also with plain buffer to estimate the sum of internalized aluminum and superficially bound aluminum (○) Inner panel: Aluminum incorporation during the first 20 min. The incorporated aluminum is shown as nmol aluminum/mg cellular protein, or the percentage of total aluminum added.

TABLE 3. Intracellular subdistribution of internalized aluminum in neuroblastoma cells

Fraction	Al content (ng Al/ mg cellular protein)	% of intracellular Al
650 g pellet (nuclear, cell debris)	28.3 ± 4.8	20.2 ± 3.4
10500 g pellet (crude mitochondria)	15.3 ± 4.2	10.9 ± 3.0
10500 g supernatant (endoplasmic reticulum, lysosomes, cytosol)	96.5 ± 10.4	68.9 ± 7.4

Cells were incubated with 25 uM aluminum in pH 6.0 MES buffer, for 2 h. Aluminum content in each fraction was determined following homogenization, differential centrifugation, and heat-acid digestion. Aluminum initially added was 3.40 ug (in 5.0 ml cell suspension). 2.34 ug aluminum was internalized, accounting for 68.8% of aluminum added, while 0.92 ug aluminum was measured extracellularly. Recovery of the added aluminum was 96.0%.

lysosomes and cytosol. About 20% of intracellular aluminum was associated with the 650 g nuclear pellet. 10% was located in crude mitochondria, a value much lower than the 40% in hepatocytes (Muller and Wilhelm, 1987), and the difference may result from hepatocytes having a highly developed mitochondrial system, accounting for 20% of the total cell volume.

Aluminum Titration

Dose-uptake experiments were performed at increasing extracellular aluminum concentrations from 0-200 uM (Figure 4). The internalized aluminum was found to increase quasilinearly in response to aluminum dose while the percentage of aluminum accumulated in cells apparently declined slightly. In other words, saturation of aluminum uptake was not observed. Our result is qualitatively consistent with that found on hepatocytes (Muller and Wilhelm, 1987) but not with that on cyanobacteria (Pettersson et al., 1986). As to the later case, a higher extracellular aluminum dose resulted in a larger percentage of aluminum accumulated intracellularly.

Effect of Transferrin

As mentioned above, aluminum was virtually excluded from uptake by cells at neutral pH in our system. However, when iron-free apotransferrin was present, the metal uptake was greater. In this

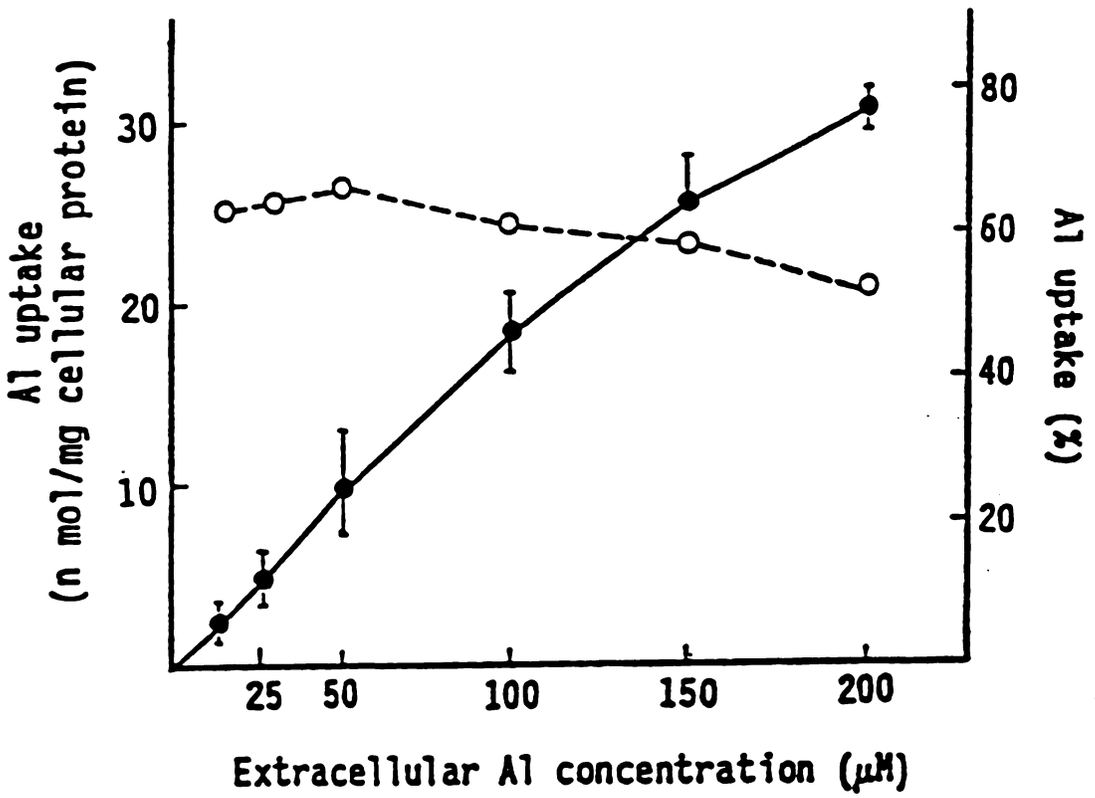

Figure 4. Dose-effect of aluminum uptake by neuroblastoma cells. Cells were subjected to extracellular aluminum of various concentrations in pH 6.0 MES incubation buffer, for 1 h. Following triple washes with buffer containing 10.0 mM citrate and hot acid digestion, the intracellular aluminum of each sample was analyzed, shown as nmol aluminum/mg cellular protein (●), or the percentage of total aluminum added (○).

study, 25 uM aluminum were preincubated with transferrin (Tf) of increasing concentrations from 0 to 12.5 uM in incubation buffer, followed by suspension of cells in buffer containing aluminum-Tf. An increase in intracellular aluminum was seen at Tf dose as low as 0.2 - 0.5 uM (Figure 5). At 2 uM Tf, a significant amount of aluminum was internalized, namely about 30% of the total metal. Whenever transferrin was used, the cells were washed with 100 uM ferric ions, in addition to citrate, to displace aluminum bound to Tf molecules adsorbed at the cellular surface (Thorstensen and Romslo, 1984), since the association constant of Fe^{+3}-Tf is 7 orders higher than that of aluminum-Tf (Cochran et al., 1984).

When transferrin was neutralized by its immunoglobulin, or saturated with iron, the increase in aluminum uptake decreased appreciably, viz, by 50% or 35% (inner panel in Figure 4). In another experiment, cells were treated with proteinase K (100 micro units) for 15 min, which only affected cell viability slightly, and aluminum uptake was found to decrease rather than increase in the presence of Tf. The protein apparently failed to enhance aluminum uptake at pH 6.0; this result agreed with the net Tf-associated aluminum uptake (Figure 2, curve d), obtained by substracting aluminum uptake in the absence of Tf (Figure 2, curve a) from that in the presence of Tf (Figure 2, curve c) in pH-titration experiments.

Figure 5. Effect of transferrin on aluminum uptake. Neuroblastoma cells were suspended in pH 7.4 Tris incubation buffer containing an aluminum-apo- transferrin mixture, prepared by preincubation of 25 uM aluminum with apotransferrin at various concentrations. After 2 h incubation, the cells were washed with buffer containing 5.0 mM citrate and 100 uM $FeCl_3$.

Inner panel: The experiments were performed similarly to those above, with 3.0 uM transferrin, except samples were treated as follows: As control, cells were incubated in the absence of apotransferrin (Con). Cells were incubated with apotransferrin (Tf), with apotransferrin which had been neutralized with antibody for 15 min (Tf + Ab). Cells were incubated with iron-saturated transferrin in the presence of 100 uM $FeCl_3$ (Fe-Tf). Cells were treated with 100 microunits proteinase for 15 min, and then incubated in the absence of apotransferrin (Pro), or in the presence of apotransferrin (Pro + Tf).

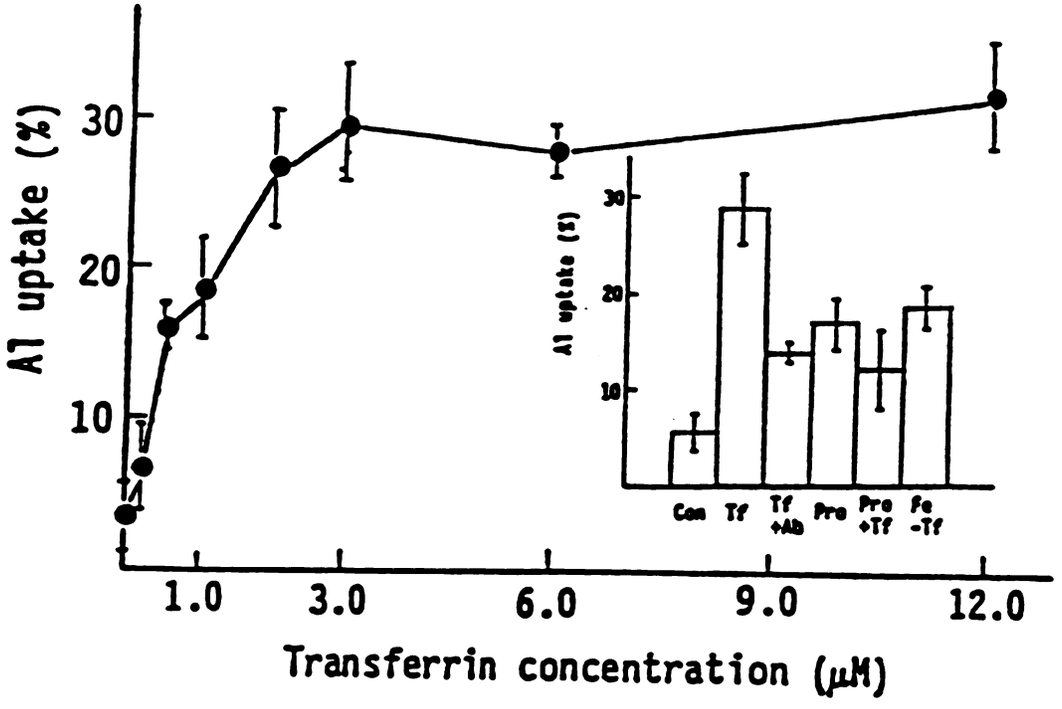

Figure 5. Effect of transferrin on aluminum uptake.

Effect of Fatty Acids

When cells were exposed to preformed fatty acid (FA)-aluminum complexes (Figure 6) at pH 6.0, nonesterified fatty acids inhibited aluminum uptake, but were appreciably less effective compared with citrate or EDTA. For instance, application of linoleic acid at 200 uM, i.e., at an 8 times higher concentration than that of aluminum, caused a decrease in metal uptake from 55% to 40%. When methyl esters of FA were applied, the inhibitory effect became much less pronounced. On the contrary, at pH 7.4, nonesterified FA, at low concentrations (0 - 200 uM), generated a moderate increase (from 10% to 25%) in aluminum uptake, followed by a further increase at higher concentrations (200 - 800 uM) whereupon many cells were not alive. There exists apparently no correlation between the efficacy of fatty acids as aluminum uptake mediators and their unsaturation degree, because all FA tested, viz., oleic, linoleic, linolenic, and arachidonic acid, produced practically the same extent of increase in aluminum incorporation. But application of corresponding methyl esters of FA had virtually no impact on aluminum uptake (Figure 6).

Alternatively, cells were loaded with fatty acids (Merrill et al., 1986) and the resuspended for aluminum stress. In this case, at pH 7.4, aluminum uptake was apparently unaffected by loading cells with 50 - 200 uM of either fatty acids or their methyl esters. Loading with 1.0 mM FA resulted in a remarkable increase (from 10% to 50%) in aluminum internalization while causing cell

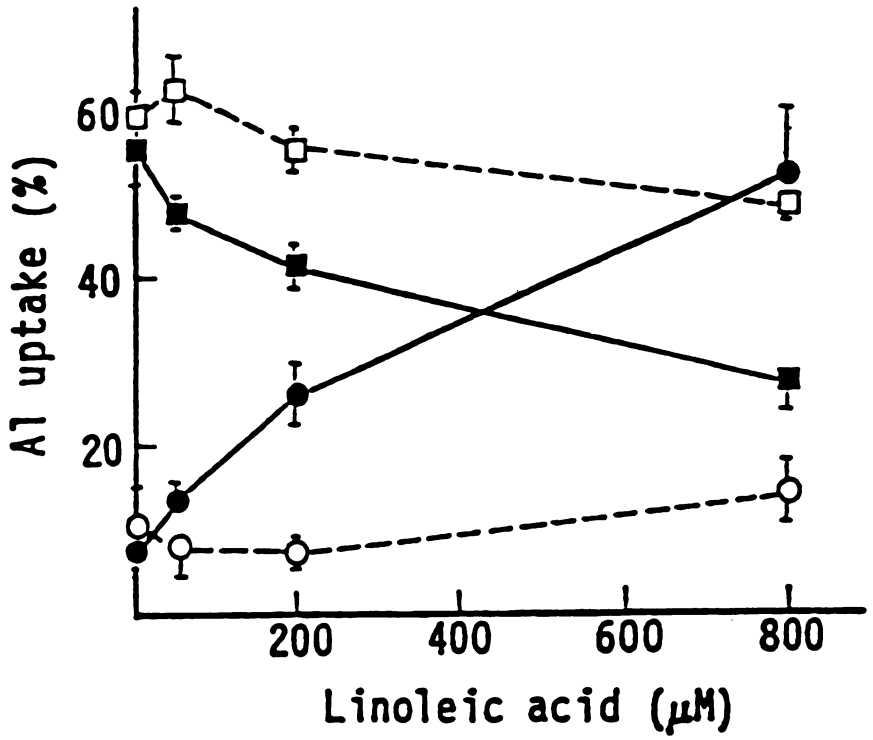

Figure 6. Effect of linoleic acid on aluminum uptake. Neuroblastoma cells were suspended in incubation buffers containing 25 uM aluminum, whose stock solution had been mixed with the colloidal suspension of fatty acids, viz., pH 7.4 Tris buffer with linoleic acid (●), or with its methyl ester (○); pH 6.0 MES buffer with linoleic acid (■), or with its methyl ester (□).

death. This high concentration FA-caused increase may be attributed to severe membrane damage caused by "detergent-like effects" of FA. The fact that depletion of FA from cells with 20 mg/ml bovine serum albumin (Simpson et al., 1988) did not affect aluminum internalization argues for such an irreversible membrane damage.

Chelator Effect

A number of aluminum chelators, either cellular metabolites such as citrate, tartrate and malate, or the lipid soluble carrier 8-hydroxy- quinoline, or the artificial compound EDTA, were tested for their roles in aluminum transport. To form metal-chelator complexes, aluminum had been preincubated with a given chelator at a molar ratio of [1 Al]:[1.5 chelator]. At neutral pH, all chelating agents studied were unable to facilitate aluminum uptake by cells (Figure 7). At acidic pH, they differentially inhibited aluminum uptake. Citrate, tartrate, and EDTA almost completely prevented the incorporation of the metal, and the intracellular aluminum diminished to less than 10% of aluminum added. 8-Hydroxy-quinoline was less effective, and the complex of aluminum with fluoride only partially inhibited the metal uptake. Whether this observation is of any biological significance is not known. Recent in vitro experiments demonstrated that specific aluminum-fluoride complexes are required for the stabilization of hepatic microsomal glucose-6-phosphatase (Lange et al. 1986), and for the activation of guanine nucleotide binding proteins (Gilman, 1987).

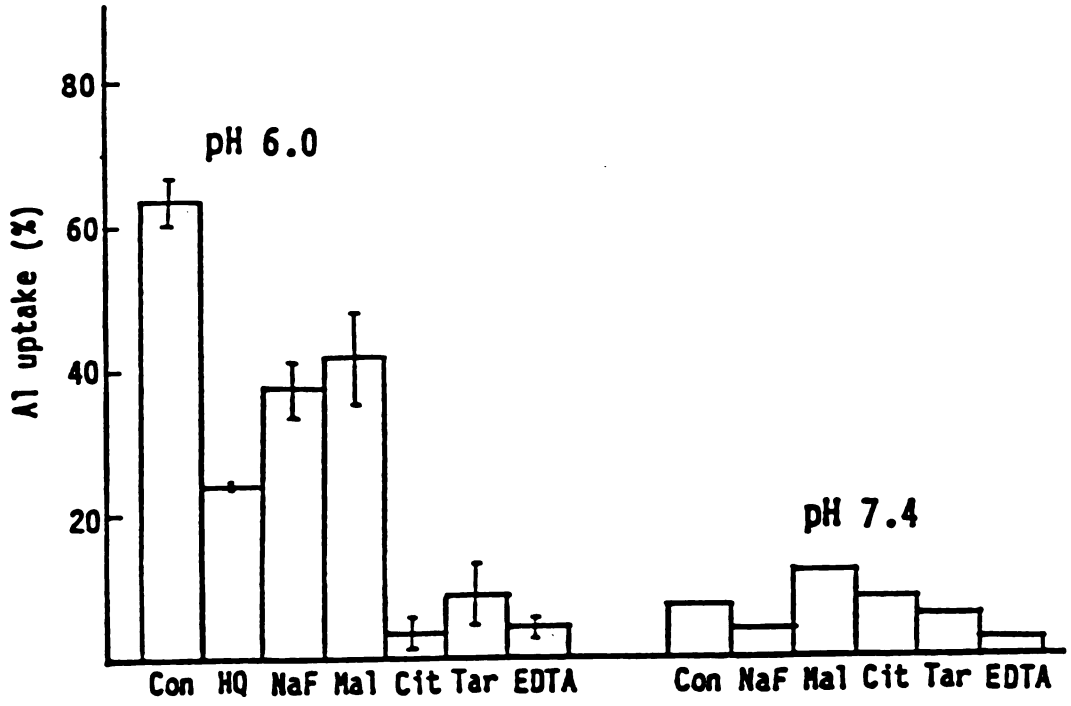

Figure 7. Effect of low molecular chelating agents on aluminum uptake. Neuroblastoma cells were incubated in pH 6.0 MES, or pH 7.4 Tris, containing 25 uM aluminum in the absence of chelator (Con), and 25 uM aluminum which had been complexed with 37.5 uM NaF, malate (Mal), citrate (Cit), tartrate (Tar), EDTA, or 25 uM 8-hydroxyquinoline (HQ). Inner panel: aluminum uptake by cells in pH 6.0 MES incubation buffer containing 25 uM aluminum precomplexed with NaF of various concentrations.

Effects of Energy Metabolism Inhibitors

The energy dependence of aluminum transport was studied by measuring the uptake by cells treated with chemicals like azide, 2,4-dinitrophenol and ouabain, which specifically block cellular energy metabolic pathways at different points. Prior to the aluminum challenge, neuroblastoma cells were pretreated with a given inhibitor of 10 uM, for 30 min, which did not influence cellular viability. At pH 6.0, application of 10 uM inhibitors showed at most marginal effects on the cell's ability to take up aluminum (Figure 8). Similar results were obtained with 250 mM inhibitors. However, at pH 7.4, it appears that treatment of cells with inhibitors (10 or 250 uM) decreased aluminum uptake. Whether the apparent slight decline at neutral pH could be interpreted as an inhibitory action of blockers is uncertain because of the low baseline uptake level and relatively high experimental errors.

Effects of Calcium, Magnesium and Phosphate.

Aluminum uptake was also compared in the presence and absence of Ca^{2+}. In this experiment, harvested cells were washed with EGTA-containing buffer to remove Ca^{2+} bound on cellular surface, then exposed to Ca^{2+} of various concentrations prior to aluminum treatment. As shown in Figure 9A, when Ca^{2+} of physiological concentration, (1 mM extracellularlly) was employed, aluminum incorporation was little affected. In the presence of 10 - 100 mM

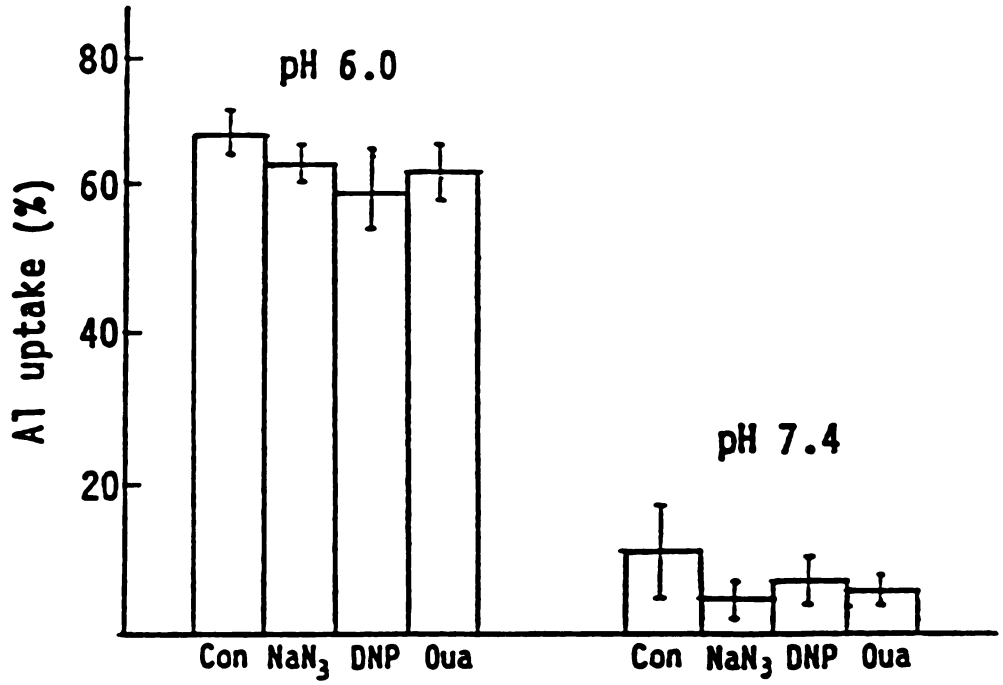

Figure 8. Effect of energy inhibitors on aluminum uptake. Neuroblastoma cells were treated with 10 uM energy inhibitors, NaN_3, dinitrophenol (DNP) and ouabain (Oua), at pH 7.4 for 30 min, and then transferred into pH 7.4 Tris, or pH 6.0 MES inhibitor-free incubation buffer, for 1 h aluminum (25 uM) stress.

Figure 9. Effect of inoganic ions on aluminum upkake.

A: Neuroblastoma cells were preincubated, 30 min, in medium containing 1.0 mM $CaCl_2$, 5.0 mM $MgCl_2$ or 0.5 mM Na_2HPO_4, then subjected to 1 h aluminum (25 uM) treatment. B: Cells were preincubated with 0 mM (●○), 10 mM (▲ △) or 100 mM $CaCl_2$ (◆◇) prior to aluminum stress. Aluminum-treated samples were taken at 20 or 60 min during the incubation for measurement of superficial binding (○ △ ◇) or uptake of aluminum (● ▲ ◆).

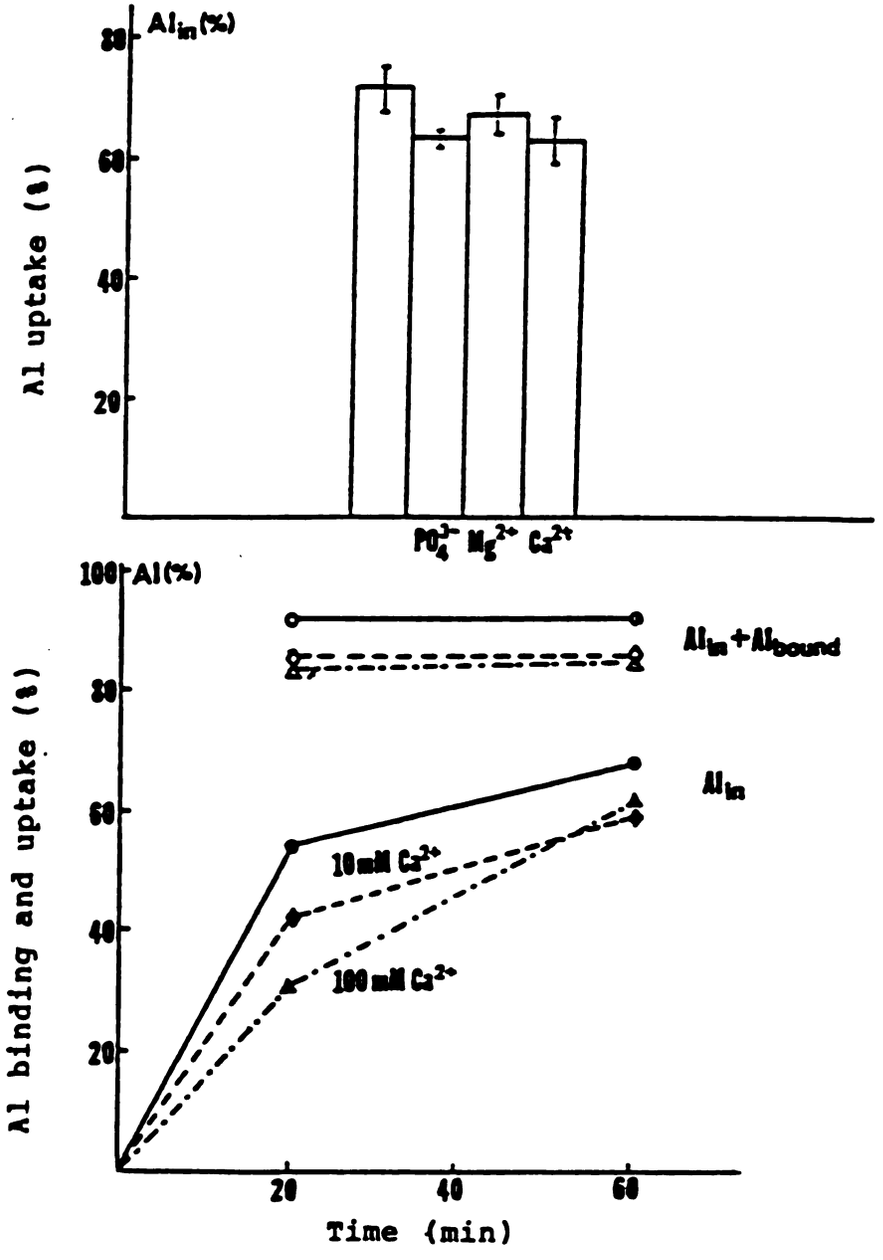

Figure 9. Effects of inorganic ions on aluminum uptake.

extracellular Ca^{2+}, superficial binding of aluminum to plasma membrane was slightly prohibited. Such high concentrations of Ca^{2+} only reduced aluminum uptake rate, but not the saturation level of aluminum incorporation (Figure 9B). Similar experiments were carried out with 5 mM Mg^{2+} and 0.5 mM PO_4^{3-}, both ions showed marginal inhibition on aluminum uptake (Figure 9A).

DISCUSSION

The major results of this investigation are that aluminum uptake by neuroblastoma cells largely depends on the pH of the suspension medium. In the neutral and acidic pH regions, the metal is probably taken up by a different mode. Transferrin and nonesterified fatty acids may facilitate aluminum uptake in the neutral pH range, while low molecular weight chelators like citrate always act as inhibitors of aluminum internalization.

To quantitatively determine aluminum uptake, chelator washes have been employed. This procedure has been widely used to *istinguish between surface bound and internalized metals including aluminum in animal tissues and cells (Bevan and Foulkes, 1989; Couri et al., 1980). Application of 1 mM EDTA reportedly removed virtually all aluminum bound onto the cellular surface of

cyanobacteria exposed to micromolar aluminum concentrations (Pettersson et al., 1986). In our experiments, a highly potent aluminum chelating agent was employed, viz., citrate, at a high concentration to enhance the washing efficacy after demonstrating that brief citrate washes did not detectably interfere with aluminum intake and exclusion. The aluminum uptake observed mainly represents a cellularly internalized aluminum fraction, even though there may be a minor metal fraction comprising metal tightly bound onto cell surfaces. This is confirmed by the following experimental observations: 1) When cells were stressed with 25 uM aluminum, the metal recovered, after more than two washes, was less than 5% of the metal in the medium (Table 1); 2) the presence of a slight excess of chelator almost completely prevented metal uptake by cells (Figure 7); 3) aluminum subcellular distribution indicated that 80% of aluminum were associated with mitochondrial and postmitochondrial fractions (Table 3).

Intracellular pH in animal cells may vary from 6.2 to 7.4 dependent on blood flow (Guyton, 1981). At neutral and slightly alkaline pH, aluminum was not taken up measurably by cells in the absence of appropriate external aluminum carriers, and the residual uptake may represent an aluminum fraction incorporated at a low level and/or specific binding on the cellular surface. This observation indicates that, at normal physiological conditions, cells do not take up toxic aluminum. However, this ability is seriously impaired as medium pH decreased (Figure 2, curve a). When neuroblastoma cells, preincubated at various pH, were transfered

into pH 7.4 medium, the aluminum uptake was indistinguishable from that of samples which remained in pH 7.4 medium. This result suggests that the elevated aluminum uptake at acidic pH is not caused by an irreversible change in membrane properties. Rather, the pH dependence of aluminum uptake may be attributed to aluminum speciation or/and reversible changes in membrane characteristics.

The potentially translocatable aluminum species have not been identified clearly (Parker et al., 1989). In the micromolar concentration range, at pH 7.4, a predominant species is $Al(OH)_4^-$, which may not be readily transported across plasma membranes. At pH 6.0, major mononuclear forms are $Al(OH)^{2+}$ and $Al(OH)_2^+$, besides small amounts of polynuclear species (Baes and Mesmer, 1976). According to our pH titration data, the positively charged mononuclear species of aluminum are more likely involved in translocation. Further characterization of transportable species is hampered by the fact that solutions of mono- and polynuclear aluminum species could be prepared only at pH 4.5 and below (Wagatsuma and Kaneko, 1987). However, at such low pH neuroblastoma cells are no longer viable.

Transferrin (Tf), the chief iron transport protein in vertebrate, has been known actively involved in iron uptake into mammalian cells (Morgan, 1988). Given similar electrochemical properties of Fe^{3+} and Al^{3+}, e.g., ionic radius and hydrolysis behavior (Birchall and Chappell, 1988), Tf are able to bind both cations with high affinities in 2 (metal) : 1 (protein) stoichiometry (Cochran et al., 1984). This protein has been shown

virtually a major carrier of aluminum, and 30% of binding sites on its molecules are occupied by aluminum (Trapp, 1983). These facts led to a hypothesis that transferrin-mediation provides a possible route for aluminum uptake by mammalian cells (Morris et al., 1987).

Our studies on neuroblastoma cells showed that transferrin may indeed mediate aluminum incorporation at neutral pH. The detailed molecular nature has not been elucidated. However, the following facts suggest that the Tf mediated-aluminum uptake may take metal-Tf-Tf receptor mechanism. First, after incubation with proteinase of low concentration (100 uM), which presumably inactivates transferrin receptors (Thorstensen and Romslo, 1984), cells were less capable of internalizing aluminum. Second, after Tf was treated with its antibody, aluminum uptake was diminished rather than enhanced, presumably neutralization of Tf impaired only its ability of binding specific receptors. The antibody-treated Tf was apparently still able of chelating aluminum but was incapable of interacting with its receptor on the membrane surface. The putative aluminum-Tf complex may be taken up per se through Tf receptor-mediated endocytosis (Morris et al, 1987), or alternatively, the metal-Tf-Tf receptor complex may deliver aluminum to a membrane-associated carrier. Recently, Roskams and Connor (1990) reported that aluminum is capable of gaining access to the cells in CNS via Tf-Tf receptor interaction under normal physiological condition. The uptake of aluminum-bound on Tf was also reported in human erythroleukaemia cells, and such interiorization was apparently responsible for downregulation of Tf

receptor expression by reducing the receptor mRNA level (Mcgregor et al., 1990). Moreover, Tf-promoted aluminum uptake was found to potentiate the antiproliferative action of aluminum in osteoblast-like cells (Kasai, et al., 1991).

Fatty acid (FA)-facilitated aluminum incorporation appears also pH- independent (Figure 6). At acidic pH, fatty acids seem to weakly block aluminum uptake as chelating agents. At neutral pH, nonesterified FA significantly enhance aluminum uptake as opposed to esterified one, implying that the carboxyl group is apparently important for mediating aluminum transport. Presumably, fatty acids facilitate aluminum uptake at by forming a transportable aluminum-FA complex, analogous to $Fe^{3+}(FA)_3$ which was reportedly involved in iron uptake by intestinal brush-border (Simpson et al., 1988). This notion is further supported by the fact that the mediating function of nonesterified FA was only observable in the presence of free FA in the incubation buffer. In experiments where FA-loaded cells had been washed with buffer, most of the remaining fatty acid molecules were incorporated into the plasma membrane and probably only few remained in suspension. As a result, mediation of aluminum uptake was no longer observable. Therefore, the mediation function of FA is not due to its modification on plasma membrane. As to esterified fatty acids, they are unable to complex aluminum with chemical bonds, rather, their molecules tend to form micellar structures which can trap aluminum from reaching the cells, resulting in the inhibition of aluminum uptake.

It is unlikely that cells have a transport device for non-essential and toxic metal cations. Hypothetically, metal cations can take advantage of non-specific transport or co-transport systems. Ca^{2+} channels were reported to provide an entry site for aluminum (Cochran et al., 1990). As to energy expenditure, in our system, none of the energy blockers tested caused a pronounced effect on aluminum uptake (Figure 8). Thus, at acidic pH, aluminum internalization occurs, at least in part, via a passive mechanism. The same conclusion has been reached with cyanobacteria (Pettersson et al., 1986). Foulkes (1988) proposed a model for the transport of non-essential and toxic metals like cadmium across cell membranes. According to this model, metal uptake first involves non-specific binding onto membrane sites, followed by metal transfer into cells via membrane carriers. Considering similarities between cadmium uptake (Planas-Bohne and Klug, 1988) and aluminum uptake processes: 1) high and rapid superficial binding on plasma membrane, 2) high level intracellular accumulation of metals, and 3) resistance to energy blockers, the Foulkes (1988) model may in part explain aluminum uptake at acidic pH in our system. The putative carrier, if any, is not known. Some lipid components in plasma membrane are presumably candidates. To illustrate, interaction of aluminum with phosphatidylcholine was reported to play a role in aluminum uptake (Akeson et al., 1989).

In our experiments, neuroblastoma cells apparently accumulated a considerable amount of aluminum. Recently, Guy et al., (1990) reported that human neuroblastoma cells (IMR-32) were able to

establish a saturation level of 10 - 20 mM intracellular aluminum, against 100 uM external aluminum in the medium. The accumulation of a large amount of aluminum in neuroblastoma cells is not necessarily linked to active transport processes, and it can be also attributed to large labile intracellular aluminum-chelating pool, including inorganic and organic polyphosphates, binding proteins, and low molecular weight ligands (Birchall and Chappel, 1988). Presumably, aluminum binds to its intracellular chelators rapidly after entering the cells, and free aluminum concentration in the cell remains very low, shifting the equilibrium for the influx of aluminum. Because a great portion of intracellular aluminum was recovered from postmitochondrial components (Table 3), aluminum may be potentially associated with the cytoskeleton in cytosol. This interaction is illustrated by the finding of aluminum-induced tangles composed of straight neurofilaments (Perl and Pendlebury, 1986).

Cellular metabolites with low molecular weight and aluminum -chelating ability, like citrate, are believed to play important roles in aluminum metabolism in living cells. There have been two conflicting models: facilitation model and detoxification model. Facilitation model suggests that complexations of aluminum with chelating metabolites provides an effective means for aluminum's translocation into cells (Martin, 1986). In animal tests, citrate chelation reportedly enhanced aluminum accumulation in plasma of human (Slinina et al., 1986) and in brain and nerve tissues of rat (Slanina et al., 1984). However, there have been more experimental

evidence for the detoxification model. In aluminum-tolerant plants, cells reduce aluminum uptake by releasing increasing amount of chelating metabolites to trap aluminum extracellularly (Koyama et al., 1988). In experimental animals, citrate and other chelating metabolites significantly increased aluminum excretion and reduced aluminum concentration in various organs and tissues (Domingo et al., 1988). Liposome studies suggest that the permeability of bilayer membrane to neutral aluminum-citrate is very small (Akeson and Munns, 1989). The data of this study are in accord with the detoxification model: all chelators tested were found to inhibit aluminum uptake by neuroblastoma cells (Figure 7). A similar finding was obtained with human neuroblastoma cells (Guy et al., 1990).

Among metal cations, Ca^{2+} is a well-known effective ameliorator to relieve aluminum intoxication. On the other hand, cellular Ca^{2+} metabolism is interfered with by aluminum in an inhibitory manner. The negative interplay between two elements has been explained by "displacement" hypothesis, i.e., they compete for binding site on crucial cellular components like receptors on plasma membrane (Parker et al., 1989). However, in our system, the presence of Ca^{2+} in the medium did not reduce the superficial binding of aluminum on cellular surface. The reduction of aluminum uptake rate is only observable at extracellular Ca^{2+} concentrations 10 - 100 times higher than the normal physiological level (Figure 9). Theoretically, the size of Ca^{2+} in its favored 8-fold coordination is 9 times greater than that of Al^{3+} in its

6-fold coordination, the substitution of one for another appears improbable (Macdonald and Martin, 1988). Therefore, it is unlikely that Ca^{2+} ameliorates aluminum toxicity simply by displacing the latter on the cellular surface, thus preventing aluminum uptake or other events. Similarly, the downregulation of aluminum on cellular Ca^{2+} metabolism may not occur at outer cellular surface but at intracellular site(s). This hypothesis is consistent with recent findings that aluminum interferes with Ca^{2+} regulation through its interactions with intracellular Ca^{2+} signalling pathway (Wukei et al., 1990).

LIST OF REFERENCES

Akeson M.A. and Munns D.N. (1989) Lipid bilayer permeation by neutral citrate and by three hydroxy carboxylic acids. Biochim. Biophys. Acta 984, 200-206.

Akeson M.A., Munns D.N. and Burau R.G. (1989) Adsorption of Al^{3+} to phosphatidylcholine vesicles. Biochim. Biophys. Acta. 986, 33-44.

Baes C.F. and Mesmer R.E. (1976) The Hydrolysis of Cations, pp. 112-123. J. Wiley & Sons, New York.

Bevan C. and Foulkes E.C. (1989) Interaction of cadmium with brush border membrane vesicles from the rat small intestine. Toxicol. 54, 297-309.

Birchall J.D. and Chappell J.S. (1988) Aluminium, chemical physiology, and Alzheimer's disease. Lancet ii, 1008-1010.

Cochran M., Coates J., and Neoh S. (1984) The competitive equilibrium between aluminium and ferric ions for the binding sites of transferrin. FEBS Lett. 176, 129-132.

Cochran M., Goddard G. and Ludwigson. N. (1990) Aluminum absorption by rat duodenum: further evidence of energy-dependent uptake. Toxicol. Lett. 51, 287-294.

Couri D., Liss L., and Ebner K. (1980) Determination of aluminum in biological samples. Neurotox. 1, 17-24.

Crapper-McLachlan D.R., and DeBoni U. (1980) Etiologic factors in senile dementia of the Alzheimer type, in Aging of the Brain and Dementia (Amaducci A., Davison A.N., and Antuono P., eds) vol. 13, pp. 173-181. Raven Press, New York.

de Laat S.W., Bluemink J.G., Boonstra J., Mummery C.L., van der Saag P.T., and van Zoelen E.J.J. (1984) Membrane fluidity in growth and differentiation; the neuroblastoma cell model, in Physiology of Membrane Fluidity (Shinitzky M., ed), vol. II, pp. 21-51. CRC Press, Boca Raton, FL.

Domingo J.L., Gomez M., and Llobet J.M. (1988) Citric, malic, and succinic acids as possible alternatives to deferroxamine in aluminum toxicity. Clin. Toxicol. 26, 67-79.

Forrester T.M. and Yokel R.A. (1985) Comparative toxicity of intracerebro ventricular and subcutaneous aluminum in the rabbit. Neurotox 6, 71-80.

Foulkes E.C. (1988) On the mechanism of transfer of heavy metals across cell membranes. Toxicol. 52, 263 - 272.

Ganrot P.O. (1986) Metabolism and possible health effects of aluminum. Environm. Health Perspect. 65, 363-441.

Gilman A.G. (1987) G protein: Transducer of receptor-generated signals. Annu. Rev. Biochem. 56, 615-649.

Guy S.P., Seagright P. and Itzhaki R.F. (1990) Uptake of aluminum by human neuroblastoma cells. J. Trace Elem. Electrolytes Health Dis. 4, 183-187.

Guyton A.C. (1981) Medical Physiology, p.448. W.B. Saunders Publ., Philadelphia.

Kasai K., Hori M.T. and Goodman W.G. (1991) Transferrin enhances the antiproliferative effect of aluminum on osteoblast-like cells. Am. J. Physiol. 260, E537-E543.

Koyama, H., Okawara, R., Ojima, K., and Yamaya, T. (1988) Reevaluation of characteristics of a carrot cell line previously selected as aluminum-tolerant cells. Physiol. Plant. 74:683-687.

Krishnan S.S., Quittkat S., and Crapper D.R. (1976) Atomic absorption analysis for traces of aluminium and vanadium in biological tissue. — A critical evaluation of the graphite furnace atomizer. Canad. J. Spectrosc. 21, 25-30.

Lai J.C.K. and Blass J.B. (1984) Inhibition of brain glycolysis by aluminum. J. Neurochem. 42, 438 - 446.

Lange A.J., Arion W.J., Burchell A., and Burchell, B. (1986) Aluminum ions are required for stabilization and inhibition of hepatic microsomal glucose-6-phosphatase by sodium fluoride. J. Biol. Chem. 261, 101-107.

Macdonald T.L. and Martin R.B. (1988) Aluminum ion in biological systems. Trends Biochem. Sci. 13/1, 15-19.

MacDonald T.L., Humphreys W.G., and Martin R.B. (1987) Promotion of tubulin assembly by aluminum ions in vitro. Science 236, 183-186.

Martin R.B. (1986) The chemistry of aluminum as related to biology and medicine. Clin. Chem. 32, 1797-1806.

McGregor S.J., Naves M.L., Oria J.K., Vass J.K. and Brock H. (1990) Effect of aluminum on iron uptake and transferrin-receptor expression by human erythroleukaemia K562 cells. Biochem. J. 272, 377-382.

Merrill A.R., Proulx P., and Szabo A. (1986) Effects of exogenous fatty acids on calcium uptake by brush-border membrane vesicles from rabbit small intestine. Biochim. Biophys. Acta 855, 337-344.

Morgan E.H. (1988) Membrane transport of non-transferrin-bound iron by reticulocytes. Biochim. Biophys. Acta 943, 428-439.

Morita K., Inoue S., Murai Y., Watanabe K., and Shima S. (1982) Effects of metals, Be, Fe, Cu and Al, on the mobility of immunoglobulin receptors. Exper. 38, 1227 -1228.

Morris C.M., Candy J.M., Court J.A., Whitford C.A., and Edwardson J.A. (1987) The role of transferrin in the uptake of aluminium and manganese by the IMR-32 neuroblastoma cell line. Biochem. Soc. Trans. 15:498.

Muller L. and Wilhelm M. (1987) Uptake and distribution of aluminium in rat hepatocytes and its effect on enzyme leakage and lactate formation. Toxicol. 44, 203 - 212.

Park D.R., Zelany L.M. and Kinraide T.B. (1989) Chemical speciation anf plant toxicity of aqueous aluminum. In Environmental Chemistry and Toxicology of Aluminum. (Lewis T.E. ed), pp 299-315. Lewis Publ. Boca Raton, FL.

Perl D.P. and Pendlebury W.V. (1986) Aluminum neurotoxicity: Potential role in the pathogenesis of neurofibrillary tangle formation. Can. J. Neurolog. Sci. 13, 441-445.

Pettersson A., Hallbom L., and Bergman B. (1986) Aluminium uptake by Anabaena cylindrica. J. Gen. Microbiol. 132, 1771-1774.

Planas-Bohne F. and Klug S. (1988) Uptake of cadmium into cells in culture. Toxicol. Environm. Chem. 18, 229-238.

Rajan K.S., Mainer S., Rajan N.L., and Davis J.M. (1981) Studies on the chelation of aluminum for neurobiological application. J. Inorg. Biochem. 14, 339-350.

Roskams A.J. and Connor J.R. (1990) Aluminum access to the brain: a role for transferrin and its receptor. Proc. Natl. Acad. Sci. USA. 87, 9024-9027.

Roll M., Banin E., and Meiri H. (1989) Differentiated neuroblastoma cells are more susceptible to aluminium toxicity than developing cells. Arch. Toxicol. 63, 231-237.

Siegel N., and Haug A. (1983) Aluminum interaction with calmodulin: Evidence for altered structure and function from optical and enzymatic studies. Biochim. Biophys. Acta 744, 36-45.

Simpson R.J., Moore R., and Peters, T.J. (1988) Significance of esterified fatty acids in iron uptake by intestinal brush-border membrane vesicles. Biochim. Biophys. Acta 941, 39-47.

Shi B. and Haug A. (1988) Uptake of aluminum by lipid vesicles. Toxicol. Environm. Chem. 17, 337-349.

Slanina P., Falkeborn Y., Frech W., and Cedergren A. (1984) Aluminium concentrations in the brain and bone of rats fed citric acid, aluminium citrate or aluminium hydroxide. Food Chem. Toxicol. 22, 391- 397.

Slanina P., Frech W., Ekstrom L., Loof L., Slorach. S and Cedergren. A.(1986) A Dietary citric acid enhances absorption of aluminum in antiacids. Clin. Chem. 32, 539-541.

Thorstensen K. and Romslo I. (1984) Albumin prevents nonspecific transferrin binding and iron uptake by isolated hepatocytes. Biochim. Biophys. Acta 804, 393-397.

Trapp G.A. (1983) Plasma aluminum is bound to transferrin. Life Sciences. 33, 311-316.

Wagatsuma T. and Kaneko M. (1987) High toxicity of hydroxy-aluminum polymer ions to plant roots. Soil Sci. Plant Nutr. 33, 57 -67.

Walker P.R.. LeBlanc J., and Sikorska M. (1989) Effects of aluminum and other cations on the structure of brain and liver chromatin. Biochem. 28, 3911-3915.

Wakui M., Itaya K., Birchall D. and Petersen O.H. (1990) Intracellular aluminum inhibits acetylcholine- and caffeine-evoked Ca^{2+} mobilization. FEBS Lett. 267, 301-304.

CHAPTER IV

SUMMARY AND PERSPECTIVES

The aim of this dissertation is to explore cellular aspects of aluminum intoxication in an effort to enhance our understanding of interactions between aluminum and living cells. Using cultured neuroblastoma N_2A cells as biological model, the study focuses on aluminum uptake by cells and modulation of aluminum on inositol phosphate formation.

Aluminum accumulation has been demonstrated clinically and experimentally in tissues, in particular brain and central nervous system, of patients and animal models. The data in this dissertation present information regarding potential uptake of aluminum by neural cells:

1. In the physiological pH region, neuroblastoma cells did not incorporate measurable amounts of aluminum, suggesting that cells do not take up the toxic element under normal physiological conditions.

2. With the aid of proper mediators, neuroblastoma cells are capable of accumulating large amounts of aluminum. Among the possible carriers, transferrin, a major aluminum ligand in plasma, may have biological importance in transporting the metal into neurons, possibly through a transferrin receptor-mediated route. On the other hand, low molecular weight cellular metabolites with aluminum-chelating ability perhaps protect cells by inhibiting aluminum internalization.

3. Enhanced aluminum uptake by cells was observed as the medium pH decreased. Cells incorporate aluminum at acidic pH probably by

a different mechanism from that at physiological pH, likely through a non-specific carrier-mediated passive pathway.

Once aluminum is internalized into neuroblastoma cells, our data suggest that a potential primary cellular lesion for aluminum intoxication is inositol phosphate metabolism, which serves as a major device to regulate intracellular Ca^{2+} mobilization and protein kinase C activity:

1. Distinct from the activation mode of the phosphoinositide signal pathway by fluoroaluminate, aluminum reduces inositol phosphate production stimulated by G_p protein activator GTP[S] or fluoride, or triggered by the receptor agonist bradykinin. As a consequence, bradykinin-evoked intracellular Ca^{2+} release is depressed.

2. Accompanying inhibition of inositol phosphate formation, aluminum lessens IPI_2 and PIP depletion. Experimental results indicated that aluminum reduces inositol phosphate production mainly by inhibiting IP_3 generation from PIP_2 by phospholipase C reaction. Aluminum apparently does not interfere with the downstream kinase or phosphatase reactions after IP_3 formation.

3. The inhibition of aluminum on inositol phosphate production is dependent on aluminum's interiorization. The aluminum's action on phosphoinositide signal pathway probably occurs at site(s) distal to receptors on the cellular surface.

4. Phosphoinositide hydrolysis in neuroblastoma cells can be stimulated directly by an increase in intracellular Ca^{2+}

concentration, bypassing G_p protein mediation. The Ca^{2+}-induced IP_3 production, like the Mg/G_p protein-induced one, is sensitive to the inhibitory effect of aluminum, but Ca^{2+}-induced IP_2 production is not affected by aluminum.

5. Proposing a mechanism, our results can be explained by ascribing changes in inositol phosphate formation to aluminum interactions with elements in the inositol phosphate signalling process. Presumably, aluminum binds at or near the nucleotide binding center of G_p protein, and the formation of nonfunctional aluminum-liganded G_p protein impedes Mg^{2+} or/and GTP binding, or prevents the activation of G_p protein in response to Mg^{2+} or/and GTP binding. Phospholipase C is also a possible target.

6. Finally, our study shows that the murine neuroblastoma N_2A cell line N_2A could be useful cell culture, in addition to conventionally used neuroblastoma cell lines human SH-SY5Y (Lambert et al., 1991), murine NIE 115 and murine neuroblastoma X glioma hybrid NG108-15 cells (Glanville et al., 1989), in investigation of phosphoinositide signalling pathway in neuronal cells.

Towards the end of this dissertation, it is important to point out that many questions remain open in the above areas. Hopefully, further investigation will yield insights into the cellular process of aluminum intoxication and generate more knowledge in developing a strategy for an therapy of the aluminum toxicity syndrome.

To explore the detailed process of aluminum's inhibition, molecular levels are certainly needed, which largely rely on

isolation and purification of key elements associated with the phosphoinositide signal transduction pathway. The attempt to isolate G_p proteins has not been successful, but in recent years, a number of distinct phospholipases C molecules, including isomers of the major enzyme found in cultured neuroblastoma cells, have been purified from a variety of mammalian tissues, and several forms have been molecularly cloned and sequenced (Rhee et al., 1991). The expression of cDNAs which encode phospholipase C and G_p protein and usage of immunological methodologies will be a promising molecular approach to elucidate the putative pathology of aluminum in the signalling pathway.

When functional preparations of phospholipase C or and/G_p protein are available, experiments can be designed in cell-free reaction systems, which contain the relevant enzyme activities and essential factors, to reexamine aluminum's effect. Alternatively, experiments can be performed in membrane vesicles, either plasma membrane preparation or lipid model membranes, which are reconstituted with receptor, G_p protein, phospholipase C and other components, but such reconstitution has not been successful yet in any system (Nozawa et al., 1991).

The purified proteins provide approaches to probe into molecular nature of interactions between aluminum and its targets, especially by physico-chemical means. For instance, the guanine nucleotide binding domain of G proteins contain a tryptophan residue (Kahn, 1991); by monitoring intrinsic tryptophan fluorescence, information will be provided as to any aluminum

binding, and how this binding changes the local environment around the nucleotide binding center. Based on the fluorescence spectra and lifetime measurement and fluoride NMR data, Hazlett et al., (1990) showed that fluoroaluminate did not bind to the nucleotide binding site of "little" monomer GTP binding proteins like EF-Tu. A similar conclusion was reached in a biochemical study which indicated that fluoroaluminate did not change proteolytic sensitivity and the aminoacyl-tRNA affinity of EF-Tu which is brought about by GTP[S] (Kraal et al., 1990).

At the cellular level, only one arm of the phosphoinositide signalling pathway, namely IP_3/Ca^{2+} messenger system, has been investigated in terms of the aluminum effect. It would be interesting to find whether and how aluminum modifies protein kinase C activity through the diacylglycerol (DAG) arm. The response of Ca^{2+}-induced phosphoinositide hydrolysis to aluminum stress is another subject worthy of further studies, because of its distinction from G_p protein-coupled pathway. For instance, Eberhard and Holz (1991) recently proposed that Ca^{2+} promotes generation of IP_3 and DAG not only by acting at phospholipase C but also by increasing the synthesis of hydrolytic substrate phosphoinositides. The experiment should be carried out in a system where intracellular Ca^{2+} concentration is well-defined. The information will be useful to locate more precisely the putative action site(s) of aluminum in IP_3/Ca^{2+} regulation, e.g., the direct inhibition of phospholipase C enzyme.

As to aluminum uptake studies, the role of transferrin in aluminum transport will remain as a hot spot of this area, e.g., what are the destinations of aluminum-carried transferrin on plasma membrane? Is it indeed bound to coated pits where it is internalized by energy-dependent endocytosis? In which intracellular compartment(s) is aluminum located following interiorization? What is the fate of transferrin following aluminum-diassociation, is it recycled to the cellular surface, or degraded in lysosomes? Experimentally, these questions may be answered by monitoring the uptake and recycling of aluminum-loaded [^{125}I]apotransferrin, using pronase digestion of cells to distinguish surface-bound from internalized Al-transferrin.

It is believed that individual vulnerability to aluminum toxicity may depend on genetic factors influencing intake, transport, or excretion (Birchall and Chappell, 1989). Therefore, a possible approach to reveal the interrelation between aluminum uptake and aluminum intoxication is to screen aluminum-tolerant or resistant cell lines, and to compare aluminum uptake in these cells with that in aluminum sensitive cells. This method has been employed in cultured plant cells to analyze the endogeous mechanism to protect plants from aluminum injury (Koyama et al., 1988). It may also find its use in neural cell study, even though the screening of aluminum-resistant mammalian cells is expected to be more difficult.

LIST OF REFERENCES

Birchall C. and Chapell J.S. (1988) Aluminum, chemical physiology, and Alzhemer,s disease. Lancet ii, 1008-1110.

Eberhard D.A. and Holz R.W. (1991) Calcium promotes the accumulation of polyphosphoinositides in intact and permeabilized bovine chromaffin cells. Cellular and Molecular Neurobiol. 11, 357-370.

Glanville N.T., Byers D.M., Cook H.W., Spence M.W. and Palmer F.B.St.C. Palmer, (1989) Differences in the metabolism of inositol and phosphoinositides by cultured cells of neuronal and glial origin. Biochim. Biophys. Acta. 1004, 169-179.

Hazlett T.L., Higashijima. T. and Jameson D.M. (1990) An aluminum fluoride binding site was not detected on elongation factor TU*GDP. Biophys. J. 57, 289a.

Kahn R.A. (1991) Fluoride is not an activator of the smaller (20-25 kDa) GTP-binding proteins. J. Biol. Chem. 266, 15595-15597.

Koyama H., Okawara R. Ojima K. and Yamaya T. (1988) Reevaluation of characteristics of a carrot cell line previously selected as aluminum-tolerant cells. Physiol. Plant. 74, 683-687.

Kraal B., de Graaf M., Mesters J.R. van Hoof P.J.M., Jacquet E. and Parmeggian A. (1990) Fluoroaluminates do not affect the guanine -nucleotide binding centre of the peptide chain elongation factor EF-Tu. Eur. J. Biochem. 192, 305-309.

Lambert D.C., Challiss R.A.J. and Nahorski S.R. (1991) Accumulation and metabolism of Ins(1,4,5)P_3 and Ins(1,3,4,5)IP_4 in muscarinic-receptor-stimulated SH-SY5Y neuroblastoma cells. Biochem. J. 273, 791-794.

Nazawa Y., Nasashima S. and Nagata K. (1991) Phospholipid-mediated signaling in receptor activation of human platelets. Biochim. Biophys. Acta. 1082, 219-238.

Rhee S.G., Kim H., Suh P.G., and Choi W.C. (1991) Multiform of phosphoinositide-specific phospholipase C and different modes of activation. Biochem. Soc. Trans. 19. 337-341.

APPENDIX A

Loss of Inositol Phospholipids in Epididymal Sperm Following Exposure of Mice to Long-term of Organophosphates

Shi B., Oswalt M.D., Chou K. and Haug A.

SHORT COMMUNICATION. Pharmacology & Toxicology 1991, 69, 150–153 ISSN 0901-9928

Short Communication

Loss of Inositol Phospholipids in Epididymal Sperm Following Exposure of Mice to Long-Term Feeding of Organophosphates

B. Shi[1], M. D. Oswald[2], K. Chou[1] and A. Haug[1]

[1]Department of Microbiology and Pesticide Research Center, and [2]Department of Animal Science, Michigan State University, East Lansing, MI 48824, U.S.A.

(Received May 22, 1991; Accepted September 2, 1991)

Organophosphates are the most widely used insecticides in our environment. Despite the short half-life of organophosphates in soil and water, humans and animals are continuously exposed to low levels of these chemicals in the environment and in the diet (Gartrell *et al.* 1986). Associated with exposure to organophosphates are potential health risks such as those involving the reproductive capacity. Little is known about mechanisms by which organophosphate exposure results in reproductive dysfunctions (Gallo & Lawryk 1991). Organophosphates have been suggested to affect sperm motility by binding to specific receptors (Nelson 1990), probably residing on the plasma membrane. These chemicals may therefore interfere with membrane-mediated processes of mammalian fertilization, e.g., sperm capacitation and the acrosome reaction. Ca^{2+} ions (Yanagimachi 1988) and membrane-bound inositol phospholipids (Roldan & Harrison 1989) appear to play a key role in the preparation of sperm for fertilization. Since these phospholipids are participating in transmembrane signalling pathways (Rasmussen 1990), we have therefore investigated changes in levels of inositol phospholipids in epididymal sperm as a result of long-term organophosphate feeding to mice.

Methods. Apart from the control group, male B6D2F1 mice were given a mixture of organophosphates as listed in table 1.

Murine epididymal sperm were collected (Chou *et al.* 1989) in Brinster's medium (Brinster 1971), modified to contain 2 percent bovine serum albumin. This medium reportedly permits *in vitro* capacitation and fertilization to take place in murine gametes (Yanagimachi 1988). Sperm concentration and motility were determined under a Zeiss microscope using a Makler counting chamber (Sefi-Medical Instruments, Haifa).

Murine epididymal sperm (1.8×10^7 cells/ml) were labelled with 200 µCi/ml ^{32}P-orthophosphoric acid (Dupont) and incubated for 2 hr, at 37° in a CO_2 incubator. The reaction was stopped with 10 percent trichloroacetic acid and lipids were extracted with various solvent mixtures composed of chloroform/methanol/HCl (Horwitz & Perlman 1987). The extract was then dried under a stream of nitrogen gas and the phospholipids separated by thin layer chromatography on silica gel plates, using chloroform/methanol/ammonium hydroxide/water (48:40:7:5) as a developing system. Using developed autoradiographs as a template, lipid spots were visualized by autoradiography, then scraped off, reextracted with chloroform/methanol/conc. HCl (200:100:0.75), and dried in a stream of nitrogen gas (Horwitz & Perlman 1987). The molecular identities of phosphatidyl inositol, PI, phosphatidylserine, PS, phosphatidyl inositol-4-phosphate, PIP, and phosphatidyl inositol-4,5-biphosphate, PIP_2, were ascertained by comigration of appropriate standard phospholipids. As to the correct identification of phosphatidyl inositols, additional information was obtained by labelling sperm cells with myo-[2-^{3}H]-inositol (Dupont), followed by analysis on thin layer chromatography plates.

Results and discussion. Labelling of inositol phospholipids was attained upon exposure to ^{32}P-labelled phosphate. Compared with the levels of PI and PIP, the level of PIP_2 was significantly decreased in sperm from mice treated with organophosphates (table 1). As to [^{32}P]Pi incorporation into total phosphatidylinositol lipids of control murine sperm, our data (table 1), if normalized to 10^6 cells, are comparable to those determined in a medium composed of Krebs-Ringer solution in the presence of bovine serum albumin (Roldan &

Table 1.

Changes in ^{32}P-labelling of inositol phospholipids in epididymal sperm from 8 months old mice, 16 mice per group, fed organophosphates in the daily diet. From weaning to 3 months, the diet (0.4 µg/kg/day) contained a mixture of diisopropyl fluorophosphate: diazinon:dimethoate:malathion:parathion = 3:160:80:2500:40 (w/w), and a diet (0.15 µg/kg/day) at a corresponding ratio of 1:50:70:760:9 from 3 months to 8 months. Sperm from each mouse were incubated with [^{32}P]Pi, then lipids extracted and separated by thin layer chromatography, and radioactivity in each lipid counted. The inositol phospholipid data listed are significant at the 5 percent level of significance according to the t-test. Results are means for six separate experiments, 2 to 4 mice each; standard errors were between 10 to 20% of the mean values. The motility values are those of sperm exposed for 95 min. to Brinster's modified medium.

	Percentage of ^{32}P-labelling (counts per min./1.8×10^7 cells)			Motility percent
	PIP_2	PIP	PI	
control group	100 (136)	100 (592)	100 (5700)	29 ± 7
treated group	74 (101)	85 (503)	105 (6050)	39 ± 8

Harrison 1989). The latter medium and that used in our studies, i.e., Brinster's medium, are capable of sustaining capacitation of murine sperm (Yanagimachi 1988). As to [^{32}P]Pi incorporation into individual phosphatidylinositol lipids of control murine sperm, our values (table 1) are significantly lower than corresponding values obtained on sperm in a medium composed of saline (Roldan & Harrison 1989) which does not support capacitation.

A large number of cell surface receptors, e.g., for neurotransmitters, are known to couple to phosphoinositide hydrolysis (Gilman 1987). Following receptor-mediated activation of phospholipase C, breakdown products of PIP_2 are inositol phosphates and diacyl glycerol, both of which play an important role in cellular regulation, e.g., during the sperm acrosome reaction (Roldan & Harrison 1989). Considerable activity of phospholipase C in bovine spermatozoa has been reported (Vanha-Perttula & Kasurinen 1989). Since sperm cells were found to exhibit membrane-bound cholinesterase activity (Bishop *et al.* 1976) and because organic phosphorus insecticides are potent inhibitors of this enzyme (Gallo & Lawryk 1991), the enhanced breakdown of PIP_2 (table 1) may thus result from organophosphate binding to membrane surface receptors of murine sperm. According to the pathway of inositol phospholipid metabolism (Berridge 1987), this biphosphate originated from PI whose level remained virtually unchanged in treated cells relative to that of the control group. At this time we cannot discard the notion that organophosphates may also bind directly to PIP kinase thus inhibiting phosphorylation of the phosphoinositide.

In summary, organophosphate binding to membrane-bound compounds probably impacts phosphatidyl inositol metabolism via receptormediated mechanism.

Acknowledgement

This work was supported in part by funds from the Pesticide Research Center.

References

Berridge, M. J.: Inositol triphosphate and diacyl glycerol, two interacting second messengers. *Annu. Rev. Biochem.* 1987, 56, 159–193.

Bishop, M. E., B. V. R. Sasti, D. E. Schmidt & R. D. Harbison: Occurrence of choline acetyltransferase and acetylcholine and other quaternary ammonium compounds in mammalian spermatozoa. *Biochem. Pharmacol.* 1976, 25, 1617–1622.

Brinster, R. L.: *In vitro* culture of the embryo. In: *Pathways to conception.* Ed.: A. I. Sherman. C. C. Thomas Publ., Springfield, IL, 1971, 245–277.

Chow, K., J. Chen, S. Yuan & A. Haug: The membrane potential changes during capacitation of murine epididymal sperm. *Biochem. Biophys. Res. Comm.* 1989, 165, 58–64.

Gallo, M. A. & N. J. Lawryk: Organic phosphate pesticides. In: *Handbook of pesticide toxicology.* Eds.: W. J. Hayes and E. R. Laws. Academic Press, New York, 1991, vol. 2, 917–1123.

Gartrell, M. J., J. C. Craun, D. S. Podrebarac & E. L. Gunderson: Pesticides, selected elements, and other chemicals in adult total diet samples, October 1980 – March 1982. *J. Ass. Off. Anal. Chem.* 1986, 69, 146–159.

Gilman, A. G.: G proteins, transducers of receptor-generated signals. *Ann. Rev. Biochem.* 1987, 56, 615–649.

Horwitz, J. & R. L. Perlman: Measurement of inositol phospholipid metabolism in PC12 pheochromocytoma cells. *Meth. Enzymol.* 1987, 141, 169–175.

Nelson, L.: Pesticide perturbation of sperm cell function. *Bull. Environ. Contam. Toxicol.* 1990, 45, 876–882.

Rasmussen, H.: The complexities of intracellular Ca^{2+} signalling. *Biol. Chem. Hoppe-Seyler* 1990, 371, 191–206.

Roldan, E. R. S. & R. A. P. Harrison: Polyphosphoinositide breakdown and subsequent exocytosis in the Ca^{2+}/ionophore induced reaction of mammalian spermatozoa. *Biochem. J.* 1989, 259, 397–406.

Vanha-Perttula, T. & J. Kasurinen: Purification and characterization of phosphatidylinositol-specific phospholipase from bovine spermatozoa. *Internat. Biochem.* 1989, 21, 997–1007.

Yanagimachi, R.: Mammalian fertilization. In: *The physiology of reproduction.* Eds.: E. Knobil and J. D. Neill. Raven Press, New York, 1988, vol. 1, 135–185.

APPENDIX B

Biochemical Basis of Aluminum Tolerance in Plant Cells

Haug A. and Shi B.

Plant and Soil 00, 000–000, 1991.

PLSO AS93

Biochemical basis of aluminium tolerance in plant cells

ALFRED HAUG and BIAO SHI
Department of Microbiology, Pesticide Research Center, and the Center for Environmental Toxicology, Michigan State University, East Lansing, MI 48824-1311, USA

Key words: aluminium, calmodulin, cytoskeleton, endocytosis, G proteins, membrane, lipid peroxidation, plant cells, tolerance, uptake

Abstract

To be considered in this treatise are recent developments on biochemical aspects of aluminium tolerance and toxicity. Advances in aluminium biochemistry are best illustrated by knowledge gained in the area of aluminium uptake across the plasma membrane and by the putative role of aluminium in transmembrane signalling pathways.

Initial studies indicate that aluminium is taken up by endocytotic mechanisms, either via non-saturable, fluid-phase endocytosis or through saturable, membrane receptor-mediated endocytosis involving specific carriers. These uptake modes are respectively exemplified by aluminium internalization involving polysaccharides and carriers, perhaps present in the rhizosphere. Regarding aluminium interiorization, a working hypothesis can be formulated explaining endocytotic uptake followed by processing along intracellular pathways that in part determine aluminium's final destination. Given the complexity of endocytotic processes, genetic defects at the plasma membrane or at internal membranes probably lead to deficiencies in aluminium's uptake and intracellular routing, respectively.

As to cellular communication, aluminium fluoride has been implicated in being a ligand for membrane-associated G proteins which function as intermediaries in signal transduction. G proteins in part control phosphoinositide hydrolysis which in turn is crucial for the release of second messenger molecules. Aluminium-related interaction with components of signalling pathways is expected to affect the cell's capability of processing sensory information.

Findings are also presented on aluminium-enhanced membrane lipid peroxidation, aluminium interference with cytoskeletal elements, calmodulin, and the chromatin structure.

The challenge will be to elucidate biochemical mechanisms of aluminium toxicity as a basis for designing aluminium tolerant plants.

Introduction

Since space does not permit an extensive report regarding the biochemical basis of aluminium toxicity and tolerance, this review is an interim account of current research as of the last few years. Within this framework it is our objective to focus on specific biochemical aspects which are beginning to emerge, *e.g.*, primary steps in the internalization of aluminium by cells. Via this discourse we also hope to stimulate interest for future research along novel lines, ultimately resulting in understanding the molecular basis of aluminium toxicity and tolerance.

In the last two decades a considerable body of evidence has accumulated implicating aluminium ions in varous disorders. This increase in information is in part summarized in reviews and aluminium toxicity/tolerance in plants (Foy *et al.*, 1978; Haug, 1984; Haug and Caldwell, 1985; Taylor, 1988; Taylor, 1988) and man (Ganrot, 1986). Within the same period of time, the chemistry of aluminium has received considerable attention as to the metal's role in our en-

vironment and in biology. This is reflected in publications concerned with physico-chemical properties of aluminium compounds (Akitt, 1989), the aqueous chemistry of aluminium in soil and water environments (Sposito, 1989), and the environmental chemistry and toxicology of aluminium (Lewis, 1989). As opposed to these fairly comprehensive surveys, we prefer selecting particular facets of aluminium biochemistry as paradigms to center attention on current and future directions of research.

The cell wall as barrier

The cell wall is a charged surface containing pores with a diameter of about 4 nm, which is roughly tenfold that of the hydrated aluminium ion. Behaving as an ion exchanger, the cell wall may therefore alleviate metal toxicity. At this time, there exists a paucity of data on interactions of aluminium wth the cell wall. Cell wall material isolated from aluminium tolerant wheat cultivars reportedly showed variances as to titrable charges and aluminium binding regardless of the presence or absence of calcium ions (Shann and Bertsch, 1988). In depth studies are required on well-defined fractions of cell wall constituents, *e.g.*, in terms of surface chemistry of genetically different cultivars. Regarding production of extracellular polysaccharide, various cereal leaf protoplasts reportedly synthesized a beta-(1→3) glucan in reponse to aluminium stress (200 μM) at pH 6.0, after 24 h incubation. However, there appeared to be no correlation between aluminium tolerance and polysaccharide production (Schaeffer and Walton, 1990).

Plasma membrane structure

The plasma membrane limits the cell from its environment. Upon interaction of aluminium (20 μM) with erythrocyte white ghosts labelled with a fluorescence probe, the rotational rates of the membrane probe were apreciably decreased. Initial aluminium-induced changes at the membrane surface are apparently translated deeply into the apolar portion of the membrane. These kinds of changes in lipid packing may be expected to influence cellular transport processes and hence cellular metabolism (Weis and Haug, 1989). This was illustrated by studies on intact root cortex cells of northern red oak. Application of aluminium decreased water and enhanced non-electrolyte permeation across the membrane (Zhao *et al.*, 1987). Dramatic membrane changes have also been observed in phosphatidylserine-containing lipid vesicles exposed to micromolar aluminium concentrations. Aluminium ions reportedly induced membrane rigidification and membrane fusion (Deleers *et al.*, 1987). For comparison, membrane rigidification was only observable at Cd^{2+} and Mn^{2+} concentrations at least tenfold higher than that used for aluminium (Deleers *et al.*, 1986).

Aluminium ions reportedly bound to the surface of phosphatidylcholine vesicles with an almost 600-fold higher affinity than Ca^{2+} does; mono- and divalent aluminium fluoride complexes did not bind measurably. Bound Al^{3+} would be expected to cause a membrane surface potential shift from −30 to +11 mV which in turn may lower the passive diffusion of cations across the membrane (Akeson *et al.*, 1989). This conclusion is in accord with observations that K^+ uptake was markedly decreased following treatment of pea seedlings with 1 mM $AlCl_3$ for 16 h; the decrease was alleviated by the presence of 10 mM Ca^{2+} (Matsumoto and Yamaya, 1986). However, aluminium-induced changes in K^+ uptake are probably not primary factors contributing to aluminium sensitivity as judged on two genetically closely related wheat cultivars with different aluminium sensitivity (Pettersson and Strid, 1989).

Because aluminium becomes mobilized at acidic pH, it is noteworthy that rice plants adaptively adjusted the phospholipid ratio to pH stress while wheat plants showed less variability in terms of lipid composition (Erdei *et al.*, 1981). Moreover, when rice roots were grown at pH 6, roots exhibited an anomalous K^+ influx, probably as a result of proton-induced changes in membrane structure (Zsoldos and Erdei, 1981).

At the present time, aluminium- and pH-induced changes in structure of plant cell membranes are poorly understood. Concerning aluminium stress, questions of alterations in heterogeneity and biological specificity of lipid and

proteins, changes in immiscibility among membrane components (Klausner and Kleinfeld, 1984), and altered lipid and protein dynamics (Yuan and Haug, 1988; Yuan and Haug, 1988) have to be addressed by employing well-defined membranes. Pathological perturbation of lipid immiscibility may provide the basis for aluminium-related changes in nutrient uptake and intracellular reorganization. An approach to this problem may be to control membranes of cultured plant cells (Conner and Meredith, 1985) by genetic and environmental means. This type of research on aluminium-related membrane changes can be facilitated by recent developments in methodology (Chapman and Hayward, 1985).

Membrane lipid peroxidation

Peroxidation of polyunsaturated fatty acids in biological membranes is a free radical-mediated reaction which causes chemical transformation of lipids and produces a wide spectrum of products (Kappus, 1987; Miquel *et al.*, 1989). Formation of peroxidation products was accompanied by changes in activities of membrane-bound enzymes and in membrane permeability (Itoh *et al.*, 1989). As to peroxidation processes, aluminium reportedly caused subtle rearrangements of membrane lipids that facilitated iron-induced peroxidative reactions in phospholipid vesicles (Gutteride *et al.*, 1985) and in erythrocytes (Quinlan *et al.*, 1988). Since a large fraction of plant iron is found associated with porphyrins (Sandman and Böger, 1983), cytochromes may be involved in the generation of free radicals similar to those produced in the presence of metmyoglobin (Xu *et al.*, 1990). Polyamine (Schuber, 1989) binding to negative charges of the membrane surface reportedly inhibited lipid peroxidation (Tadolini *et al.*, 1984). To the best of our knowledge, no data are available as to aluminium-accelerated lipoxidation processes in plant membranes. In this context it appears worth noting that root hairs are capable of accumulating large amounts of iron (Branton and Jacobson, 1962). Furthermore, following exposure of young bean foliage to simulated acid rain, radical-mediated peroxidation was detectable in membranes characterized by the formation of gel-phase lipid (Thompson *et al.*, 1985). Clearly more studies are required to establish a firm basis for aluminium's role in membrane lipid peroxidation and the possible remedial action of plant associated radical scavengers.

Aluminium and signal transduction

Cells have a need to sense their microenvironment and to respond to external signals. These signal are detected at the cellular surface and are translated into a cascade of intracellular second messengers. One class of signal transmitters involves membrane-bound guanine nucleotide binding proteins, or G proteins (Naccache, 1989), which play a predominant role in phosphoinositide breakdown (Rana and Hokin, 1990). Among the hydrolysis products are two second messengers, *viz.*, diacylglycerol and inositol triphosphate. The latter messenger signals the release of intra-cellular calcium, presumably involving calmodulin. The presence of phosphatidylinositol and phosphatidylinositol 4-phosphate kinase has been established in plant plasma membranes with similar characteristics as those found in various animal membranes, *e.g.*, as to ATP dependence, ion requirement and pH optima (Sommarin and Sandelius, 1988). Polyamines have been shown to affect the formation and metabolism of inositol triphosphate (Berridge, 1987) and to play a role in Ca^{2+} homeostasis (Schuber, 1989). Via a signal cascade, cells are thus capable of converting an external stimulus into intracellular second messengers, which in turn trigger metabolic activities and eventually appropriate cellular responses.

G proteins could be activated by fluoride plus aluminium. AlF_4^- was bound to GDP and seemed to mimic the role of the gamma phosphate of GTP (Gilman, 1987). Studying human vein endothelial cells, stimulation of cells with aluminium fluoride caused a dose- and time-dependent generation of inositol phosphates and a calcium-dependent release of arachidonic acid (Magnusson *et al.*, 1989). At this time it appears rather speculative to correlate aluminium

fluoride activated G proteins with findings on the stimulatory effects of aluminium on growth of tea plants (Konishi *et al.*, 1985).

Since aluminium is known to bind to phosphate groups (Haug, 1984), there are valid reasons to assume that aluminium may also strongly attach to adjacent phosphate groups of inositol. In view of electrochemical similarities between Al^{3+} and Fe^{3+} (Hartley *et al.*, 1980), it is noteworthy that Fe^{3+} reportedly formed a complex with myo-inositol phosphate and can thus be used as a mobile phase additive to enhance the detection of inositol phosphate isomers by high performance liquid chromatography (Henderson *et al.*, 1989). As a result of the high stability of aluminium phosphate complexes, inositols chelated with aluminium are probably less susceptible to hydrolysis, which in turn may be of great significance for signals triggered by external stimuli. Moreover, aluminium was found to impair incorporation of inositol into phospholipids (Johnson and Jope, 1986).

Our knowledge on the involvement of aluminium – beneficially or pathologically – in signal transduction is rudimentary. Studies on aluminium interactions with plant membrane phosphoinositides and G proteins warrant special attention as to early events (if any) in the aluminium toxicity syndrome.

Uptake of aluminium

Numerous studies have been performed regarding aluminium uptake and distribution in plant tissue or in intact plants (Foy, 1988). Relatively few data are available on the effects of aluminium at the cellular and molecular levels. A fundamental question that has to be resolved is that of the mode(s) of aluminium uptake across the plasma membrane, the interface between the cell and its environment. Any such molecular study must take into account the unique physico-chemical properties of aluminium in the hydrated and complexed states (Lewis, 1989; Sposito, 1989). In the following we are discussing the role of pH and specific carriers in aluminium uptake across the plasma membrane.

pH-dependent uptake

Examining aluminium uptake by multilamellar phospholipid vesicles, maximal aluminium uptake was strongly dependent on the lipid composition of the liposome and the pH of the suspension medium (Shi and Haug, 1988). Characterized by an aluminium uptake maximum in the range from pH 4.0 to 5.0, low pH in the suspension medium facilitated aluminium entry into vesicles composed of dimyristoyl phosphatidylcholine (DMPC) and acidic phosphatidylserine at a ratio of 4:1. However, using DMPC liposomes, which carry a zero net charge at neutral pH, the maximum of aluminium uptake was shifted into the range from pH 6.0 to 7.0. Viable murine neuroblastoma cells also displayed a pH-dependent aluminium uptake pattern. Maximum uptake took place around pH 6.0, whereas in the physiological pH region, neuroblastoma cells did not take up aluminium measurably, and after 1 to 4 h of incubation the intracellular aluminium content was generally less than 10 percent of total aluminium (25 μM) added. The time course of aluminium uptake (pH 6.0, 25 μM, 37°C) was biphasic and reached a plateau at about 1 h. In the presence of millimolar Ca^{2+} or Mg^{2+} concentrations, the initial rate of aluminium uptake was substantially lower compared with that in the absence of these bivalent cations. However, as the incubation time progressed to about 1 h, the overall uptake of aluminium was indistinguishable from that obtained with no bivalent cations present. The pH-dependence of aluminium uptake was attributed to aluminium speciation and/or reversible changes in membrane properties, *e.g.*, phase separation, changes in nonbilayer lipid configurations, relevant for aluminium transport (Shi and Haug, 1990). Being most pronounced at slightly acidic pH, a pH-dependent aluminium uptake was also observed in cyanobacteria (Pettersson *et al.*, 1985).

Regarding pH-dependent aluminium uptake, these types of studies permit us to view the plant-induced pH hypothesis (for review see: Foy, 1988) from a novel perspective. The original idea was that certain plants can reduce aluminium toxicity by maintaining a fairly high pH in the rhizosphere or root apoplasm thus

generating conditions favourable for the formation of less toxic aluminium species (for review see: Taylor, 1988).

Taking into account the above results, we suggest to advance the expanded pH hypothesis: certain aluminium tolerant plants are capable of modifying their membrane structure under acidic stress thus rendering the membrane less conducive to aluminium uptake. To test this hypothesis, various avenues of experimentation are available. Information on protein and lipid composition is required on well-defined membranes as opposed to whole cell extracts (Zsoldos and Erdei, 1981). Since membrane lipids are able to adopt nonbilayer configurations (Cullis *et al.*, 1980), subtle changes in lipid composition are expected to influence metastable lipid configurations which in turn impact the membrane's functional capability as to aluminium uptake. It may suffice to point out that the membrane lipid structure of erythrocytes can be modulated by 3 to 4 prostaglandin molecules per cell (Kury *et al.*, 1974). Spectroscopic tools (Chapman and Hayward, 1985) can be applied to elucidate dynamic aspects of membrane lipids and proteins in aluminium tolerant and sensitive plants. For certain types of studies, tissue cultures (Conner and Meredith, 1985) may be applied to modify cells by genetic means.

Role of aluminium chelators

An aluminium tolerant carrot cell line was found to secrete large amounts of citrate into the medium containing millimolar amounts of insoluble aluminium phosphate. Citrate secretion was not detectable in the absence of insoluble phosphate source (Koyama *et al.*, 1988). Since citrate is a potent aluminium chelator (Öhman, 1988), and because neutral complexes are favoured to permeate a lipid bilayer, the question arises as to lipid permeation of neutral aluminium citrate. Recent studies on multilamellar (Shi and Haug, 1988) and unilamellar lipid vesicles (Akeson and Munns, 1989) demonstrated that prior aluminium chelation by citrate virtually prevented aluminium from being taken up by the vesicles. Hydrogen bonding between water and citrate carboxyl groups and metal hydration apparently are in part responsible for restricted diffusion of aluminium/citrate complexes across the water/lipid interface (Akeson and Munns, 1989). The above findings on artificial membranes are consistent with results of aluminium uptake by viable neuroblastoma cells in the presence of a slight excess of citrate or EDTA, at neutral pH (Shi and Haug, 1990). In conclusion, exudation of citrate by plant cells is a means of detoxifying aluminium, albeit requiring considerable energy.

Speaking of chelator-assisted aluminium uptake, nonesterified unsaturated fatty acids (up to 200 μM in the medium) were found to appreciably enhance aluminium uptake by viable neuroblastoma cells at neutral pH compared with uptake in the presence of esterified fatty acids. The mediating function of fatty acids was only detectable in the presence of free fatty acids in the suspension medium. The types of complexes formed are not known (Shi and Haug, 1990). Conceivably, metal-fatty acid complexes may be similar to those found for Fe^{3+}, *viz.*, Fe^{3+} (fatty acid)$_3$, which was reportedly involved in iron uptake by internal brush border membrane vesicles derived from murine small intestine (Simpson *et al.*, 1988). Given the composition of the rhizosphere in the proximity of the plant root (Lynch, 1976), there is the distinct possibility that organic molecules, *e.g.*, fatty acids, may serve as instruments for aluminium transport across the root plasma membrane.

Aluminium interiorization via endocytosis

Concerning mechanisms of aluminium uptake via endocytotic processes, available knowledge is in its infancy, both in plant and mammalian cells. There exist two distinct mechanisms of endocytotic uptake, *viz.*, fluid-phase endocytosis and receptor-mediated endocytosis (Pastan and Willingham, 1985). As opposed to receptor-mediated endocytosis, fluid-phase endocytosis is not saturable with respect to the ligand. A classical endocytotic pathway is that of ferri-transferrin internalization by receptor-mediated endocytosis in mammalian cells (Pearse and Crowther, 1987). Given similar electrochemical properties of Fe^{3+} and Al^{3+} (Hartley *et al.*, 1980; Nightingale, 1959), and the observation that transferrin bound two aluminium ions per protein (Ichimura *et al.*, 1989), we recently hypoth-

esized that transferrin-mediated endocytosis is an important mode of aluminium uptake at neutral pH by mammalian cells (Shi and Haug, 1990). By working with viable neuroblastoma cells, evidence was established that aluminium uptake reached a plateau upon addition of micromolar amounts of apotransferrin, at pH 7, 37°C. Furthermore, aluminium uptake decreased considerably when the carrier protein had been neutralized by anti-transferrin antibodies. The antibody-treated apotransferrin probably lost its ability of recognizing and binding membrane associated receptors. Gentle proteinase treatment of cells also diminished aluminium uptake presumably by inactivating in part transferrin receptors at the membrane surface. As to aluminium-associated apotransferrin, no information is available addressing questions pertaining to transit structures involved and the initial destination of aluminium (lysosome, Golgi apparatus), degradation (if at all) of apotransferrin, recycling of apotransferrin, pathways of iron vs those of aluminium. Following differential centrifugation, we have demonstrated that in the absence of apotransferrin (pH 6.0, 37°C) the major portion (70%) of interiorized aluminium was associated with post-mitochondrial components, consisting of endoplasmic reticulum, lysosomes and cytosol (Shi and Haug, 1990).

As to iron uptake by animal cells, receptor-mediated endocytosis may be briefly described as follows (Pearse and Crowther, 1987): Apotransferrin binds iron at neutral pH extracellularly, then iron-loaded transferrin binds to specialized membrane regions (coated pits), the receptor/transferrin complexes are internalized and move to endosomes mainly responsible for iron dissociation, whereas apotransferring attached to its receptor, recycles to the plasma membrane surface.

In plant cells an endocytotic pathway is also operable (Coleman *et al.*, 1988; Robinson and Depta, 1988) as demonstrated, for example, on primary roots of maize seedlings treated with lead salts. Lead deposits were also found in the Golgi apparatus and on small vacuoles (Hübner *et al.*, 1985). As to aluminium internalization, histochemical and ultrastructural experiments indicated that the first observable effect involved the migration of secretory vesicles of the Golgi apparatus following exposure of maize plants to a millimolar aluminium solution for several hours (Bennet *et al.*, 1985a). The presence of acidic muco-polysaccharides appeared to play a role in aluminium uptake (Bennet *et al.*, 1985b). Aluminium interiorization may have taken place by a fluid-phase endocytotic proceess of aluminium bound to polysaccharides. In yeast, for example, dextran was incorporated by non-saturable, fluid-phase endocytosis and accumulated in the vacuole in a time-, temperature-, and energy-dependent fashion (Makarow, 1985). The intracellular routes taken by the aluminium-loaded polysaccharides and their fate are not known at this time. Genetic studies on cells deficient in defined steps of the endocytotic pathway may be valuable in analyzing molecular aspects of endocytotic metal uptake.

Since iron is an essential element for higher plants and most micro-organisms, it is reasonable to assume that certain microbial siderophores (Castignetti and Smarrelli, 1986; Neilands, 1981) are also capable of delivering a nonphysiological cargo, *viz.*, aluminium, across the root membrane possibly involving specific cell surface receptors. The notion that siderophores are capable of chelating aluminium is illustrated, for example, by ferrisiderophores which are therapeutically used to effectively remove aluminium from patients suffering from high aluminium levels in various tissues (Domingo *et al.*, 1988; Stummvoll *et al.*, 1984; Yokel and Kostenbauder, 1987). As to plants, hydroxamate siderophores were found to significantly enhance growth and reduce chlorosis of an Fe-inefficient variety of sorghum. The siderophore presumably acted as a shuttle agent between the iron pool in the nutrient solution and the membrane of absorbing root cells (Cline *et al.*, 1984). Siderophore concentrations in soils reportedly varied from about 3 to 34 n*M* desferrioxamine methane-sulfonate equivalents (Castignetti and Smarrelli, 1986). Grasses, exemplified by barley (Marschner *et al.*, 1974), can solubilize iron by their own iron chelators termed phytosiderophores. Ferrichrome reportedly served as a source of iron for tomato and duckweed (Neilands and Leong, 1986). This siderophore also formed isostructural diamagnetic complexes with aluminium and has been studied by NMR spec-

troscopy (Neilands, 1981). Taken together, iron chelators present in the rhizosphere may serve as carriers for aluminium uptake by plants.

Aluminium and the cytoskeleton

The topographical arrangement of membrane macromolecules is in part dependent upon underlying cytoskeletal structures like microtubules and microfilaments. As to interactions with deleterious aluminium ions, *in vitro* experiments of tubilin assembly into microtubules demonstrated that Al^{3+} effectively competed with Mg^{2+} for support of tubulin polymerization. Moreover, the Al^{3+}-produced microtubules were less susceptible to Ca^{2+}-induced depolymerization than microtubules produced in the presence of Mg^{2+} (Macdonald *et al.*, 1987). A major regulatory component of the cytoskeleton is calmodulin, a pivotal calcium-regulating protein which has been localized in microfilament bundles and in microtubules (Piazza and Wallace, 1985; Stoclet *et al.*, 1987). Calmodulin is also believed to play a key role in mitotic cell division (Rasmussen and Means, 1987), a process requiring extensive reorganization of cytoskeletal proteins. Interrelationships between calmodulin and cytoskeletal elements are further exemplified by recent evidence suggestive of coordinate gene regulation of calmodulin and specific tubulin genes (Slaughter *et al.*, 1989). Aluminium-triggered changes in microtubular structure, either directly or indirectly by way of aluminium-altered calmodulin (Haug, 1984), are expected to result in repercussions on processes critically dependent on these organelles, *e.g.*, mitotic apparatus, intracellular vesicle trafficking. These types of changes may in part be responsible for aluminium-inhibited cell division in the root tip meristem of cowpea (Horst *et al.*, 1983). Whether aluminium-related alterations of cytoskeletal assembly constitute an early biochemical lesion remains to be investigated.

Aluminium in the cytosol

The final destination, or at least long-term residency, of internalized aluminium is not accurately known. In evaluating the nature of aluminium's fate, a unique feature of aluminium complexation has to be taken into account, *viz.*, kinetic routes and time required to establish true equilibrium. For example, recent studies have demonstrated that equilibrium times up to 6 h may be required from the time of mixing aluminium with citrate until true equilibrium has been reached (Öhman, 1988). Moreover, aluminium complexes may be reversible, such as those of Al^{3+} with transferrin (Ichimura *et al.*, 1989), or irreversible – or at most very slowly reversible. Intracellularly aluminium is thus expected to eventually bind to ligands having the highest affinity towards the metal; an important factor is the intracellular pH dictating metal speciation. As to toxicological aspects, ligands formation and slowness of ligand exchange are therefore of great import (Ganrot, 1986) since aluminium toxicity may be underestimated in short-term exposure studies of biological tissues.

In plants, chelation in aluminium by acidic polypeptides (Putterill and Gardner, 1988) and low molecular weight ligands like citric acid (Suhayda and Haug, 1986) have been suggested as playing a role in tolerance against aluminium (see also review: Taylor 1988). ATP is also a strong aluminium chelator (Akitt, 1989; Laussac *et al.*, 1983). This was illustrated by experiments to assess the effect of aluminium on ATP pools in a cyanobacterium. Addition of micromolar quantities of aluminium enhanced the ATP pool within 24 h, presumably forming stable Al^{3+}–ATP complexes which were no longer available for cellular metabolism (Pettersson and Bergman, 1989).

Both in cyanobacteria (Pettersson *et al.*, 1986) and in neuroblastoma (Shi and Haug, 1990), aluminium internalization apparently occurred, at least in part, via passive mechanism(s) following exposure of cells to aluminium at slightly acidic pH. The intracellular accumulation of large amounts of aluminium by neuroblastoma cells, about 65 percent of externally added metal (25 μM), at pH 6.0, is probably attributable to an appreciable intracellular metal chelating pool. In these cells, intracellular complexation rather than transport across the plasma membrane seemed to be the rate limiting reaction determining the interiorization process of aluminium. The

significance of an intracellular chelator pool as a means for aluminium detoxification was also demonstrated on wheat roots. At sublethal and lethal aluminium concentrations in the medium, the total aluminium content in mitochondrial and cytosolic fractions was about sixfold higher in the aluminium tolerant than that in the aluminium sensitive wheat genotype (Niedziela and Aniol, 1983). Considerable aluminium concentrations have also been found in the leaves of aluminium tolerant trees and shrubs in central Brazil. High levels of aluminium in the leaves were not correlated with low levels of magnesium, iron, zinc, or phosphorus as compared with native cerrado species which do not accumulate aluminium (Haridasan, 1982; Haridasan and De Araujo, 1988). Under the same soil and climatic conditions, aluminium tolerant species of trees and shrubs were identified which seemed to exclude rather than incorporate aluminium (Haridasan, 1982). Aluminium exclusion was also found in aluminium tolerant blueberry (Wagatsuma *et al.*, 1987) and barley cultivars (Wagatsuma and Yamasaku, 1985). There is obviously a need to identify intracellular aluminium chelators and to clarify molecular mechanisms of aluminium exclusion vs. those involving aluminium accumulation.

Calmodulin is a highly conserved protein crucial for calcium regulation in eukaryotic cells. This protein is mainly found in the cytosol, where changes in calmodulin levels and intracellular distribution may reflect regulatory processes involved in calcium regulation (Stoclet *et al.*, 1987). At present, NAD kinase is the best characterized calmodulin-dependent plant enzyme (Muto and Miyachi, 1986). In pea root apex, NAD kinase was reportedly present in two forms, a calmodulin-dependent and a calmodulin-independent form (Allan and Trewavas, 1985). In the presence of aluminium, calmodulin underwent pronounced structural and functional changes (Haug, 1984) that impaired the efficacy of interfacing with target proteins (Weis and Haug, 1987). Therefore NAD kinase activity in root tips of two wheat genotypes of different aluminium tolerance was examined. Genetic differences were found to be reflected in the proportion of calmodulin-dependent to calmodulin-independent NAD kinase activity. Under aluminium stress the aluminium tolerant wheat genotype was apparently able to replace in part the calmodulin-dependent enzyme by the calmodulin-independent enzyme (Slaski, 1989). Application of calmodulin inhibitors to rye and wheat seedling inhibited root growth concomitant with enhanced aluminium toxicity. It cannot be excluded, however, that some of the inhibitors tested interfered with the cellular membrane rather than calmodulin (Slaski and Aniol, 1987). To further elucidate the role of calmodulin in aluminium toxicity, there are several directions of research. For example, with the availability of calmodulin antibodies and immunological techniques, calmodulin redistribution, such as translocation to the plasma or internal membranes, can be studied under aluminium stress. Moreover, expression of calmodulin and calmodulin-related genes (Braam and Davis, 1990) by aluminium stress deserves particular attention. As to calmodulin dependent calcium regulation, the apparent relationships between aluminium and calcium are far from being understood. These types of studies may be of import to understand aluminium-related forest decline which has been attributed in part to aluminium-triggered calcium disorders (Godbold *et al.*, 1988; Shortle and Smith, 1988).

Concerning aluminium interations with cytosolic components, aluminium ions were found to be required for stabilization and inhibition of hepatic microsomal glucose-6-phosphatase by sodium fluoride. The apparent dissociation constant for interaction of the enzyme and AlF_4^- was 0.1 μM (Lange *et al.*, 1986). Yeast glucose-6-phosphate dehydrogenase apparently bound 1 mol of aluminium per mol of enzyme subunit. The enzyme was inhibited by aluminium by pseudo-first-order reaction (Cho and Joshi, 1989).

Aluminium and the nucleus

Confirming findings on beans (Deufel, 1951), numerous studies (Taylor, 1988) have demonstrated that application of aluminium salts can inhibit cell division and produce chromosome

aberrations in plant cells. Blocking of cell division was attributed to the interaction of aluminium with DNA (Matsumoto *et al.*, 1976). Chromosome aberrations may partially originate from aluminium's action of the cytoskeleton as discussed above. Binding of aluminium to the phosphate backbone appeared to be mainly driven by ionic forces, taking place at all pH values. Regarding interstrand DNA cross-linking with aluminium, saturation of cross-linking has been observed at a 0.4 ratio of aluminium to nucleotide phosphate; cross-links were broken at elevated pH (Karlik and Eichhorn, 1989). At micromolar concentrations, aluminium reportedly caused considerable alterations in the structure of chromatin isolated from rat brain and liver. Of all the di- and trivalent cations tested, aluminium ions were the most relative as to their ability to induce precipitation of chromatin. Some of the toxic effects of aluminium may therefore result from disruption of the physiological processes of gene expression (Walker *et al.*, 1989) since a transcriptionally competent chromatin structure is crucial for controlling gene expression. Such a chromatin structure is necessary to render the coding DNA strand accessible to RNA polymerase. Structural changes were also observed in pea chromatin following *in vitro* or *in vivo* treatment with aluminium. Interestingly, analysis of the melting profile indicated that chromatin prepared from aluminium-treated pea roots were more stable to thermal changes than chromatin from control roots (Matsumoto, 1988). Employing energy-dispersive X-ray analysis, a considerable amount of aluminium was detected in mitotic chromosomes of mays compared with that of control regions (Whallon and Flegler, 1986). Data suggest that aluminium might bind between the linker histone and DNA (McLachlan, 1988). Studying aluminium teated rabbit brain, experiments also demonstrated that aluminium severely reduced messenger RNA levels such as those of calmodulin and tubulins (MacLachlan, 1988). Whether these changes in RNA levels are a consequence of direct aluminium effects on gene transcription is not known. Since differences in calcium nutrition reportedly altered pea chromatin structure (Matsumoto, 1987), the interplay between aluminium and calcium has to be further examined.

Future directions

In this review we have provided an appraisal of recent biochemical developments in the field of aluminium toxicity. Although a large background knowledge has been built over the years, our fundamental understanding on the temporal development of aluminium toxicity is rudimentary.

Nevertheless, the last few years have apparently heralded a new phase in the study of the modes of aluminium uptake, *viz.*, aluminium interiorization by endocytotic mechanisms. Application of improved biochemical/biophysical techniques and genetic engineering methods is thus expected to provide new insights into the role of the plasma membrane and into internal membrane traffic promoting aluminium internalization and distribution. Genetic defects in membrane receptor structure or in proteins crucial for intracellular processing may lead to deficiencies and/or changes in the intracellular itinerary of toxic aluminium ions. What, at present, appear to be pleiotropic aluminium effects in the plant cell, may in the end prove to emerge from a basic, underlying molecular mechanism crucial for the pathogenesis of the aluminium toxicity syndrome.

Recent discoveries in the field of transmembrane signalling pathways suggest a scenario whereby aluminium ions are capable of interfering with key elements of signal transduction. In plants, research on signalling pathways and their modulation by aluminium ions must be further pursued. The challenge will be to identify some common principles by which aluminium possibly interferes with the cell's ability to communicate with its environment. The expression of cDNA's which encode G protein subunits and usage of immunological methodologies are promising molecular approaches to address putative beneficial and pathological functions of aluminium in signalling pathways. Given calcium's recognized role as second messenger and experimental evidence implicating calcium as being part of transmembrane signalling pathways, there is an urgent need to analyze intracellular calcium fluctuations in response to aluminium stress in genetically different plant cell and in intact plants. Understanding the significance of

aluminium-induced changes in calcium regulation will certainly yield insights into the likely involvement of signalling pathways in aluminium tolerance/toxocity.

Finally, these considerations may contribute to our knowledge of molecular aspects of aluminium tolerance thus permitting development of aluminium resistant varieties by biotechnological means. Research on the biochemistry of aluminium tolerance will continue to fuel the interest of scientists from diverse fields.

References

Akeson M A, Munns D N and Burau R G 1989 Adsorption of Al^{3+} to phosphatidylcholine vesicles. Biochim. Biophys. Acta 986, 33–40.

Akeson M A and Munns D N 1989 Lipid bilayer permeation by neutral aluminum citrate and by three alpha-hydroxy carboxylic acids. Biochim. Biophys. Acta 984, 200–206.

Akitt J W 1989 Multinuclear studies of aluminium compounds. Progr. NMR Spectr. 21, 1–149.

Allan E and Trewavas A 1985 Quantitative changes in calmodulin and NAD kinase during early cell development in the root apex of *Pisum sativum* L. Planta 165, 493–501.

Bennet R J, Breen C M and Fey M V 1985a The primary site of aluminium injury in the root of *Zea mays* L. South Afr. J. Plant Soil 2, 8–17.

Bennet R J, Breen C M and Fey M V 1985b Aluminium uptake sites in the primary root of *Zea mays* L. South Afr. J. Plant Soil 2, 1–7.

Berridge M J 1987 Inositol triphosphate and diacylglycerol: two interacting second messengers. Annus. Rev. Biochem. 56, 159–193.

Braam J and Davis R W 1990 Rain-, wind-, and touch-induced expression of calmodulin and calmodulin-related genes in Arabidopsis. Cell 60, 357–364.

Branton D and Jacobson L 1962 Iron localization in pea plants. Plant Physiol. 37, 546–551.

Castignetti D and Smarrelli J 1986 Siderophores, the iron nutrition of plants, and nitrate reductase. FEBS Lettr. 209, 147–151.

Chapman D and Hayward J A 1985 New biophysical techniques and their application to the study of membranes. Biochem. J. (London) 228, 281–295.

Cho S W and Joshi J G 1989 Time dependent inactivation of glucose-6-phosphate dehydrogenase from yeast by aluminum. Toxicol. 47, 215–219.

Cline G R, Reid C C P, Powell P E and Szaniszlo P J 1984 Effects of a hydroxamate siderophore on iron absorption by sunflower and sorghum. Plant Physiol. 76, 36–39.

Coleman J, Evans D and Hawes C 1988 Plant coated vesicles. Plant, Cell Environment 11, 669–684.

Conner A J and Meredith C P 1985 Simulating the mineral environment of aluminum toxic soils in plant tissue culture. J. Exp. Bot. 36, 870–880.

Cullis P R, De Kruijff B, Hope M J, Nayar R and Schmid S L 1980 Phospholipids and membrane transport. Can. J. Biochem. 58, 1091–1100.

Deleers M, Servais J P and Wülfert E 1986 Neurotoxic cations induce membrane rigidification and membrane fusion at micromolar concentrations. Biochim. Biophys. Acta 855, 271–276.

Deleers M, Servais J P and Wülfert E 1987 Aluminum-induced lipid phase separation and membrane fusion does not require the presence of negatively charged phospholipids. Biochem. Int. 14, 1023–1034.

Deufel J 1951 Untersuchungen über den Einfluss von Chemikalien und Röntgenstrahlen auf die Mitose von *Vicia faba*. Chromosoma 4, 239–272.

Domingo J L, Gomez M, Llobet J M and Corbella J 1988 Citric, malic and succinic acids as possible alternatives to deferoxamine in aluminum toxicity. Clin. Toxicol. 26, 67–79.

Erdei L, Berczi A and Zsoldos F 1981 Membrane and ion transport properties in cereals under acidic alkaline stress. Physiol. Plant 53, 471–474.

Foy C D, Chaney R L and White M C 1978 The physiology of metal toxicity in plants. Annu. Rev. Plant Physiol. 29, 511–566.

Foy C D 1988 Plant adaptation to acid, aluminum-toxic soils. Comm. Soil Sci. Plant Anal. 19, 959–987.

Gemrot P O 1986 Metabolism and possible health effects of aluminum. Environm. Health Perspect. 65, 363–441.

Gilman A G 1987 G proteins: transducers of receptor-generated signals. Annu. Rev. Biochem. 56, 615–649.

Godbold D L, Fritz E and Hüttermann A 1988 Aluminum toxicity and forest decline. Proc. Nat. Acad. Sci. USA 85, 3888–3892.

Gutteridge J M C, Quinlan G J, Clark I and Halliwell B 1985 Aluminium salts accelerate peroxidation of membrane lipids stimulated by iron salts. Biochim. Biophys. Acta 835, 441–447.

Haridasan M 1982 Aluminium accumulation by some cerrado native species of central Brazil. Plant and Soil 65, 265–273.

Haridasan M and De Araujo G M 1988 Aluminium-accumulating species in two forest communities in the Cerrado region of central Brazil. Forest Ecol. Managem. 24, 15–26.

Hartley F R, Burgess C and Alcock R M 1980 Solution Equilibria. Wiley, New York, NY. 361 p.

Haug A 1984 Molecular aspects of aluminum toxicity. CRC Crit. Rev. Plant Sci. 1, 345–373.

Haug A and Caldwell C R 1985 Aluminum toxicity in plants: The role of the root plasma membrane and calmodulin. *In* Frontiers of Membrane Research in Agriculture. Eds. J B St. John, E Berlin and P C Jackson. pp 359–381. Rowman & Allanheld, Totowaa, NJ.

Henderson S K, Desplaines K and Henderson D E 1989 HPLC separation and detection of inositol phosphate isomers. Biochrom. 4, 89–93.

Horst W J, Wagner A and Marschner H 1983 Effect of aluminium on root growth, cell division rate and mineral

element contents in roots of *Vigna unguiculata* genotypes. Z. Pflanzenphysiol. 109, 95–103.

Hübner R, Depta H and Robinson D G 1985 Endocytosis in maize root cap cells. Protoplasma 129, 214–222.

Ichimura K, Kihara H, Yamamura T and Satake K 1989 Negative cooperativity of chicken ovotransferrin on Al(III)-binding. J. Biochem. (Tokyo) 106, 50–54.

Itoh F, Minamide Y, Horie T and Awazu S 1989 Time dependent changes occurring in rat liver microsomes upon lipid peroxidation. Lipids 24, 905–908.

Johnson G V W and Jope R S 1986 Aluminum impairs glucose utilization and cholinergic activity in rat brain in vitro. Toxicol. 40, 93–102.

Kappus H 1987 Oxidative stress in chemical toxicology. Arch. Toxicol. 60, 144–149.

Karlik S J and Eichhorn G L 1989 Polynucleotide cross-linking by aluminum. J. Inorgan. Biochem. 37, 259–269.

Klausner R D and Kleinfeld A M 1984 Lipid domains in membranes. *In* Cell Surface Dynamics: Concepts and Models. Eds. A S Perelson, C DeLisi and F W Wiegel. pp 23–58. Marcel Dekker, Inc., New York, NY.

Konishi S, Miyamoto S and Taki T 1985 Stimulator effects of alu[illegible]um on tea plants grown under low and high phosphorus supply. Soil Sci. Plant Nutr. 31, 361–368.

Koyama H, Okawara R, Ojima K and Yamaya T 1988 Reevaluation of characteristics of a carrot cell line previously selected as aluminum-tolerant cells. Physiol. Plant. 74, 683–687.

Kury P G, Ramwell P W and McConnell H M 1974 The effects of prostaglandins E_1 and E_2 on the human erythrocyte as monitored by spin labels. Biochem. Biophys. Res. Comm. 56, 478–483.

Lange A J, Arion W J, Burchell A and Burchell B 1986 Aluminum ions are required for stabilization and inhibition of hepatic microsomal glucose-6-phosphatase by sodium fluoride. J. Biol. Chem. 261, 101–107.

Laussac J P and Commenges G 1983 ^1H, ^{13}C, ^{31}P and ^{27}Al NMR study of aluminium-ATP complexes. A possible relation with its biological application. Nouv. J. Chim. 7, 579–585.

Lewis T E 1989 (Ed.) Environmental Chemistry and Toxicology of Aluminum. Lewis Publ., Chelsea, MI. 344 p.

Lynch J M 1976 Products of soil microorganisms in relation to plant growth. CRC Crit. Rev. Microbiol. 5, 67–107.

Macdonald T L, Humphreys W G and Martin R B 1987 Promotion of tubulin assembly by aluminum ion. Science 236, 183–186.

Magnusson M K, Halldorsson H, Kjeld M and Thorgeirsson G 1989 Endothelial inositol phosphate generation and prostacyclin production in response to G-protein activation by AlF_4^-. Biochem. J (London) 264, 703–711.

Makarow M 1985 Endocytosis in *Saccharomyces cerevisiae*: Internalization of alpha-amylase and fluorescent dextran into cells. EMBO J. 4, 1861–1866.

Marschner H, Kalisch A and Romheld V 1974 Mechanism of iron uptake in different plant species. Proc. 7th Internat. Colloquium on Plant Analysis and Fertilizer Problems. pp 273–281. Hannover, Germany.

Matsumoto H, Hirasawa E, Torikai H and Takahashi E 1976 Localization of absorbed aluminum in pea root and its binding to nucleic acids. Plant Cell Physiol. 17, 127–137.

Matsumoto H and Yamaya T 1986 Inhibition of potassium uptake and regulation of membrane-associated Mg^{2+}-ATPase activity of pea roots by aluminium. Soil Sci. Plant Nutr. 32, 179–188.

Matsumoto H 1987 Reduced stability of chromatic structure of pea roots grown under calcium starvation. Plant Cell Physiol. 28, 643–652.

Matsumoto H 1988 Changes of the structure of pea chromatin by aluminum. Plant Cell Physiol. 29, 281–287.

McLachlan D R C 1989 Aluminum neurotoxicity: criteria for assigning a role in Alzheimer's disease. *In* Environmental Chemistry and Toxicology of Aluminum. Ed. T E Lewis. pp 299–315. Lewis Publ., Chelsea, MI.

Miquel J, Quintanilha A T and Weber H 1989 Handbook of free radicals and antioxidants in biomedicine. Vol. I. CRC Press, Boca Raton, FL. 337 p.

Muto S and Miyachi S 1986 Roles of calmodulin dependent and independent NAD kinases in regulation of nicotinamide coenzyme levels of green plant cells. *In* Molecular and Cellular Aspects of Calcium in Plant Development. Ed. A J Trewavas. pp 107–114. Plenum Press, New York, NY.

Naccache P H 1989 G Proteins and Calcium Signaling. CRC Press, Boca Raton, FL. 160 p.

Neilands J B 1981 Microbial iron compounds. Annu. Rev. Biochem. 50, 715–731.

Neilands J B and Leong S A 1986 Siderophores in relation to plant growth and disease. Annu. Rev. Plant Physiol. 37, 187–208.

Niedziela G and Aniol A 1983 Subcellular distribution of aluminium in wheat roots. Acta Biochim. Polon. 30, 99–105.

Nightingale E R 1959 Phenomenological theory of ion solvation: Effective radii of hydrated ions. J. Phys. Chem. 63, 1381–1387.

Öhman L O 1988 Equilibrium and structural studies of silicon(IV) and aluminum(III) in aqueous solutions. 17. Stable and metastable complexes in the system H^+-Al^{3+}-citric acid. Inorgan. Chem. 27, 2565–2570.

Pastan I and Willingham M C 1985 (Eds.) Endocytosis. Plenum Press, New York, NY. 326 p.

Pearse B M F and Crowther R A 1987 Structure and assembly of coated vesicles. Annu. Rev. Biophys. 16, 49–68.

Pettersson A, Hällboom L and Bergman B 1986 Aluminium uptake by *Anabaena cylindrica*. J. Gen. Microbiol. 132, 1771–1774.

Pettersson A and Bergman B 1989 Effects of aluminium on ATP pools and utilization in the cyanobacterium *Anabaena cylindrica*: A model for the *in vivo* toxicity. Physiol. Plant. 76, 527–534.

Pettersson S and Stid H 1989 Effects of aluminium on growth and kinetics of K^+(^{86}Rb) uptake in two cultivars of wheat with different sensitivity to aluminium. Physiol. Plant. 76, 255–261.

Piazza G A and Wallace R W 1985 Calmodulin accelerates the rate of polymerization of human platelet actin and alters the structural charateristics of actin filaments. Proc. Nat. Acad. Sci. USA 82, 1683–1687.

Putterill J J and Gardner R C 1988 Proteins with the potential to protect plants from Al^{3+} toxicity. Biochim. Biophys. Acta 964, 137–145.

Quinlan G J, Halliwell B, Moorhouse C P and Gutteridge J M C 1988 Action of lead(II) and aluminium(III) ions on iron-stimulated lipid peroxidation in liposomes, erythrocytes and rat liver microsomal fractions. Biochim. Biophys. Acta 962, 196–200.

Rana R S and Hokin L E 1990 Role of phosphoinositides in transmembrane signaling. Physiol. Rev. 70, 115–164.

Rasmussen C D and Means A R 1987 Calmodulin as regulator of cell growth and gene expression. J. Gen. Physiol. 19, 288–293.

Robinson D G and Depta H 1988 Coated vesicles. Annu. Rev. Plant Physiol. 39, 53–99.

Sandmann G and Böger P 1983 The enzymological function of heavy metals and their role in electron transfer processes of plants. *In* Inorganic Plant Nutrition. Eds. A Läuchli and R L Bieleski. pp 563–596. Springer-Verlag, Berlin.

Schaeffer H J and Walton J D 1990 Beta-(1→3) glucan synthesis by aluminum ions. Plant Physiol. (*In press*).

Schuber F 1989 Influence of polyamines on membrane functions. Biochem. J. (London) 260, 1–10.

Shann J R and Berruch P M 1988 Al and Ca interactions with isolated cell wall preparations. 80th annual meeting of ASA/SSSA, Anaheim, CA. p. 249.

Shi B and Haug A 1988 Uptake of aluminum by lipid vesicles. Toxicol. Environm. Chem. 17, 337–349.

Shi B and Haug A 1990 Aluminum uptake by neuroblastoma cells. J. Neurochem. (*In press*).

Shortle W C and Smith K T 1988 Aluminum-induced calcium deficiency syndrome in declining red spruce. Science 240, 1017–1018.

Simpson R J, Moore R and Peters T J 1988 Significance of non-esterified fatty acids in iron uptake by intestinal brush border membrane vesicles. Biochim. Biophys. Acta 941, 39–47.

Slaski J J 1989 Effect of aluminium on calmodulin-dependent and calmodulin-independent NAD kinase activity in wheat root tips. J. Plant Physiol. 133, 696–701.

Slaski J J and Amiot A 1987 Effect of calmodulin inhibitors on aluminium toxicity in cereals. Acta Physiol. Plant. 9, 13–23.

Slaughter G R, Meistrich M L and Means A R 1989 Expression of RNA's for calmodulin, actins, and tubulins in rat testis cells. Biol. Reproduct. 40, 395–405.

Sommarin M and Sandelius A S 1988 Phosphatidylinositol and phosphatidyl-inositolphosphate kinases in plant plasma membranes. Biochem. Biophys. Acta 958, 268–278.

Sposito G 1989 The Environmental Chemistry of Aluminum. CRC Press, Inc., Boca Raton, FL. 336 p.

Stoclet J C, Gerard D, Kolhoffer M C, Lugnier C, Miller R and Schaeffer P 1987 Calmodulin and its role in intracellular calcium regulation. Progr. Neurobiol. 29, 321–364.

Stummvoll H K, Graf H and Meisinger V 1984 Effect of desferrioxamine on aluminum kinetics during hemodialysis. Mineral Electrolyte Metab. 10, 263–266.

Suhayda C G and Haug A 1986 Organic acids reduce aluminum toxicity in maize root membranes. Physiol. Plant. 68, 189–195.

Tadolini B, Cabrini L, Landi L, Varani E and Pasquali P 1984 Polyamine binding to phospholipid vesicles and inhibition of lipid peroxidation. Biochem. Biophys. Res. Comm. 122, 550–555.

Taylor G J 1988 The physiology of aluminum tolerance. *In* Metal Ions in Biological Systems. Ed. H Sigel. Vol. 24, pp 165–198. Marcel Dekker, Inc., New York, NY.

Taylor G J 1988 The physiology of aluminum tolerance in higher plants. Comm. Soil Sci. Plant Anal. 19, 1179–1194.

Thompson J E, Chia L S, Barber R F and Sridhara S 1985 Comparative effects of senescence and chemical stress on the molecular organization of plant membranes. *In* Frontiers of Membrane Research in Agriculture. Eds. J B St. John, E Berlin and P C Jackson. pp 319–334. Rowan and Allanheld, Totowan, NJ.

Wagatsuma T and Yamasaku K 1985 Relationship between differential aluminum tolerance and plant-induced pH change of medium among barley cultivars. Soil Sci. Plant Nutr. 31, 521–535.

Wagatsuma T, Kyuuda T and Sakuraba A 1987 Aluminum accumulation characteristics of aluminum-tolerant plants. Bull. Yamagata Univ., Agr. Sci. 10, 355–359.

Walker P R, LeBlanc J and Sikorska M 1989 Effects of aluminum and other cations on the structure of brain and liver chromatin. Biochem. 28, 3911–3915.

Weis C and Haug A 1987 Aluminum-induced conformational changes in calmodulin alter the dynamics of interaction with melittin. Arch Biochem. Biophys. 254, 304–312.

Weis C and Haug A 1989 Aluminum-altered membrane dynamics in human red blood cell white ghosts. Thromb. Res. 54, 141–149.

Whallon J H and Flegler S L 1986 Determination of bound elements in mitotic chromosomes of *Zea mays* by energy-dispersive X-ray analysis. Cytobios 48, 45–61.

Xu Y, Ashgar A, Gray J L, Pearson A M, Haug A and Grulke E A 1990 ESR spin trapping of free radicals generated by hydrogen peroxide activation of metmyoglobin. J. Agr. Food Chem. (*In press*).

Yokel R A and Kostenbauder H B 1987 Assessment of potential aluminum chelators in an octanol/aqueous system and in the aluminum-loaded rabbit. Toxicol. Appl. Pharmacol. 91, 281–294.

Yuan S and Haug A 1988 Frictional resistance to motions of bimane-labelled spinach calmodulin in response to ligand binding. FEBS Lettr. 234, 218–223.

Yuan S and Haug A 1988 Ligand-triggered conformational perturbations elicit changes at the single cysteinyl residue in spinach calmodulin. Eur. J. Biochem. 175, 119–124.

Zhao X J, Sucoff E I and Stadelmann E J 1987 Al^{3+} and Ca^{2+} alteration of membrane permeability of *Quercus rubra* root cortex cells. Plant Physiol. 83, 159–162.

Zsoldos F and Erdei L 1981 Membrane and transport properties in cereals under acidic and alkaline stress. Physiol. Plant. 53, 468–470.

APPENDIX C

Changes in Intracellular Calcium of Porcine Sperm During in vitro Incubation with Seminal Plasma and A Capacitating Medium

Zhou R., Shi B., Chou K.C.K., Oswalt M.D. and Haug A.

Vol. 172, No. 1, 1990 BIOCHEMICAL AND BIOPHYSICAL RESEARCH COMMUNICATIONS
October 15, 1990 Pages 47-53

CHANGES IN INTRACELLULAR CALCIUM OF PORCINE SPERM DURING IN VITRO INCUBATION WITH SEMINAL PLASMA AND A CAPACITATING MEDIUM

R. Zhou,[1] B. Shi,[1] K.C.K. Chou,[2] M.D. Oswalt,[2] and A. Haug[1,*]

[1]Department of Microbiology and Pesticide Research Center, [2]Department of Animal Science and Center for Environmental Toxicology, Michigan State University, East Lansing, MI 48824

Received August 13, 1990

The intracellular free Ca^{2+} concentration in ejaculated, porcine sperm was determined with a fluorescent, Ca^{2+}-specific probe, Fura 2. Following suspension of sperm in a medium capable of sustaining capacitation and the acrosome reaction, the intracellular [Ca^{2+}] increased from an initial value of about 75 nM to a peak value of 130 nM, after about 4 to 5 h of incubation. Within this period of time, a peak value of 246 nM was attained when sperm was incubated in seminal plasma. Ca^{2+} uptake is presumably not associated with membrane potential-dependent channels. The results indicate that a pronounced increase in intracellular free Ca^{2+} occurs towards the end of the incubation period when rather synchronous acrosome reactions take place in the sperm population, either in capacitating medium or in seminal plasma.

Immediately following release from the male reproductive tract, mammalian sperm are incapable of fertilizing eggs. A series of sequential processes, namely capacitation and the acrosome reaction, must take place to confer upon sperm the full fertilizing potential (1). In the course of sperm activation the cellular surface is profoundly altered, in part by the interaction of macromolecules and ions present in the female reproductive tract (1,2,3). For some mammalian species, in vitro systems have been established (1), thus facilitating research on mechanisms involved in the capacitation and acrosome reaction phases of sperm activation. In the coordination of sequential phases Ca^{2+} appears to play a key role. Extracellular Ca^{2+} is essential for triggering the acrosome reaction (1) while Ca^{2+} has only recently been implicated to be involved at the end of the capacitation phase as opposed to early stages (4). Our knowledge about biochemical mechanisms of Ca^{2+} entry and regulation in

*To whom correspondence should be addressed.

0006-291X/90 $1.50

sperm is rather fragmentary. Concerning Ca^{2+} uptake, Na^{+}/Ca^{2+} antiports (5), calcium channels (6), and calmodulin-dependent, energy-requiring Ca^{2+} transporters (7) may be responsible. These types of uptake mechanisms may operate alone or in unison during various phases of sperm activation. Evidently, information is needed on the role of Ca^{2+} in integrating sequential processes of sperm activation.

The current study was therefore designed to examine temporal changes in the intracellular Ca^{2+} concentration, $[Ca^{2+}]_i$, of ejaculated boar spermatozoa during incubation in a capacitating medium and in seminal plasma. Employing a highly selective fluorescent Ca^{2+} indicator, Fura 2, $[Ca^{2+}]_i$ was found to vary dramatically after 4 to 5 h of incubation, especially in the presence of seminal fluid.

MATERIAL AND METHODS

Media and reagents: (a) Physiological medium (PM) comprises 145 mM NaCl, 0.5 mM $MgSO_4$, 5 mM KCl, 1 mM Na_2HPO_4, 1 mM $CaCl_2$, 5 mM glucose, and 10 mM HEPES buffer, pH 7.4. (b) Capacitation medium (CM) comprises 88 mL medium 199 (GIBCO, Gaithersburg, MD), 12 mL foetal calf serum, 2.3 g bovine serum albumin, 2.9 mM calcium lactate, 7.5 mg penicillin G (1670 U/mg), 5 mg streptomycin (750 U/mg), 100 mM HEPES, pH 7.8. Boar sperm reportedly acquired fertilizing ability after 4 to 5 h of incubation in this medium (8).

The fluorescent Ca^{2+} chelator, Fura 2/AM, was purchased as the cell- permeant ester, (1-[2-(carboxyoxazol-2-yl)-6-aminobenzofuran-5-oxyl]-2- (2'-amino-5'-methyl-phenoxy)-ethane-N,N,N',N'-tetraacetic acid, pentaacetoxy- methyl ester), from Molecular Probes (Eugene, OR). Fura 2/AM was maintained as a 1 mM stock solution in dimethyl sulfoxide, -20°C. All chemicals were of the highest grade available. Doubly glass-distilled water was used to prepare the buffer systems.

Boar sperm collection: Freshly ejaculated sperm were collected at room temperature from 2 years old Yorkshire boars (weight about 270 kg) at the Swine Research Center of Michigan State University. Semen samples were immediately filtered through Miracloth (Calbiochem, La Jolla, CA) to remove semen gel, and maintained at 38°C. Using a Makler counting chamber (Sefi-Medical Instruments, Haifa), sperm concentration and motility were measured with a Zeiss bright field microscope.

Filtered sperm were washed twice with physiological medium (PM), followed by further incubation in the same medium, or in a capacitating medium (CM). In experiments dealing with the effect of seminal fluid on Ca^{2+} uptake, filtered sperm were first centrifuged followed by incubation with seminal fluid. Incubated sperm (3.4×10^7 cells/ ml) were maintained at 38°C in an atmosphere of 5 percent carbon dioxide in air.

Intracellular Ca^{2+}: The relative fluorescence intensity was measured with a Perkin-Elmer luminescence spectrometer, model LS-5B. The excitation wavelength was set at 339 nm with 5 nm slits; emission was recorded at 500 nm with 10 nm slits.

Sperm suspensions were incubated with Fura 2/AM at a final concentration of 1 µM, 38°C, 1 h. 3 mL of Fura 2-loaded sperm were transferred to a quartz cuvette (final concentration 1.7×10^7 cells/ml), thermostatically maintained at 38°C. The concentration of dimethyl sulfoxide in the Fura 2/AM loading

solution was 0.25 percent (w/w). Control experiments showed no detectable influence of dimethyl sulfoxide on sperm motility and intracellular $[Ca^{2+}]$, at the solvent concentrations used. Regardless of the incubation media (PM, CM, seminal fluid) and time employed, subsequent dye loading (duration 1 h) and fluorescence studies were always performed in the presence of PM medium.

In dye-loaded cells, the intracellular Ca^{2+} concentration, $[Ca^{2+}]_i$, was determined following a procedure recently described (9). Briefly, the presence of extracellular Fura 2 (including leakage of Fura 2) was ascertained by addition of EGTA (3.3 mM) and then Tris (20 mM), at pH 8.2. The fluorescence minimum, F_{min}, was obtained by dye release from sperm in the presence of digitonin (0.06 mg/mL). Following addition of HCl (20 mM), the fluorescence maximum, F_{max}, was measured in the presence of 3.3 mM Ca^{2+} added, pH 7.5 (Fig. 1). Autofluorescence was spectrally subtracted. Generally the autofluorescence intensity was less than 20 percent that of F_{max}; autofluorescence intensity remained constant regardless of the presence of EGTA, Tris, digitonin, HCl, and Ca^{2+}. The intracellular concentration of Ca^{2+} was calculated from the relation $[Ca^{2+}]_i = k_d (F - F_{min})/(F_{max} - F)$, where k_d = 224 nM is the dissociation constant of calcium binding to Fura 2 (10).

RESULTS

Time course of $[Ca^{2+}]_i$ during incubation (Fig. 1). At the onset of incubation, $[Ca^{2+}]_i$ amounted to 70-80 nM. With an increase in incubation time, $[Ca^{2+}]_i$ increased concomitantly, its associated rate and peak value depen-

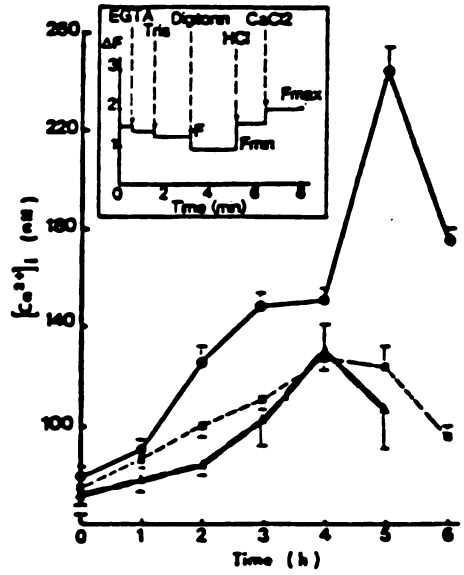

Fig. 1. Dependence of the intracellular free Ca^{2+} concentration in ejaculated porcine sperm on incubation time, in the presence of a physiological medium (■), a capacitating medium (▲), or seminal plasma (●), respectively. 1.7 x 10^7 cells/ml were loaded with a Ca^{2+}-specific, fluorescent chelator, Fura 2 (1 μM), 38°C. Following incubation in the respective medium, spectral measurements were always performed on cells suspended in physiological medium. Insert: Typical time dependence of changes in relative fluorescence intensity (ΔF) of Fura 2-loaded sperm following addition of EGTA (3.3 mM), Tris (2.2 mM), digitonin (0.05 mM), and HCl (20 mM). From these values the minimum and maximum values of fluorescence intensity were derived.

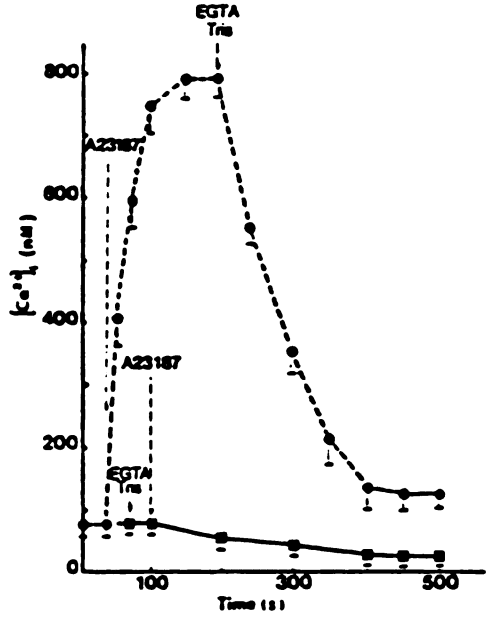

Fig. 2. Response of the intracellular free Ca^{2+} concentration in ejaculated porcine sperm, incubated in a physiological medium, to the application of a Ca^{2+}-specific ionophore, A23187 (25 nM), then followed by the application of EGTA (3.3 mM) and Tris (2.2 mM), respectively. These sperm were washed twice after collection. Without any preceding incubation, sperm were loaded with Fura 2/AM (duration 1 h), followed by A23187 treatment. Bottom: Response of intracellular $[Ca^{2+}]$ when the order of application of these agents was reversed.

dent on the type of incubation medium employed. Upon incubation in seminal plasma for 5 h, a peak value of $[Ca^{2+}]_i$ =246±10 nM was obtained which was almost twice as high as the corresponding peak values in the presence of the artificial media tested.

As determined in a physiological medium (PM), the peak value of $[Ca^{2+}]_i$ was independent of the presence or absence of monovalent Na^+ or K^+ in the incubation medium. This was illustrated, for example, by findings that in a PM medium devoid of K^+ (150 mM Na^+ added to maintain osmolarity), the maximal value of $[Ca^{2+}]_i$ was found to be 126±17 compared with the corresponding value of 129±4 measured after 4 h of incubation in the full PM medium.

Experiments were also performed regarding $[Ca^{2+}]_i$ in response to incubation in a medium deficient in Ca^{2+}; to this end 3.3 mM EGTA were added. Following incubation in EGTA-containing seminal plasma for 5 h, $[Ca^{2+}]_i$ was 108±7 nM, as opposed to 246±10 nM in the absence of the Ca^{2+} chelator. A

similar reduction in $[Ca^{2+}]_i$, viz., from 129 nM to 82 nM, was measured in sperm incubated in PM supplemented with EGTA (3.3 mM).

Intracellular $[Ca^{2+}]$ following induction of acrosome reaction. Since the acrosome reaction was reportedly (11) inducible by the application of a Ca^{2+} specific ionophore, A23187, the intracellular Ca^{2+} concentration was determined in response to the application of A23187 (25 µM) to the sperm suspension in PM (Fig. 2). These sperm were washed twice after collection. Without any preceding incubation, sperm were loaded with Fura 2/AM (duration 1 h, PM). Starting at a basal value of 75±5 nM, upon A23187 application $[Ca^{2+}]_i$ promptly increased (in about 2 min) to a maximal value of 791±37 nM. Subsequent administration of EGTA (3.3 mM) and Tris (2.2 mM) diminished $[Ca^{2+}]_i$ to a value of 125±23 nM, within less than 4 min. The latter Ca^{2+} concentration, 125 nM, is higher than that evaluated prior to the application of the ionophore, viz. 75 nM. Presumably, some Ca^{2+} became trapped in intracellular compartments following application of the Ca^{2+} chelator and Tris which enhances Ca^{2+} chelation at slightly alkaline pH. Reversing the sequence of treatment, viz., Tris/EGTA first, then A23187, yielded a value of 22±5 nM for $[Ca^{2+}]_i$ after about 6 min (Fig. 2). The presence of the ionophore apparently facilitated Ca^{2+} efflux, thus lowering the interior $[Ca^{2+}]$.

Sperm motility. Since sperm acquire unique motility patterns in the course of capacitation and the subsequent acrosome reaction (2, 12), sperm motility was evaluated. Irrespective of the incubation medium employed, 80-90 percent of sperm was found to be motile at the onset of incubation. Sperm motility declined to about 40-50 percent after 5 h of incubation in artificial media (PM and CM). In the presence of EGTA, motility further declined to a value of 30-40 percent (5 h). The observed motility decline with time is in accord with recent findings on boar sperm in a similary reconstituted medium 199 (13). Upon incubation of sperm in seminal plasma (5 h), however, motility remained at 70-80 percent, a value only slightly lower than that found at the onset of incubation. When cell viability was assessed with the Trypan blue assay (14), the initial viability was about 85 percent, and after 5 h of incubation (PM, SM) approximately 80 percent.

At the onset of incubation, the sperm motility pattern was characterized by linear swimming. After 5 h of incubation, this pattern was converted into one typified by nonprogressive, tumbling sperm movements, called "hyperactivation" (1,2,12).

As judged by motility and viability criteria, the micromolar Fura 2 concentration used exerted no detectable toxic influence upon sperm. This observation is consistent with motility studies employing a closely related dye, quin 2, for measurements of $[Ca^{2+}]$ in boar epididymal sperm (15).

Dye compartmentation: Since a spermatozoon is compartmentalized, the question arises as to the intracellular localization of free Ca^{2+} which is monitored in boar sperm by the fluorescent dye, Fura 2. Using a fluorescence microscope, examination of freshly Fura 2-loaded spermatozoa suggested that the sperm head was uniformly stained with the dye. This qualitative result is consistent with data obtained in response to digitonin application (Fig. 1). At the low concentration used, this membrane-disruptive agent reportedly released constituents of cytoplasmic rather than mitochondrial origin (16). It seems therefore that Fura 2 mainly monitored the Ca^{2+} concentration in the cytosol of the sperm head. In this context it appears noteworthy that recent ultrastructural findings demonstrated that bound Ca^{2+} can be detected in the anterior regions of the spermatozoon head during various stages of the acrosome reaction (17).

DISCUSSION

In this study we demonstrated temporal changes of intracellular $[Ca^{2+}]$ in ejaculated porcine sperm exposed to a capacitating medium, or to seminal plasma. Compared with $[Ca^{2+}]_i$ at the onset of incubation, enhancement of $[Ca^{2+}]_i$ is pronounced after 4 to 5 h in the media tested, especially upon incubation in seminal plasma. This period of time is in accord with recent data on boar sperm capacitation (8, 13). The dramatic increase of $[Ca^{2+}]_i$ of sperm in seminal plasma is perhaps related to several claims asserting that sperm capacitated in vivo are more effective in fertilizing ova than sperm capacitated in artificial media (1).

The pronounced increase (4-5 h) in $[Ca^{2+}]_i$ appears to coincide with the time required to achieve maximal fertilizing ability of boar sperm incubated in vitro (8). A relationship between enhanced $[Ca^{2+}]_i$ and the acrosome reaction is indicated by the manifold increase of $[Ca^{2+}]_i$ in the presence of A23187, a Ca^{2+} ionophore known to rapidly trigger the acrosome reaction in sperm in the presence of extracellular Ca^{2+} (2,11). Besides morphological parameters (hyperactivation, acrosome exocytosis), the enhanced $[Ca^{2+}]_i$ may thus be a useful biochemical marker suggestive of sperm fertilizing ability.

The virtual independence of $[Ca^{2}]_i$ on the presence of extracellular $[K^+]$ argues against a major involvement of voltage-gated channels in Ca^{2+} uptake by boar sperm because at the millimolar $[K^+]$ employed depolarization of the K^+-dependent membrane potential is to be expected (18).

ACKNOWLEDGMENTS

This study was supported in part by a grant from USDA, Food Toxicology Program. The authors are grateful to Alan Snedegar for the expert technical assistance in providing fresh boar sperm.

REFERENCES

1. Yanagimachi (1988) In The Physiology of Reproduction (Knobil, E. and Neill, J.D., eds), vol. 1, pp. 135-185. Raven Press, New York.
2. Blottner, S. (1989) Biol. Zentr. bl. 108, 41-62.
3. Blaquier, J.A., Cameo, M.S., Cuasnicu', P.S., Echeverria, M.F.G., Pineiro, L., Tezon, J.G., and Vazquez, M.H. (1988) Reprod. Nutr. Develop. 28, 1209-1216.
4. Fraser, L.R., and McIntyre, K. (1989) J. Reprod. Fertil. 86, 223-233.
5. Bradley, M. P. and Forrester, I.T. (1980) FEBS Lettr. 121, 15-18.
6. Breitbart, T., Rubinstein, S., and Nass-Arden, L. (1985) J. Biol. Chem. 260, 11548-11553.
. Silvestroni, L. and Menditto, A. (1989) Arch. Androl. 23, 87-96.
8. Saxena, M., Peterson, R.N., Saxena, N.K., and Russell, L.D. (1986) J. Reprod. Fertil. 78, 601-614.
9. Capponi, A.M., Lew, P.D., Schlegel, W., and Pozzan, T. (1986) Meth. Enzymol. 124, 116-135.
10. Grynkiewicz, G., Poenie, M., and Tsien, R.Y. (1985) J. Biol. Chem. 260, 3440-3450.
11. Byrd, W. (1981) J. Exp. Zool. 215, 35-46.
12. Lindemann, C.B. and Kanous, K.S. (1989) Arch. Androl. 23, 1-22.
13. Berger, T. and Horton, M.B. (1988) Gamete Res. 19, 101-111.
14. Shi, B. and Haug, A. (1990) J. Neurochem. 55, 551-558.
. Simpson, A.M. and White, I.G. (1988) Cell Calcium 9, 45-56.
. Akerman, K.E.A. (1989) FEBS Lettr. 242, 337-340.
17. Ruknudin, A. (1988) Gamete Res. 22, 375-384.
18. Chou, K., Chen, J., Yuan, S. and Haug, A. (1989) Biochem. Biophys. Res. Comm. 165, 58-64.

APPENDIX D

Uptake of Aluminum by Lipid Vesicles

Shi B. and Haug A.

Toxicological and Environmental Chemistry, Vol. 17, pp. 337–349
Reprints available directly from the publisher
Photocopying permitted by license only

Printed in Great Britain

Uptake of Aluminum by Lipid Vesicles

BIAO SHI and ALFRED HAUG

Department of Microbiology and Pesticide Research Center, Michigan State University, East Lansing, MI 48824, USA

(*Received in final form 4 January 1988*)

Aluminium uptake and tight binding were studied in multilayered phospholipid liposomes, as a model for cellular uptake of aluminum ions. Most of these studies were conducted with an initial aluminum concentration of 10 μM, while aluminum superficially bound to liposomes was removed by citrate chelation. Maximum uptake and tight binding of aluminium were pH-dependent. In dimyristoyl phosphatidylcholine (DMPC) liposomes, this maximum occurred in the neutral pH region, while it was shifted towards more acidic pH values in DMPC liposomes containing 20% of acidic phosphatidylserine. The initial rate of aluminum uptake was apparently dependent on the physical state of the liposome membrane. Prior formation of an aluminum-citrate chelate prevented aluminum uptake and tight binding to DMPC liposomes.

KEY WORDS: Aluminum, aluminum-citrate, aluminum uptake, atomic absorption, liposomes, membranes.

INTRODUCTION

Recently, aluminum has been implicated as a potentially toxic agent for various cellular constituents. Chromatin and DNA,[1] enzymes,[2] regulatory proteins like calmodulin,[3] cytoskeleton,[4] and cellular membranes[5] seem to emerge as critical factors in the expression of aluminum toxicity.

Irrespective of the primary lesion site, the plasma membrane is involved in the expression of aluminum toxicity by controlling the

entry of aluminum prior to its interaction with intracellular targets. A body of information suggests that in the plasma membrane aluminum is capable of altering physico-chemical properties of membrane lipids. For example, perturbations were observed in the plasma membrane of Thermoplasma acidophilum,[6] in oak root cells[7] and in phospholipid liposomes.[8] Membrane constituents such as proteins and carbohydrates can also act as lesion sites of aluminum.[9,10] Gross features of aluminum accumulation and distribution in plant and animal tissues have been investigated.[11,12] Only recently has aluminum uptake by individual cells been investigated with rat hepatocytes[13] and cyanobacterial cells.[14]

There is a profound lack of experimental data regarding cellular and molecular mechanisms of aluminum transport, e.g., the translocated aluminum species, the carriers involved (if any), the limiting reactions for the transport, and the role of the membrane's physical state and external factors. In this article we are therefore reporting on the application of phospholipid liposomes as model membranes in studies on aluminum interactions with membrane lipids.

MATERIALS AND METHODS

Chemicals

Phospholipids, i.e., dimyristoyl phosphatidylcholine (DMPC), dimyristoyl phosphatidylethanolamine (DMPE) and phosphatidylserine were purchased from Sigma Chemical Co. (St Louis, MO). Other reagents used were all of the highest quality available.

Liposome preparation

Phospholipids were dissolved in chloroform which had been redistilled and treated with molecular sieve (M-514, type 4A). The lipid suspension was dried in a rotary evaporator under a stream of nitrogen for 6 hours. The residual organic solvent was removed by further evaporating the sample in vacuum for another 6 hours. The multilamellar liposomes (vesicles) were prepared by the mechanical shaking technique. Dried lipids were added in the appropriate volume of PIPES buffer (5 mM, pH 6.5), which had been passed over a Chelex-100 column to remove any residual metals, and the mixture

was dispersed by violently shaking on a vortex rotamixer for 10 times, 1 min each. The resulting lipid vesicle suspension was diluted to 0.5 mg/ml of lipid. The suspension was allowed to stand for 2 hours to facilitate liposome swelling. Examination with a phase contrast microscope demonstrated the presence of large amounts of lipid vesicles.

Aluminum assay

The liposome samples were incubated with $AlCl_3$, at room temperature by gentle shaking, dissolved in 5 mM PIPES buffer. Aluminium stock, $AlCl_3$, was freshly prepared before the experiment. After incubation the liposome suspension was centrifuged at 10 000 g for 10 to 15 min. A portion of the sample was treated with EDTA or sodium citrate (final concentration 1 mM) for 10 to 15 min, followed by recentrifugation at 10 000 g for 10 min to remove aluminium bound onto the outer surface. The pellet was washed with 1 mM EDTA or citrate buffer once more. Two supernatants were combined for the determination of the aluminium concentration outside the liposomes. Another fraction of the sample was washed with chelator-free buffer. Furthermore, liposome pellets were also washed with chelator-containing buffer and subjected to acid digestion,[14] and the amount of aluminium coprecipitated with liposomes was measured. Within experimental errors both methods yielded the same result. The recovery was 93–104% of the aluminium added.

Furnace atomic absorption spectrophotometry was applied to quantitatively assay aluminum. The samples were analyzed with a Hitachi polarized Zeeman atomic absorption spectrophotometer, model 180-80, and the 309.3 nm wavelength was employed. The optimal furnace program was established in pre-experiments. An aliquot of a 20 μl sample solution was injected into a graphite cup (Hitachi Nr. 180-7402). Glassware was avoided for preventing contamination with aluminum.

RESULTS

In all of our experiments an aluminum concentration of 10 μM was used, i.e., a value lower than aluminum levels generally found in acidic soils.[15] After liposomes had been washed with 1 mM EDTA or

citrate, only a portion of aluminum added could be removed, and a fairly large amount of the metal was found to coprecipitate with liposomes after centrifugation. We attribute coprecipitated aluminum to that metal fraction taken up by liposomes and tightly and specifically bound to the liposomes. We define the latter fraction as that where the metal specifically interacted with lipid membrane, and thus distinguish this particular fraction from that characterized by superficially bound aluminum which is easily removed by the chelator wash. For convenient data analysis, we adjusted the experimental conditions (e.g., lipid concentration and incubation time) in such a manner as to produce 70–80% of coprecipitated aluminum.

pH effect on neutral phospholipid vesicles

In the neutral pH range both the major aluminum species[16] and the DMPC lipid have zero net charge. Regardless of the washing procedure applied, the interaction of aluminum with neutral liposomes was found to be pH-dependent (Figure 1). The maximum binding and uptake of aluminum appeared to take place in the range of pH 6.0–7.0. Beyond this range the amount of coprecipitated aluminum decreased remarkably as the pH changed in both the acidic and alkaline regions; in the alkaline region the decrease was more pronounced. At pH 4.0 or pH 8.0, the majority of aluminum (approximately 90%) was removed by EDTA treatment.

Liposomes were also prepared from DMPE, a neutral phospholipid at neutral pH. Rather similar uptake and binding patterns were obtained as indicated by a maximum of coprecipitated aluminum at pH 6.0–7.0.

pH effect in phosphatidylserine-containing liposomes

Phosphatidylserine is an acidic phospholipid, carrying a net negative charge at neutral pH. Acidic membrane vesicles were prepared containing 20% phosphatidylserine and 80% (w/w) DMPC. The peak of the curve shifted about 2 pH units compared with that obtained in DMPC or DMPE liposomes (Figure 2). In other words, aluminum uptake by and tight binding to the acidic lipid vesicles occur mostly in the pH range 4.0 to 5.0.

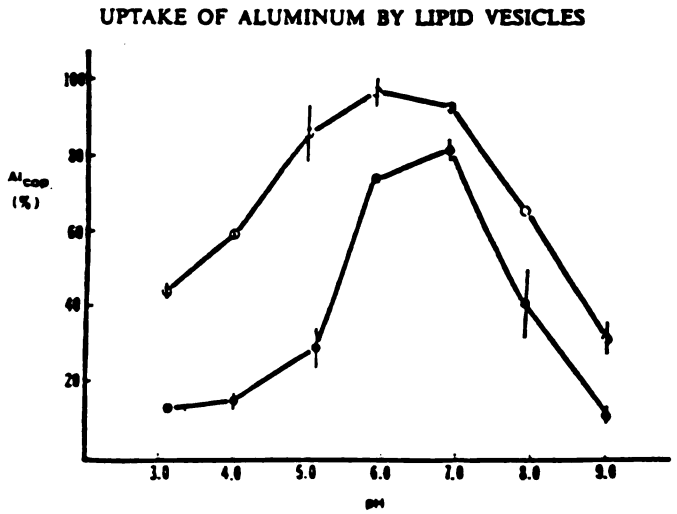

Figure 1 Auminum coprecipitation with DMPC liposomes at various pH values. DMPC liposomes were incubated with 10.0 μM (270 μg/l) aluminum (added from $AlCl_3$ stock solution) at room temperature for 12 hours. Aluminum-stressed liposomes were washed with 1.0 mM EDTA in 5 mM PIPES (●) or EDTA-free PIPES buffer (○), pH 6.5. Data are the average of three replicates. Error bars represent standard deviation.

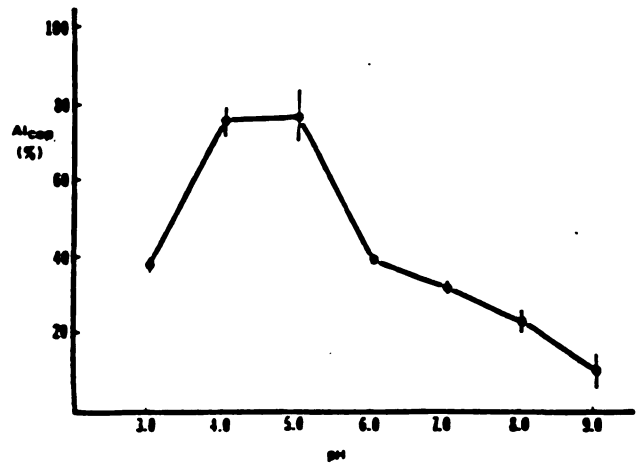

Figure 2 Aluminum coprecipitation with phosphatidylserine-containing liposomes (80% DMPC + 20% (w/w) phosphatidylserine) at various pH values. Following exposure to 10.0 μM aluminum for 12 hours, the liposomes were washed with 1.0 mM sodium citrate in 5 mM PIPES. Error bars represent standard deviation.

Time course and citrate effect

The time course of aluminum-liposome interaction was followed on DMPC liposomes at pH 6.5. For the aluminum assay an aliquot of the sample was taken out at various incubation times, followed by treatment with chelator-free or chelator-containing buffer. The results are presented in Figure 3. Superficial binding of aluminum to lipid membranes seems to be fairly rapid, being completed within a few minutes. However, the specific interaction of aluminum with membrane lipids was relatively slow, as reflected by the extent of aluminum coprecipitation. In the first hour there was a rapid phase of aluminum coprecipitation although the reaction rate decreased

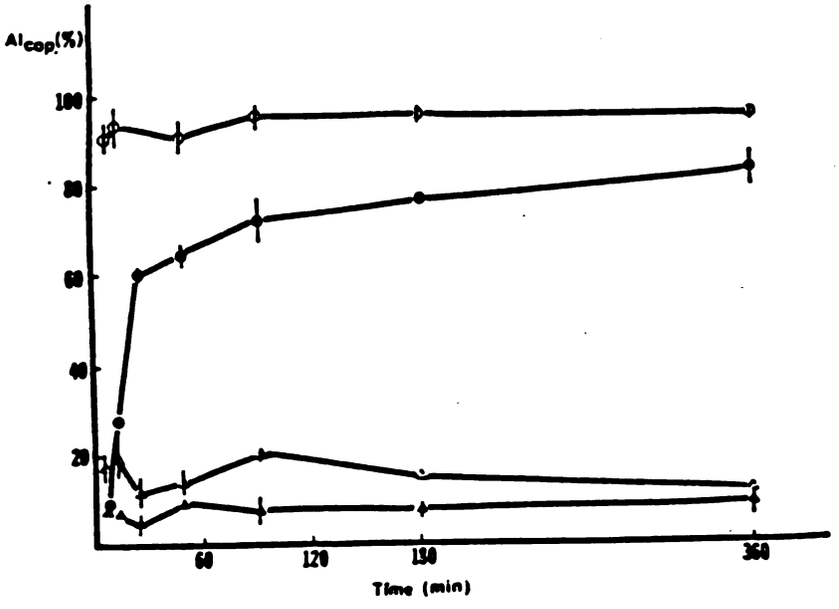

Figure 3 Time course of aluminum coprecipitation with DMPC liposomes in the absence (● ○) or presence (▲ △) of citrate (final concentration 12.0 μM). In the latter case, aluminum stock was preincubated with sodium citrate for 15 min, before being applied to liposomes. Liposomes were incubated with $AlCl_3$ 10.0 μM. Aliquots were taken from the sample at 6, 12, 24, 48, 90, 180 and 360 min following aluminum application. For aluminum determination the sample was washed with 2 mM citrate in 5 mM PIPES buffer (● ▲) or citrate-free PIPES buffer (○ △). Error bars represent standard deviation.

remarkably. After two hours the coprecipitated metal quantity still increased slightly and the reaction system did not attain equilibrium even after 6 hours.

To determine whether citrate-mediated aluminum transport across the lipid bilayer is taking place, aluminum stock was preincubated with sodium citrate (final [Al]/[citrate] molar ratio = 1.0:1.2) in slight excess prior to application of DMPC liposomes. Most of the aluminum was retained in the supernatant, and only a small portion (approximately 10–20%) was detected in liposome pellets after the solution had been treated with either citrate-free buffer or buffer containing 1 mM citrate. Consequently prior aluminum chelation by citrate prevented aluminum from being bound to membrane lipids or from being taken up by lipid vesicles. This inhibition was also observed when other organic acid aluminum chelators, e.g., malate and succinate, were used, and the inhibitory effect of the organic acids was in accord with their chelating abilities.

Temperature effect

As to the influence of the physical state of the lipid bilayer on aluminum-membrane interaction, experiments were conducted at temperatures below and above the phase transition point for DMPC vesicles. For our sample we confirmed a temperature of 22.5°C as the transition temperature by monitoring the temperature dependent motion of a spin probe, viz., that of 2,2,6,6-tetramethyl-piperidine-1-oxyl, incorporated into the lipid matrix.[17] Aluminum-treated DMPC liposomes were incubated at 15° and at 37°C, respectively. Initially, binding and uptake of aluminium by lipid vesicles (Figure 4) were faster in the liquid-crystalline membrane state, i.e., at the higher temperature, compared with that in the gel state at 15°C. Within experimental error, however, the total amount of aluminum co-precipitated after 3 hours of liposome incubation was virtually the same regardless of the incubation temperature. This indicates that the membrane fluidity mainly influenced the interaction rate but did not affect the aluminium distribution when the interaction equilibrium was established at a given temperature.

Calcium effect

The effect of Ca^{2+} on aluminum-lipid membrane interaction was also investigated with DMPC liposomes. For the duration of 2

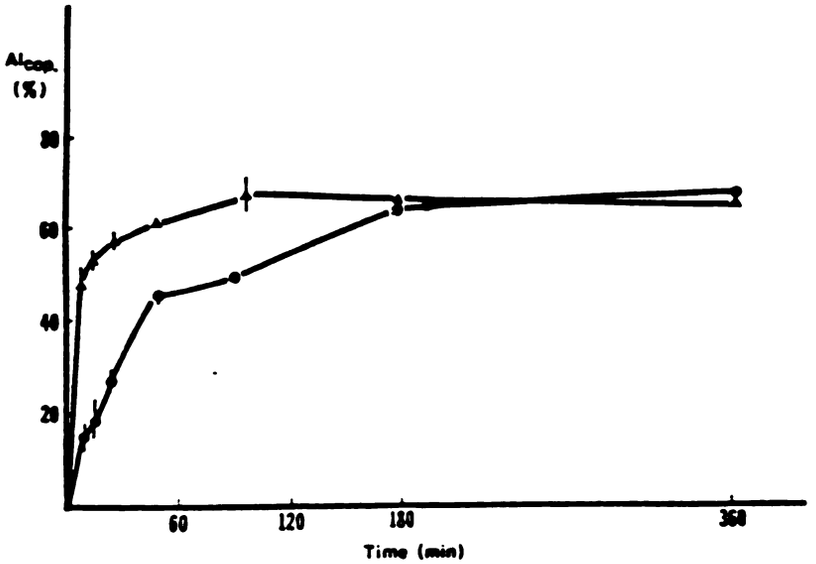

Figure 4 Time course of aluminum coprecipitation with DMPC liposomes at two different temperatures. Liposomes were incubated with aluminium (10.0 μM) at 15°C (•) and 37°C (▲), respectively. Following addition of aluminum, samples were taken at 6, 12, 24, 48, 90, 180 and 360 min. For determining the aluminum content, samples were washed with 1 mM citrate in 5 mM PIPES buffer. Error bars represent standard deviation.

hours, the liposome suspension was preincubated with Ca^{2+} of varying concentrations prior to aluminum administration. A higher citrate concentration was used in the washing procedure to prevent the possible competition of Ca^{2+} for the metal-chelator, even though the dissociation constant, K_d, of citrate for Al(III) (10^{-8} to $10^{-9}M^{-1}$)[18] is known to be 4 orders of magnitude lower than that for Ca^{2+}.[19] Results in Table 1 show that binding and uptake of aluminium were not affected by the presence of Ca^{2+}, at a concentration up to 5 mM, the normal extracellular Ca^{2+} level. It is noteworthy that Ca^{2+} does not interfere in atomic absorption measurements of aluminum when the concentration ratio of [Ca^{2}]/[aluminum] is 50000:1.[20] We verified these findings by a control experiment in which Ca^{2+}-treated DMPC liposome suspensions were incubated with aluminum-free buffer and standard aluminum was added into the supernatants after centrifugation (Table 2).

UPTAKE OF ALUMINUM BY LIPID VESICLES

Table 1 Aluminum coprecipitation with DMPC liposomes in the presence of Ca^{2+}. Lipid vesicle solutions (pH 6.5) were preincubated with $CaCl_2$ solution for 2 hours and then stressed by 10.0 μM $AlCl_3$ for 6 hours. The liposomes were washed with 10.0 mM citrate, followed by assay for aluminium. Data listed are averages for values obtained in 10 independently treated samples

$[Ca^{2+}]$	$^{Al}_{cop}$ percent ± SD
0	81.8 ± 2.5
1.0 mM	79.3 ± 4.2
2.0 mM	81.0 ± 3.1
5.0 mM	83.7 ± 3.6

Table 2 Aluminum recovery in the presence of Ca^{2+}. Lipid vesicle suspensions were preincubated with $CaCl_2$ solution for 6 hours and the Ca^{2+}-loaded liposomes were treated with 10 mM citrate. After centrifugation, 270 μg/l aluminum was added to the supernatants and aluminum was determined. Data are the average of 8 independent experiments

$[Ca^{2+}]$	$^{Al}_{measured}$
0	280.8 ± 7.7 μg
1.0 mM	290.5 ± 5.8 μg
2.0 mM	276.0 ± 13.0 μg
5.0 mM	278.0 ± 12.0 μg

DISCUSSION

In our experiments multilayer liposomes were selected as model membranes for the purpose of simulating membrane systems of eukaryotic cells. Incubating a liposome suspension with $AlCl_3$, a fairly large portion of aluminum could not be removed with chelator solution but coprecipitated with liposomes, suggesting aluminum

accumulation in the liposome lumen. To reach the liposome lumen, neutral aluminum species are favored since the apolar portion of the lipid matrix constitutes a barrier for the movement of charged species across the membrane. At neutral pH and at micromolar concentration, aluminium predominantly exists in the forms, $Al(H_2O)_3(OH)_3$[16] and $Al(H_2O)_4(OH)_2Cl$.

This conclusion is in accord with findings that nonionic complexes of mercury, $HgCl_2$, $Hg(OH)_2$ and TlCl, traverse lipid bilayers at significant rates.[21] Passive diffusion has also been implicated in aluminum uptake by plants[22] and cyanobacteria.[14]

Resembling somewhat cellular membranes in terms of heterogeneous lipid compositions and membrane properties, phosphatidylserine-containing acidic liposomes showed a maximum of aluminum coprecipitation at pH 4.0 to 5.0, compared with a neutral pH range for neutral liposomes. Probably different species and mechanisms are involved in aluminum uptake by and interactions with phosphatidylserine-containing liposomes relative to neutral liposomes. At pH 4.0 to 5.0, ionic forms like $Al(H_2O)_6^{3+}$ and $Al(H_2O)_5(OH)^{2+}$ become major species in solution.[16] Appreciable diffusion of these charged ions across the lipid bilayer is only feasible via appropriate carriers or by leakage of the lipid matrix. Increased liposome permeability may result from aluminum-induced phase separation and/or liposome aggregation.[23] Aluminum ion transport may also occur with phosphatidylserine as mobile, negatively-charged carriers. This type of ionophoretic capacity was demonstrated on lipids from barley root plasma membranes.[3]

Concerning our experimental results, the question has to be addressed whether aluminum coprecipitation with liposomes may be considered a valid estimate of intraliposomal accumulation rather than that of binding of the metal to phospholipid molecules on the liposome's outer surface.

For the purpose of removing aluminum ions we used most of the time citric acid, a potent aluminum chelator. Aluminum-citrate chelates are characterized by a dissociation constant of 10^{-8}–$10^{-9}M^{-1}$.[18] As to phospholipids, phosphatidylserine forms the most stable complex with aluminum typified by a dissociation constant varying from 10^{-4} to $10^{-5}M^{-1}$,[24] i.e., 3 to 4 orders of magnitude lower than that of the citrate-aluminum chelate. Noting that in our studies a molar ratio of about 1.5:1 for [citrate]/

[phospholipids] was used, and because that of [citrate]/[aluminum] was at least 100:1, it seems that 1 mM citrate is sufficient in removing bound aluminum from liposomes effectively. This notion is supported by several observations: (a) No further aluminum was removed in the supernatant when the citrate concentration in the washing solution was increased up to 10 mM. (b) Preincubation of aluminum with a slight excess of citrate almost completely prevented metal binding to phospholipid vesicles (Figure 3). (c) Adsorption of metal by phospholipids occurs rapidly[25] while diffusion of aluminum through the lipid matrix is expected to proceed much slower, as reflected by the time course curves (Figure 3). (d) Application of Ca^{2+} of up to 5 mM (i.e., 500 times that of aluminum) caused little displacement of aluminum from phospholipid liposomes (Table 2). (e) Generally associations are less likely as the temperature rises. On the other hand, permeants seem to traverse the membrane at a faster rate at higher temperatures, presumably facilitated by a more fluid matrix of the liposome. Our results on the temperature dependence (Figure 4) are in general accord with temperature-facilitated aluminum permeation.

Neverthless, probably not all aluminum adsorbed on the outer surface of liposomes was removed following application of a chelator. For example, aluminum might be trapped by phospholipids at certain sites or might have altered the lipid bilayer conformation in such a manner that aluminum becomes inaccessible for washing agents.

We therefore suggest that aluminium coprecipitated with liposomes, after chelator wash, is composed of two fractions, viz., a major fraction taken up by lipid vesicles and accumulated in the lipid lumen and a minor fraction of specifically and tightly bound aluminium on the liposome surface. Only superficially bound metal can be easily removed by washing with chelator solution. Because of the low aluminium concentration used, it is reasonable to assume that multilayered lipid vesicles can incorporate the bulk of metal administered, even though the exact amount is not known.

In studies on aluminum uptake by cyanobacteria, optimal recovery of cellularly bound aluminum was achieved by incubating cells with 1 mM EDTA for 10 min.[14] EDTA-washing was also widely used to distinguish metals adsorbed onto the cell surface from metals taken up by cells. Dilute EDTA solutions (molar ratio of [EDTA]/

[metal] = 2:1) rapidly removed in a few min 98–100% of adsorbed Cd, Cu and Zn by the blue-green alga, Chroococcus paris.[25] This technique was also employed to separate bound aluminum from intracellular one. It appears more difficult to remove bound metal from the intact cell surface than that from the phospholipid membrane because of the complexity of biological membranes and the presence of cell wall constituents.

Results from our experiments also indicate that application of citrate, as low as 10 μM, greatly inhibited both binding and uptake of aluminum by phospholid vesicles (Figure 3). These findings are in general accord with results obtained on plant membranes. Both membrane-bound ATPase activity and membrane structure could in part be protected from aluminum injury when citric acid was administered prior to the metal.[26] Furthermore, aluminum-tolerant carrot cells reportedly reduced aluminum uptake by releasing increasing amounts of citric acid to chelate the metal in the medium.[27] On the other hand, when rats were fed aluminum citrate, distinctly elevated aluminum levels were found in the brain compared with animals similarly treated with aluminum hydroxide, indicating that aluminum citrate may be a chemical form preferentially taken up and transported.[12]

Acknowledgement

This work was supported by a grant from the National Institutes of Health No. 1-RO1 ES04468-01. We thank Dr J. Giesy for use of the Hitachi Zeeman atomic absorption spectrophotometer. Thanks are extended to John Nesterod for technical assistance with the atomic absorption measurements.

References

1. S. J. Karlik, G. L. Eichhorn and D. R. Crapper McLachlan, *Neurotoxicol.* 1, 83 (1980).
2. J. C. K. Lai and J. P. Blass, *J. Neurochem.* 42, 438 (1984).
3. A. Haug, *CRC Crit. Rev. Plant Sci.* 1, 345 (1984).
4. D. R. Crapper and G. J. Tomko, *Brain Res.* 97, 253 (1980).
5. A. Pettersson, L. Hällbom and B. Bergman, *Physiol. Plant* 63, 153 (1985).
6. R. Vierstra and A. Haug, *Biochem. Biophys. Res. Commun.* 84, 138 (1978).
7. X. J. Zhao, E. Sucoff and E. J. Stadelmann, *Plant Physiol.* 83, 159 (1987).
8. M. Deelers, J. P. Servais and E. Wülfert, *Biochem. Internat.* 14, 1023 (1987).
9. K. Morita, S. Inoue, Y. Murai, K. Watanabe and S. Shima, *Exper.* 38, 1227 (1982).
10. C. Moreno, M. R. Lifely and J. Esdaile, *Infect. Immun.* 9, 587 (1985).

11. A. Goransson and T. D. Eldhuset, *Physiol. Plant.* **69**, 193 (1987).
12. P. Slanina, Y. Falkeborn, W. Frech and A. Cedergren, *Fd. Chem. Toxicol.* **22**, 391 (1984).
13. M. Muller and M. Wilhelm, *Toxicol.* **44**, 203 (1987).
14. A. Pettersson, L. Hällbom and B. Bergman, *J. Gen. Microbiol.* **132**, 1771 (1986).
15. C. S. Andrew, *Limitations and Potential for Biological Nitrogen Fixation in the Tropics*, in: J. Doebereiner, R. H. Burris, A. Hollaender, A. A. Franco, C. A. Neyra and D. B. Scott, eds. (Plenum Press, New York, 1979), pp. 135–160.
16. C. F. Baes and R. E. Mesmer, *The Hydrolysis of Cations* (J. Wiley & Sons, New York, 1976), pp. 112–123.
17. R. S. Phedke, N. V. Kumar, R. V. Hosur, V. W. Kulkarni, A. Saran and G. Goril, *Int. Quantum Chem.* **20**, 85 (1981).
18. K. E. Neet, T. C. Furman and W. J. Hueston, *Arch. Biochem. Biophys.* **213**, 14 (1982).
19. A. E. Martell and R. M. Smith, *Critical Stability* (Plenum Press, New York, 1977), Vol. 3, p. 167.
20. S. S. Krishnan, S. Quittkat and D. R. Crapper, *Can. J. Spectroscopy* **21**, 25 (1975).
21. T. Gutknecht, *Biophys. J.* **41**, 183a (1983).
22. A. Aniol, *Biochem. Physiol. Pflanzen* **178**, 11 (1983).
23. M. Deleers, J. P. Servais and E. Wüllert, *Biochim. Biophys. Acta* **813**, 195 (1985).
24. M. Deleers, *Res. Commun. Chem. Pathol. Pharmacol.* **49**, 277 (1985).
25. A. Les and R. W. Walker, *Water, Air and Soil Pollution* **23**, 129 (1984).
26. C. G. Suhayda and A. Haug, *Physiol. Plant.* **68**, 189 (1986).
27. K. Ojima, H. Abe and K. Ohira, *Plant and Cell Physiol.* **25**, 855 (1984).

APPENDIX E

Channel-closing Activity of Porins from *Escherichia coli* in Bilayer Lipid Membranes

Xu G., Shi B., McGroarty E.J. and Tien H.T.

Biochimica et Biophysica Acta 862 (1986) 57–64
Elsevier

BBA 73321

Channel-closing activity of porins from *Escherichia coli* in bilayer lipid membranes

Guangzhou Xu [a], Biao Shi [b], Estelle J. McGroarty [a] and H. Ti Tien [b]

[a] *Department of Biochemistry and* [b] *Department of Physiology, Michigan State University, East Lansing, MI 48824 (U.S.A.)*

(Received 12 May 1986)

Key words: Porin; Ion channel; Planar bilayer membrane; (*E. coli*)

The opening and closing of the ompF porin from *Escherichia coli* JF 701 was investigated by reconstituting the purified protein into planar bilayer membranes. The electrical conductance changes across the membranes at constant potential were used to analyze the size and aggregate nature of the porin channel complexes and the relative number of opening and closing events. We found that, when measured at pH 5.5, the channel conductance diminished and the number of closing events increased when the voltage was greater than 100 mV. The results suggest that the number of smaller sized conductance channels increases above this potential. There was also an increase in the smaller subunits and in the closing events when the pH was lowered to 3.5, and these changes were further enhanced by increasing the voltage. We propose that both lowering the pH and elevating the potential across the membrane stabilize the porin in a conformation in which the subunits are less tightly associated and the subunits open in a non-cooperative manner. These same conditions also appear to stabilize the closed state of the pore.

Introduction

The porin proteins in the outer membranes of mitochondria and Gram-negative bacteria have been studied extensively in recent years [1]. These porins, which are thought to have evolved from a common ancestral protein, function as molecular sieves, allowing small hydrophilic molecules to pass across the membrane. The best characterized porin is the ompF protein of *Escherichia coli*. The primary sequence of this protein is known [2]. Its secondary structure, as revealed by circular dichroism of detergent solubilized protein [3] and X-ray diffraction analysis of crystallized protein [4,5], is high in β-structure.

Electron micrographs of bacterial porin [6,7] and conductance measurements across bilayer membranes containing porin suggest that, in the membrane, the protein exists as trimeric units of three identical polypeptides [8,9]. However, information on the tertiary and quaternary structure of these porin aggregates and conformational changes that occur in these complexes is still far from complete. Analysis of the structure of the ompF trimer in the electron microscope has indicated that three openings exist on the outer face of the complex. These channels appeared to fuse in the middle of the membrane, forming a single channel exiting on the inner face of the membrane [7]. Such a branched channel model would predict that the porin subunits, if separated from the other subunits, would be unable to form a chan-

Abbreviations: SDS, sodium dodecyl sulfate; CIE, current increment events; CDE, current decrement events; PC, phosphatidylcholine; PE, phosphatidylethanolamine.

Correspondence: Dr. E.J. McGroarty, Department of Biochemistry, Michigan State University, East Lansing, MI 48824, U.S.A.

0005-2736/86/$03.50

nel. Furthermore, in such a complex, the central constriction would be limiting for the movement of ions [1]. Closing of only one of the three external portals would decrease the current across the pore by only about 5% and closing a second external entrance would decrease the current by another 10–20% [1]. In contrast, if each of the porin subunits within the trimer contained a complete and separate channel through the membrane, closing one or two of the subunits would decrease the conductance by 33% or 66%, respectively, of that for the entire complex. In this study, we detected conductance changes of the ompF protein in a bilayer membrane of 33% and 66% of that of the main channel event. Our results suggest that units containing three channels are the major conductance channel, but monomers and dimers had channel-forming activity and that these smaller conductance channels increase under conditions where the interactions between the subunits within the trimer were weakened. In the present study, we have also analyzed voltage controlled properties of bacterial porin channels. The size of the porin channels of the mitochondrial outer membrane has been shown to be voltage-dependent: that is, the size of the single-channel conductance decreases and the number of closing events increases with increasing voltage [10–12]. Also, Schindler and Rosenbusch [8.13] found that bacterial porins inserted in a bilayer lipid membrane close when the electrical potential exceeds a threshold value of about 140 mV. Others [14.15], however, have been unable to show such effects and some investigators have asserted that the small number of channel closing events is unaffected by the sign or size of the membrane potential [16].

In this study, we analyzed conductance across bilayer lipid membranes containing ompF porin. We measured more than 10^3 discrete electrical current increment events (CIE), presumably reflecting channel opening, and current decrement events (CDE), representing channel closing. We found that the size distribution of the channels and the percent of total events which were CIEs decreased with increasing membrane potential.

Material and Methods

Porin preparation

The ompF protein was isolated and purified from *E. coli* strain JF 701 [17]. The bacteria were grown and the protein-lipopolysaccharide-peptidoglycan complex was isolated as described by others [18]. The isolation and purification of the protein was similar to that used by Benz and co-workers [14] with some modification. The trypsin treatment was repeated four times to remove the peptidoglycan layer. A CL-Sepharose-4B column was used for the fractionation of the protein aggregates. The protein content in the eluted solution was monitored by measuring absorption at 280 nm. The main protein-containing peak eluted as an aggregate of about 800 kDa [19] and was collected and stored at −20°C. The isolate produced a single band on sodium dodecyl sulfate (SDS)-polyacrylamide gels. Before addition to the membrane system, the sample was solubilized in solution A, comprised of 0.1% SDS, 3 mM NaN_3, 5 mM Tris-HCl (pH 8) and frozen and thawed multiple times (> 20). Between 1 and 5 μl of porin in solution A at 200 μg/ml was added to a 7 ml solution of 0.1 M NaCl or of 0.1 M KCl (pH 3.5 or pH 5.5) for 30 to 120 minutes prior to analysis in a bilayer lipid membrane.

Bilayer lipid membrane

The principle and techniques used to study bilayer lipid membranes have been described previously [20]. The lipids used to form the membrane included oxidized cholesterol, soybean phosphatidylcholine (PC, Sigma Chemical Co.), and L-α-phosphatidylethanolamine (PE, type V, from *E. coli*, Sigma Chemical Co.). Oxidation of cholesterol (Eastman Chemicals) was performed by the method of Tien et al. [21]. The membrane was formed by applying a 1.5% lipid solution in *n*-decane to a hole in a teflon chamber submersed in a bathing solution at pH 5.5 or 3.5. The lifetime of the bilayer lipid membranes was > 0.5 h and the resistance was $> 10^8\ \Omega \cdot cm^2$ in the absence of porin. The pH was adjusted using HCl and measured with a pH meter. The membrane was monitored with a microscope until it turned black, indicating that a bimolecular leaflet had formed. Porin was added either before or after the membrane became black. Constant voltage was maintained during all experiments, and the current across the membrane was measured using a Keithley model 610 electrometer.

The stepwise conductance changes, Λ, across the membrane were measured and divided by the specific conductance, σ, of the solution. Assuming that the porin channel is a hollow water-filled cylinder, then $\Lambda/\sigma = \pi r^2/l$ where r is the inner radius of the channel at its narrowest section and l is the channel length. In this study, most conductance changes are reported as the size parameter Λ/σ since this parameter is proportional to the cross-sectional area of the channel and corrects for the changes in conductances at different pH values and in different salt solutions.

Results

Abrupt stepwise increases and decreases in the current across the bilayer lipid membrane in the presence of porin were recorded from the electrometer, as shown in Fig. 1. We assume that the CIE represent opening of porin channels, while the CDE represent closing events (arrows, Fig. 1). The size parameter, Λ/σ, represents the conductance change of the membrane (Λ) divided by the specific conductance of the bathing solution (σ) and is presumed to be proportional to the cross sectional area of the channel at its narrowest point (see Material and Methods). At low voltages (< 100 mV), the majority of conductance changes had size parameter values of approx. 3.1 Å, while a few smaller current jumps, indicated by M (Fig. 1), were detected which had size values approximately one-third of the main conductance change.

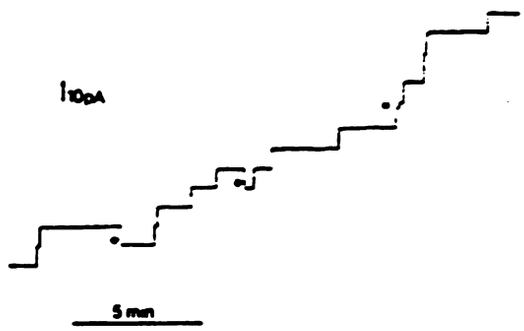

Fig. 1. Stepwise current changes across a membrane comprised of PC/oxidized cholesterol (2:1) in the presence of 60 ng/ml of ompF protein in a bathing solution of 0.1 M NaCl (pH 5.5). The porin was pretreated by repeated freezing and thawing in solution A, followed by preincubation in the bathing solution for 30 to 60 min at room temperature. The current decrements, indicated by arrows, presumably represent channel closing events of porin trimers and have the same size as the majority of increment events. The current change, indicated by M, has a magnitude one-third of the majority of events and is assumed to indicate the opening of a single channel. The voltage across the membrane was 50 mV. The baseline of the tracing was omitted.

The size parameters of both CIE and CDE were recorded at different transmembrane potentials. In these studies the bilayer lipid membrane, comprised of a 2:1 mixture of PC/oxidized cholesterol (by weight), was bathed in 0.1 M NaCl (pH 5.5), and the transmembrane potential maintained at values between 25 and 150 mV. At each voltage, approximately 200 individual events were measured, and histograms of the relative number (P) of CIE and CDE events were plotted against the Λ/σ values (Fig. 2). One can see that at all voltages studied, the main channel size was approx. 3 Å (Table I). However, with increasing voltage, smaller channel events became prominent (Fig. 2, Table I). At a transmembrane potential of 125 mV, three distinct populations of channels were evident: the main channel of size 3.1 Å, and two smaller channels, 0.9 and 1.7 Å in size. These smaller channels have cross-sectional areas approximately one-third and two-thirds the size of the main conductance channel. Above 75 mV, the number of large conductance jumps ($\Lambda/\sigma > 4$ Å) increased, which may reflect protein aggregation

TABLE I

SIZE (Λ/σ) OF SINGLE-CHANNEL EVENTS AT pH 5.5 FOR ompF MEASURED AT DIFFERENT MEMBRANE POTENTIALS

Voltage (mV)	CIE + CDE		CDE
	Main peak (Å)	$\overline{\Lambda/\sigma}$ [a] (Å)	$\overline{\Lambda/\sigma}$ [b] (Å)
25	3.1	2.9	n.d. [c]
50	3.1	2.9	n.d.
75	3.1	2.7	n.d.
100	3.0	2.9	2.6
125	3.1	2.4	2.1

[a] Average size of all CIE and CDE smaller than 4 Å, as shown in Fig. 2.
[b] Average size of all CDE as shown in Fig. 3.
[c] n.d., not determined.

induced by the high potentials. Also, the uniformity in the size of the conductance channels decreased at the high potentials, as has been reported in studies of mitochondrial porin [11].

From the experiments described in Fig. 2, the CDE measurements alone were plotted as separate histograms and are shown in Fig. 3. The number of CDE was relatively small when the transmembrane potential was under 75 mV, but increased above this voltage. At 100 and 125 mV, the average sizes of the CDEs were significantly smaller than the size of the total events (Table I). Furthermore, the average size of the CDE shifted to smaller values when the potential was raised from 100 to 125 mV (Table I).

In preliminary studies, we have found that the size distribution of the ompF porin channels was essentially identical when the bathing solution surrounding the bilayer lipid membrane was changed from 0.1 M NaCl to 0.1 M KCl (pH 5.5) (unpublished data). However, when the pH of the bathing solution was lowered to 3.5, a treatment which reportedly decreases subunit interaction within the porin trimers [16], the size distribution of porin channel conductance is dramatically altered. The size distribution histograms of ompF porin channels inserted into bilayer lipid membranes bathed in 0.1 M KCl (pH 3.5) are shown in Fig. 4. When the transmembrane potential was maintained at

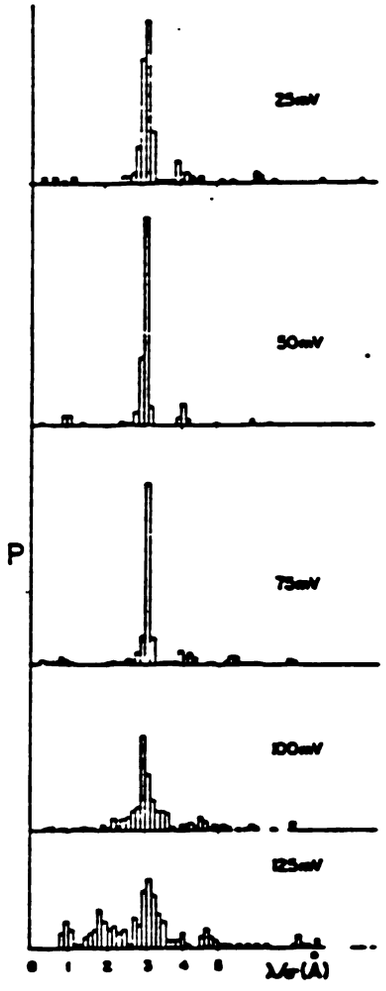

Fig. 2. Distribution of the size parameter, Λ/σ, for ompF protein added to a bilayer lipid membrane comprised of PC/oxidized cholesterol (2:1) at different transmembrane potentials. Λ is the conductance change and σ is the specific conductance of the bathing solution. P, in arbitrary units, is the relative number of events with the give size parameter values. The experimental conditions were the same as that described for Fig. 1, except that the porin used in the top histogram (25 mV) was added at a concentration of 30 ng/ml, and this protein was added to the bilayer lipid membranes without pretreatment. Both the opening and closing events are included in the histograms.

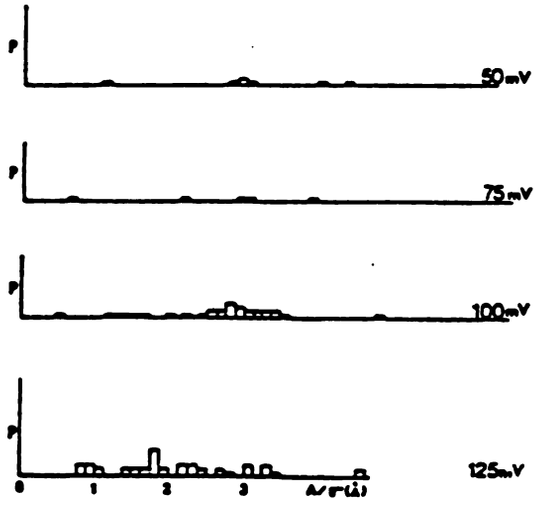

Fig. 3. The distribution of the size parameter of only the closing events from Fig. 2 at different transmembrane potentials. The experimental conditions were the same as for Fig. 2.

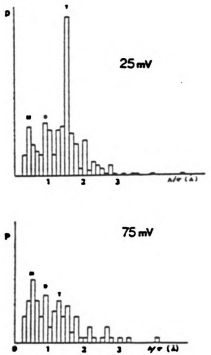

Fig. 4. Distribution of the size parameter, A/σ, for the ompF protein in a bilayer lipid membrane comprised of PE/oxidized cholesterol (2:1). The porin sample, at a final concentration of 140 ng/ml, was incubated in the bathing solution of 0.1 M KCl (pH 3.5), for 0.5 to 2 h at room temperature prior to addition to the bilayer lipid membrane. 195 events measured at the two voltages were analyzed.

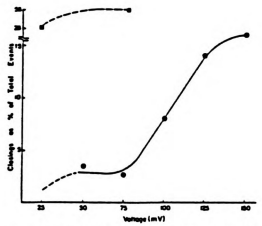

Fig. 5. Voltage dependence of porin channel closing from ompF protein suspended at pH 5.5 in 0.1 M NaCl (●) or at pH 3.5 in 0.1 M KCl (■). The bilayer lipid membrane systems used for the pH 5.5 studies were as described for Figs. 2 and 3, and for the pH 3.5 studies, as described for Fig. 4.

25 mV, the majority of channels (both CIE and CDE) had a size of 1.6 Å, while there were a significant number of channels with one-third and two-thirds the size of the major peak. Furthermore, when the voltage across the membrane was raised to 75 mV, the channel size distribution at pH 3.5 shifted to even smaller values (Fig. 4, 75 mV), and the majority of channels now had a size of 0.6 Å, approximately one-third the cross-sectional area of the channel at 25 mV.

Not only did the size of the channels decrease at low pH values, but the number of closing events also increased. Fig. 5 shows the percent of total events that were CDEs. At pH 5.5, using transmembrane potentials below 100 mV, the CDEs were less than 5% of the total events, while at pH 3.5, the CDEs were > 25% of the total, and approached 50% of the total at 75 mV. The results indicate that lowering the pH and increasing the transmembrane potential both decrease the size distribution of ompF porin channels and increase the probability of channel closing for ompF porin inserted into a bilayer lipid membrane. Furthermore, when the transmembrane potential was decreased from 125 mV to 25 mV, the number of closing events decreased and the channel size increased, indicating that changes induced at high voltage were reversible (data not shown).

Discussion

The changes in conductance across a bilayer lipid membrane containing porin protein are of two basic types; increases in conductance (CIE) and decreases in conductance (CDE). In most bilayer lipid membrane studies of porins the majority of events have been reported to be CIE and are interpreted to represent the opening of porin channels [8,13]. Others have noted infrequent CDE and suggest that, under the conditions used in bilayer lipid membrane studies, porin channels close relatively infrequently [16].

In our studies, we have noted two types of CDE. The vast majority of CDE occur very fast (< 0.3 ms) and are of a magnitude essentially identical to the CIE. On rare occasions at low pH or in high ionic strength, we detected very slow closing events which occurred over a period of seconds to minutes. These slow events showed random fluctuations in the conductance during this time. We propose that the fast CDE represent a reversible conformational change in the porin proteins from an 'open' to a 'closed' state. The slow process seen on rare occasion is thought to reflect an irreversible denaturation of an open porin channel.

In analyzing both the CDE and CIE at pH 5.5, the peak value of the channel size at all voltages was 3.1 Å. Assuming a channel length of 7.5 nm [22], we calculated that this size corresponds to an interior diameter of 1.7 nm, consistent with other bilayer lipid membrane results [8,16]. Below 100 mV, there was little change in the size distribution histogram of conductance changes measured at pH 5.5. Thus, the structure of the ompF complex was unaltered by these changes in the electric field. Within this range, Ohm's law has been shown to be valid for porin single-channel conductance measurements [16]. However, above 100 mV, the channel size distribution histogram changed dramatically (Fig. 2). In addition to the main channel of 3.1 Å, two additional peaks at approx. 1 and 2 Å were evident.

We propose that the main conductance change with a size parameter value of 3.1 Å represents the opening of a porin complex that contains three separate channels which open cooperatively. At high membrane potential, the cooperativity between the units within the complex appears to be weakened and the channels more readily open independently. This would account for conductance changes corresponding to channel cross-sectional areas of one-third and two thirds that of the main complex. For the single channel with a size parameter of 0.9 Å, the calculated diameter would be 0.9 nm, consistent with the size exclusion limit of the ompF porin determined by liposome swelling assays [19,23]. Our results, however, cannot determine whether, in this model, the single channel with a 0.9 nm diameter represents a protein trimer with a single fused channel or a single protein subunit. Channel conductance studies of mitochondrial porins also have shown that the size of the conductance channels decreases with increasing membrane potentials [10–12]. In these studies, distinct size populations of channels were also detected which changed in levels with membrane potential [11,12]. These results, however, were interpreted in terms of multiple conformations of the porin channel with different channel sizes. We do not believe that the three populations of channel sizes that we see for the ompF protein represent three conformations with three sizes of channels. If this were the case, the predominant conformation with a conductance size of 3.1 Å would have a diameter of 1.7 nm, much larger than the exclusion limit of the ompF protein.

In addition to the change in the size distribution of the channels, high voltage also affected the stability of the open channel conformation. At low voltage, the number of CDE was very small, and below 100 mV, the size distribution of the CDE was difficult to assess. However, above 100 mV, the stability of the closed state increased with increasing voltage (Fig. 5). The size of the CDE was distinctly smaller than that of the total events (Table I), suggesting that, for our model, the closing event shows less cooperativity between the subunits than the opening event. A similar increase in number of CDE with increasing potential has been noted for mitochondrial porins, and CDE of the mitochondrial porins are also reported to be smaller in size than the opening events [10–12].

Processes similar to those seen at high voltage were also detected at low voltage when the pH of the bathing solution was decreased to 3.5. As shown in Fig. 4, at 25 mV, channels of one-third and two-thirds the size of the main channel were detected in sizable amounts. Furthermore, when the voltage was increased to 75 mV, the monomeric channels were the major channels detected. Thus, even at low pH, increased voltage further reduced either the aggregation state or the cooperativity in the opening of the porin channels. The smaller size of the porin trimer at pH 3.5 (Λ/σ = 1.6 Å) compared to pH 5.5 (Λ/σ = 3.1 Å) is thought to reflect a specific pH-dependent alteration in protein structure that significantly affects the apparent channel size. The change in confor-

mation that alters the diameter of the channel at low pH is probably not the cause of the increase in channel closing events. High voltage caused these later changes, but did not affect the size of the main channel event. Furthermore, increasing the voltage at low pH to 75 mV further enhanced the level of monomeric units and CDE, but did not alter trimer or monomer channel size.

At pH 5.5, there appears to be a threshold potential, above which the porin subunits undergo a reversible, voltage-dependent change in conformation. This second, voltage-induced structural change triggered above 75 mV and enhanced at low pH induces two detectable changes in porin function in the bilayer lipid membrane. The first is an increase in the number of smaller subunit channels (CIE and CDE), and the second is an increase in the probability of channel closing. These two changes are likely caused by the same structural alteration in the protein. We propose that, both at low pH and at high transmembrane potential, the proteins within the trimeric unit become less tightly associated. In the loosened complexes, the separate channels open and close independent of the other subunits, and the closed conformation becomes more favorable. This model is consistent with the studies of Markovic-Housley and Garavito [24] and Schindler and Rosenbusch [3], who show that, below pH 4.5, structural changes are detected which are at least partially reversible and are dependent on the detergent used to solubilize the sample. These pH-dependent structural changes are thought to weaken inter-subunit contacts and change the porin structure [24], and thus, may decrease the cooperativity of the CIE/CDE of the subunits and increase the stability of the closed state. Furthermore, this less tightly associated complex is stabilized in a bilayer lipid membrane by elevated membrane potentials.

Whether transmembrane potentials control porin activity on the intact cell has been a controversial question. It has been calculated that the Donnan potential across the outer membrane usually does not exceed approximately 30 mV [25]. Furthermore, in studies where the Donnan potential was elevated to as high as 80 mV, the rate of cephaloridine diffusion through the porin channels was unaffected [26]. However, we found that such a potential may have been near the threshold value needed to induce an alteration in porin structure. In addition, lowering the pH may dramatically drop the threshold potential required to induce channel closing events. Thus, several environmental factors, such as pH and salt concentration, may dramatically affect porin-channel activity and allow for voltage-dependent control of diffusion across the channel. We found that we could detect distinct size populations of porin subunits and CDEs when the porin samples were pretreated by repeated freeze-thaw cycles, followed by preincubation in 0.1 M NaCl. In the absence of such pretreatment, the histograms were very broad and almost no CDEs were detected, even above 75 mV (data not shown). We believe that the pretreatment did not denature the protein, but allowed for dissociation of porin aggregates to trimeric units and perhaps weakened the interactions within the trimers.

Acknowledgements

This work was supported in part by Public Service Grants GM14971 and GM31202 (H.T.T.).

References

1 Benz, R. (1985) CRC Rev. Biochem. 19, 145–190
2 Chen, R., Krämer, C., Schmidmayr, W., Chen-Schmeisser, U. and Henning, U. (1982) Biochem. J. 203, 33–43
3 Schindler, M. and Rosenbusch, J.P. (1984) FEBS Lett. 172, 85–89
4 Garavito, R.M., Jenkins, J., Jansonius, J.N., Karlsson, R. and Rosenbusch, J.P. (1983) J. Mol. Biol. 164, 313–327
5 Kleffel, B., Garavito, R.M., Baumeister, W. and Rosenbusch, J.P. (1985) EMBO J. 4, 1589–1592
6 Chang, C., Mizushima, S. and Glaeser, R.M. (1985) Biophys. J. 47, 629–639
7 Dorset, D.L., Engel, A., Massalski, A. and Rosenbusch, J.P. (1984) Biophys. J. 45, 128–129
8 Schindler, H. and Rosenbusch, J.P. (1981) Proc. Natl. Acad. Sci. USA 78, 2302–2306
9 Paul, C. and Rosenbusch, J.P. (1985) EMBO J. 4, 1593–1597
10 Freitag, H., Neupert, W. and Benz, R. (1982) Eur. J. Biochem. 123, 629–636
11 Roos, N., Benz, R. and Brdiczka, D. (1982) Biochim. Biophys. Acta 686, 204–214
12 DePinto, V., Tommasino, M., Benz, R. and Palmieri, F. (1985) Biochim. Biophys. Acta 813, 230–242
13 Schindler, H. and Rosenbusch, J.P. (1978) Proc. Natl. Acad. Sci. USA 75, 3751–3755
14 Benz, R., Janko, K., Boos, W. and Läuger, P. (1978) Biochim. Biophys. Acta 511, 305–319

15 Benz, R., Janko, K. and Läuger, P. (1979) Biochim. Biophys. Acta 551, 238–247
16 Lakey, J.H., Watts, J.P. and Lee, E.J.A. (1985) Biochim. Biophys. Acta 817, 208–216
17 Foulds, J. and Chai, T.-J. (1979) Can. J. Microbiol. 25, 423–427
18 Coughlin, R.T., Tonsager, S. and McGroarty, E.J. (1983) Biochemistry 22, 2002–2007
19 Nakae, T. (1976) Biochem. Biophys. Res. Commun. 71, 877
20 Tien, H.T. (1985) Prog. Surf. Sci. 19, 169–274
21 Tien, H.T. (1974) Bilayer Lipid Membrane (BLM): Theory and Practice, Marcel Dekker, New York
22 Matsuyama, S.I., Inokuchi, K. and Mizushima, S. (1984) J. Bacteriol. 158, 1041–1047
23 Nikaido, H. (1983) Meth. Enzymol. 97, 85–100
24 Markovic-Housley, Z. and Garavito, R.M. (1986) Biochim. Biophys. Acta 869, 158–170
25 Stock, J.B., Rauch, B. and Roseman, S. (1977) J. Biol. Chem. 252, 7850–7861
26 Nikaido, H. and Vaara, M. (1985) Microbiol. Rev. 49, 1–32